A Dissertation

Entitled

Synthesis and Applications of Carbon Nanotubes in Nano-Electro-Mechanical System

by

Kun Guo

Submitted as partial fulfillment of the requirement for

the Doctoral of Philosophy in Engineering

Advisor: Dr. Ahalapitiya H. Jayatissa

College of Graduate Studies

The University of Toledo

August 2008

The University of Toledo

College of Engineering

I HEREBY RECOMMEND THAT THE DISSERTATION PREPARED UNDER MY

SUPERVISION BY *Kun Guo*

ENTITLED *Synthesis and Applications of Carbon Nanotubes in Nano-Electro-Mechanical System*

BE ACCEPTED IN PARTIAL FULFILLMENT OF THE REQUIREMENTS FOR

THE DEGREE OF DOCTOR OF PHILOSOPHY IN ENGINEERING

Dissertation Advisor: Dr. Ahalapitiya H. Jayatissa

Recommendation concurred by

Dr. Abdollah Afjeh

Dr. Alvin Compaan

Dr. Lesley Berhan

Dr. Mehdi Pourazady

Committee

On

Final Examination

Dean, College of Engineering

An Abstract of

Synthesis and Applications of Carbon Nanotubes

in Nano-Electro-Mechanical System

Kun Guo

Submitted as partial fulfillment of the requirement for

the Doctor of Philosophy in Engineering

The University of Toledo

August 2008

Synthesis and applications of Carbon Nanotubes (CNTs) in nanotechnology and Nano-Electro-Mechanical System (NEMS) have been investigated. A hot filament assisted Chemical Vapor Deposition (CVD) system was developed to synthesize the CNTs in a low temperature region of 450 - 700 °C at atmospheric pressure. The carbon source, methane (CH_4), was decomposed into carbon radicals by a hot filament heated to 2000 °C. The 5% hydrogen (H_2) in argon (Ar) or pure Ar was used as the carrier gas of the carbon radicals to the reaction zone. Cobalt (Co), nickel (Ni), iron (Fe), and gold (Au) were coated on substrates as catalyst by Physical Vapor Deposition (PVD). The CNTs were synthesized on the patterned catalyst coated on the silicon and glass substrates. Using this hot filament CVD, it is possible to synthesize CNTs on glass substrates at a temperature as low as 450 °C. The

synthesis conditions, such as filament temperature, catalyst type, substrate pre-heating temperature and carbon source feeding rate were optimized to control the formation of CNTs. The effects of catalyst type, catalyst particle size and substrate treatment conditions for the growth of CNTs were also investigated. The CNTs were characterized by Scanning Electron Microscopy (SEM), Transmission Electron Microscopy (TEM), Raman spectroscopy and X-ray Diffraction (XRD). It was found that the present hot filament CVD system produced multi-walled carbon nanotubes (MWCNTs). The SEM images indicated that the CNTs were formed faster and longer at higher temperatures than lower temperatures. In this hot filament CVD system, the CNTs were grown as long as 60 μm in length and as small as 4 nm in diameter on silicon and glass substrates at low temperature and atmospheric pressure.

Applications of the CNTs were investigated by combining nanotechnology and Micro-Electro-Mechanical system (MEMS) in a few advanced devices such as gas detectors, pressure sensors, and field emission displays. The CNTs were grown on the patterned catalyst as the core parts to fabricate gas detectors, pressure sensors, and field emission test devices. The resistances of CNT-based sensors were measured and recorded after being assembled in an electrode circuit. The gas detectors were tested mainly for hydrogen. It was found that the MWCNTs have high sensitivity and fast response in the operating temperature range of 150 - 300 °C. For the pressure sensors, the CNTs were synthesized on a micro-fabricated silicon nitride (SiN_x) membrane. The SiN_x membrane was fabricated by employing advanced bulk MEMS technology. It was observed that CNT-based pressure sensors have the potential to measure gas pressure. The resistance of the CNTs grown on the membrane was changed by the stress developed by the applied pressure. Two types of possible mechanisms of the actions of the CNTs on the pressure sensor membranes were proposed based on the

experimental results. For the thin CNTs film on the membranes, the resistances of pressure sensors increased with the increase of pressure, while for the thick CNTs film, the resistance of pressure sensors decreased. Finally, the electron field emission phenomena of these CNTs were investigated. It was observed that these CNTs have an emission threshold electric field as low as 1-5 V/μm and high emission current levels. The CNT-based Field Emission Display (FED) devices have advantages of low temperature synthesis of CNTs at atmospheric conditions as compared to other synthesis methods that require high temperature and vacuum conditions. All these applications of CNTs proved that the CNTs grown by the hot filament CVD system at atmospheric pressure have similar or improved properties and several technical advantages over the CNTs produced by conventional methods.

Acknowledgements

The writing of this dissertation was not possible without the personal and practical support of numerous people. Thus I would like to offer my sincere gratitude go to my advisor, my committee members, my friends and all people providing help to me over the last few years.

I would like to express my gratitude to my advisor, Dr. Ahalapitiya H. Jayatissa, for his support, patience, and encouragement throughout my PhD studies. It is not often that one finds an advisor who co-work with students and provide advice and support any time. I admire his hard work, and appreciate his help for me on the research. He led me into the interesting world of this research and taught me lots of knowledge in classes and laboratory experiments. His academic and editorial advices were essential to the completion of this dissertation and taught me innumerable lessons and insights on the academic research.

My thanks go to the committee members, Dr. Abdollah Afjeh, Dr. Alvin Compaan, Dr. Abdul-Majeed Azad, Dr. Lesley Berhan, and Dr. Mehdi Pourazady for their time, advices and comments on my previous proposal and manuscript of this dissertation. I really thank all of them for providing many valuable comments that improved the presentation and contents of this dissertation. I also thank Dr. Sarit Bhaduri for careful reading and checking of the dissertation.

My gratitude also goes to my lab mates, Dennis J. Wagner, Zhiyu Li, Linhao Wu, Dr. Pubudu Samarasekara, for their support on research. I am thankful to the staff that maintained machines and resources for our laboratory. I thank those people in other labs or universities who assisted on our research. I thank the Physics, Chemistry, Bio-Engineering

departments in the University of Toledo, and EMAL laboratory in the University of Michigan for using their instruments.

I thank the chairman, faculty, and staff of the department of Mechanical, Industrial and Manufacturing Engineering for giving me the opportunity and providing financial support to study here.

I am grateful to many friends who helped me stay through hard time in life and study and shared happy time. I thank Hua for editing the dissertation. I thank my parents for understanding and supporting all those years. I am always proud of you just as you are proud of me.

This research was supported by a grant (Grant number ECS-0401690) from the National Science Foundation (NSF), USA.

Table of Contents

List of Tables

List of Figures

Nomenclature

A	ampere meter, or area
Ar	argon
C	carbon
CNTs	carbon nanotubes
Co	cobalt
d	distance
E	energy
Fe	iron
FED	field emission display
G	conductance of carbon nanotubes
ΔG	change of conductance of carbon nanotubes
g	conductance of single carbon nanotube
Δg	change of conductance of single carbon nanotubes
H	hydrogen
hr	hour
I	current
ITO	Indium Tin Oxide
L	length
M	metal

m meter, or the number of unit vectors along two directions in the honeycomb crystal lattice of graphite

MEMS Micro-Electro-Mechanical system

MWCNTs multi-walled carbon nanotubes

min minutes

N number of carbon nanotubes

NEMS Nano-Electro-Mechanical system

Ni nickel

n The number of unit vectors along two directions in the honeycomb crystal lattice of graphite

nm nanometer

O oxygen

P pressure

psi pounds per square inch

PVD physical vapor deposition

R resistance

Rm resistance of metallic tubes

rpm revolutions per minute

Rs resistance of semi-conducting tubes

S sensitivity

s second

Si silicon

SiN_x silicon nitride

sccm	Standard Cubic Centimeters per Minute
SWCNTs	single-walled carbon nanotubes
UV	ultra violet light
V	voltage
X	coordinate axis
Y	coordinate axis
θ	chiral angle in graphite sheet
Ω	resistance
ρ	the electrical resistivity of material
α	the area of emission sites
β	the field enhancement factor
ϕ	the work function of the emission surface
μm	micron

Chapter One

1 Introduction

In the history of human beings, materials have been the driving force of human civilization since the beginning, from the natural materials of pre-history such as wood and stone, to little complicated processed copper and bronze, and then to more complicated featured iron. Those periods are so named as the Stone Age, the Bronze Age, and the Iron Age according to the widely used materials in each period [1]. Today, there are more than 80,000 materials for use at this age of advanced materials [2]. New or improved materials are now evolving faster than ever before due to the growing demand of the industry producing and scientific research interest. The efforts of materials and mechanical scientists and engineers are to develop better materials and apply them in productions. An impressive generalization is shown in Figure 1-1. Following the history, possibly the current age will be named after one of the most involved materials by the people in the future.

Carbon is the most versatile element that exists on the earth. It has many different properties which can be used in different ways depending on how the carbon atoms are arranged and how combined with other elements [4]. Carbon is the important component of living organism. Carbon is one of the main components of widely used fuels such as wood, coal, petroleum and natural gas. Carbon was discovered in the form of graphite in 1779 and

in the form of diamond in 1789 [4]. After about 200 years, Kroto, Smalley and Curl discovered the fullerenes in 1985 [5]. A few years later, the Carbon Nanotubes (CNTs) were discovered by Sumio Iijima in 1991 [6].

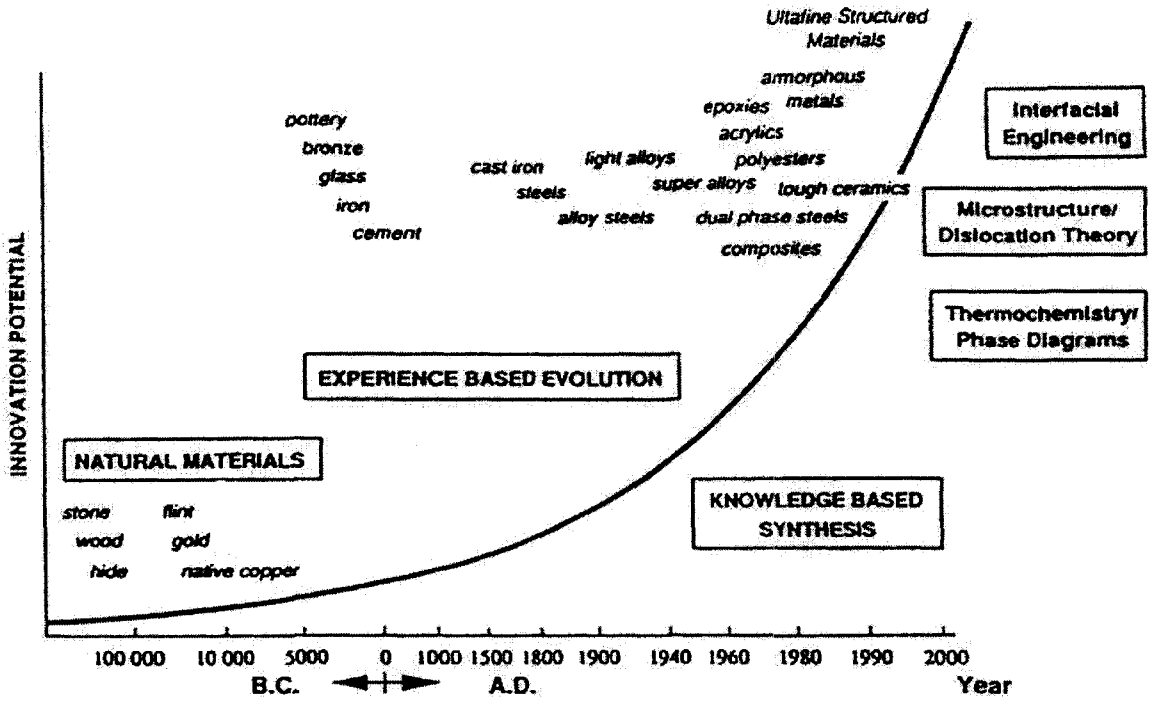

Figure 1-1 The evolution of the innovation content of materials [3]

The structures of diamond, graphite and fullerene are shown in Figure 1-2. After the discovery of CNTs, carbon was considered as one of the important materials that could be widely used in engineering. Some smart materials developed using modern technologies, such as nanotechnology, have the potential to start a new technology revolution. Among those possible materials, CNTs have aroused great interests because of their remarkable mechanical, electrochemical, piezoresistive and other physical and chemical properties [7]. After more than 17 years of research, many interesting properties of CNTs have been discovered, such as structural and electrical characteristics, including large surface, piezoresistivity and electrochemical properties that make them a promising material in many

applications such as sensors, pressure gas store, composite component, high-intensity products, property-enhance additive and micro-chips. The CNTs are possibly the strongest and most super-elastic materials that have been found. The electronic properties of CNTs are interestingly a strong function of their atomic structure. Mechanical deformation or chemical functionalization of the surface can induce changes in the conductance of CNTs [8]. Their tiny size makes it possible to fabricate extremely small sensors that are sensitive to chemical and mechanical changes without causing influence to the objects being detected. Those important properties of CNTs provide a potential for developing sensors with high sensitivity, low operating voltage, and multi-functional sensor array.

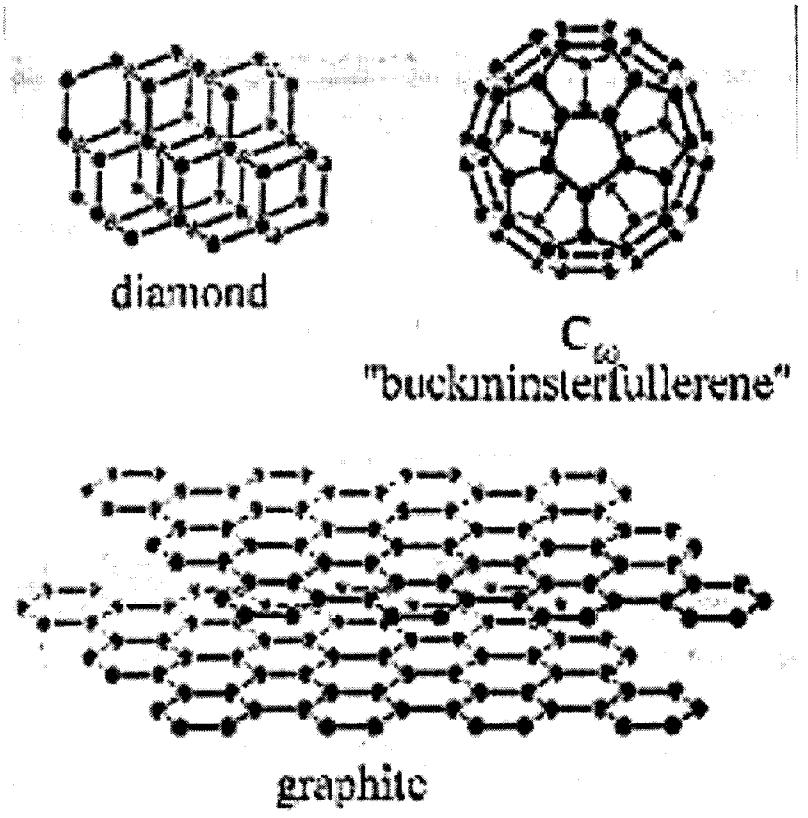

Figure 1-2 Structure of diamond, fullerene and graphite [9]

Since the beginning of the 20th century, the development of sciences and technologies

had been accelerated so fast that more and more new theories and technologies appeared, such as Theory of Relativity and Quantum Theory, and research had been done widely in almost all fields. But as Albert Einstein said, all the future researches should be extended in two directions: macro-world, such as universe celestial body, and micro-world, such as atoms. The range of the objects will be from light-year (9.46×10^{15} m) to nanometer (10^{-9} m) and even picometer (10^{-12} m). For the demands of research in the micro-world, one of most important theories and technologies appeared in the modern sciences was nanotechnology, which was considered as the key to lead us into the new Nanometer Times. As some rules in the micro-world may be different from the macro-world, hence many of them need to be examined and studied again. Nanotechnology is helpful for researches in the nano-scale world. Another related technology is Micro-Electro-Mechanical System (MEMS), which combines micro-scale actuator/sensor and circuit together and reduces the size of devices by using semiconductor-processing technologies [10]. When the core parts of the sensors are nanometer scale, the devices are called Nano-Electro-Mechanical System (NEMS). With the help of semiconductor industry technologies, the CNTs can be used to fabricate many high-quality functional products using nanotechnology. The main application areas include: composites, sensors / probes, field emission devices, flat panel display, nanotubes-based lamps, energy storage, electrochemical devices, and nanometer-size electronic devices [4]. Potential practical applications of CNTs have been reported such as chemical sensors [11], field emission materials [12], catalyst support [13], electronic devices [14], high sensitivity nano-balance for nano-scopic particles [14], nano-tweezers [15], reinforcements in high performance composites, and as nano-probes in meteorology and biomedical and chemical investigations, anode for lithium ion in batteries [16], nano-electronic devices [17], super

capacitors [18] and hydrogen storage [19].

1.1 Motivation

It has been 17 years since the discovery of CNTs. While so many researches have investigated this important material, the CNTs are still very expensive because of the high cost of processing, equipment, energy, and source materials. There are few products made of CNTs in industry because of many limitations, including mass production, technological difficulties, and economical factors.

Currently, there are many methods to synthesize CNTs, such as arc discharge, CVD, plasma-enhanced chemical vapor deposition (PECVD), laser-pulse chemical vapor deposition (LPCVD), and laser ablation. Every method has advantages and disadvantages as shown in Table 1-1. Most methods require high temperature (> 600 ^{o}C), and the typical temperature is about 700 - 800 ^{o}C. Some methods cannot control the nucleation position of CNTs, therefore CNTs are coated on unwanted area of the device component. Some methods cannot grow CNTs on large area, which prevent them from being used for industry batch producing. As some methods need extra energy (plasma or laser), the equipments and processes are complex. It is important to develop a better method to synthesize CNTs and apply CNTs in productions. The novel technology must synthesize CNTs at low temperature, selected place as the nucleation position of CNTs, and favorable conditions such as vacuum requirement and scalability. If a technology had the above advantages, it could be used to grow CNTs on large area, and the equipment and processes would be simple.

Table 1-1 Comparing Current Synthesis Methods of CNTs

Methods	Temperature (°C)	Position control	Large scale area	Complexity
Arc discharge	750 - 800	No	No	Yes
CVD	750 - 800	Yes	Yes	No
PECVD	700 - 800	No	Yes	Yes
LPCVD	700 - 800	No	Yes	Yes
Laser ablation	600 - 800	No	No	Yes

In this research project, the investigation was made to grow CNTs using a hot filament CVD system at low temperature, low gas flow rate, and atmospheric pressure conditions. Several applications were investigated by applying CNTs in gas detection, gas pressure measurement and field emission devices. The position of CNTs was controlled by making catalyst pattern. This hot filament CVD system can grow CNTs on large area substrates with high reproducibility and in a well controlled manner.

1.2 Objectives

The overall objectives of this research were:

1. To grow CNTs by hot filament assisted CVD system at low temperature, low gas flow rate, on many kinds of catalysts and substrates, under atmospheric pressure;
2. To develop CNT-based gas sensors to detect gases;
3. To develop CNT-based pressure sensors to measure gas pressure;
4. To develop CNT-based field emission display unit.

1.3 Overview of the Dissertation

This dissertation involves several main parts. These are: (1) background study on CNTs and their applications; (2) synthesis of CNTs using a hot filament CVD system; (3) fabrication and testing of CNT-based gas detectors; (4) fabrication and testing of CNT-based pressure sensors; (5) fabrication and testing of CNT-based field emission displays; (6) conclusions and recommendation for future research.

In this chapter, some background technologies related to this research are presented. These sections include the basic concept and structure of CNTs, synthesis methods, and fundamentals of synthesis mechanisms. The applications of CNTs such as gases detectors, mechanical actuators, and field emission displays are described. Some basic knowledge about NEMS will be discussed at the end of this chapter.

In Chapter 2, the hot filament CVD system used in this research is introduced, and the process of synthesis of CNTs using this system is described in detail. Characterization of CNTs by SEM, TEM, RAMAN and XRD are also discussed.

Chapter 3 covers the fabrication and testing of CNT-based gas detectors are presented. The analysis of testing results of gas detectors for different gases is discussed.

In Chapter 4, the fabrication and testing of CNT-based pressure sensors are presented. Two types of response of pressure sensors were observed and discussed based on the results of the research.

In Chapter 5, the fabrication and testing of CNT-based field emission testing device are described. The field emission phenomenon of CNTs was analyzed.

In Chapter 6, the conclusions of this research are presented, and recommendations for future research are given on synthesis of CNTs and several applications.

1.4 Carbon Nanotubes

The CNTs were first discovered in 1991 by Sumio Iijima in fullerene soot [6]. They were produced by carbon-arc discharge method, which was similar to the method of preparing fullerenes. Fullerenes are closed cage structures of 60 carbon atoms, which look like soccer ball [20]. The first synthesized CNTs were multi-walled carbon nanotubes (MWCNTs), which comprised coaxial cylinders of graphite sheets ranging from 2 to 50 and up, and single-walled carbon nanotubes (SWCNTs) were observed two years later [21]. The SWCNTs are basically a single fullerene molecule that is stretched out so the length is thousands to millions times its diameter [22].

1.4.1 Properties of Carbon Nanotubes

Since the discovery of CNTs [6], intense interests have been focused on them because of their special properties, which make them potentially useful in extremely small-scale electrical and mechanical applications [23]. The CNTs have unique properties due to their seamless carbon-sheet structure with high aspect ratios and their symmetric structure [24]. The CNTs are long, slender fullerenes where the walls of the tubes are hexagonal carbon (graphite structure) and often capped at each end. The CNTs can be considered as cylindrically shaped molecules formed of rolled-up single or multilayer sheets of graphitic planes as shown in Figure 1-3. Figure 1-3 (a) is the graphite sheet to be cut along the dotted lines and rolling the tube so that the tip of the chiral vector touches its tail. The way the graphite sheet wrapped is represented by a pair of indices (n, m) called the chiral vector. The integer n and m denote the number of unit vectors along two directions in the honeycomb crystal lattice of graphite. According to the different chiral angle, θ, in the cutting, there are

two atomic structures: zigzag (0^{o}) and armchair (30^{o}) based on the geometry of the carbon bonds around the circumference of the CNT as shown in Figure 1-3 (b) and (c). If there are many graphite sheets that were cut and rolled up together to form the CNT, it is MWCNT as shown in Figure 1-4 (b).

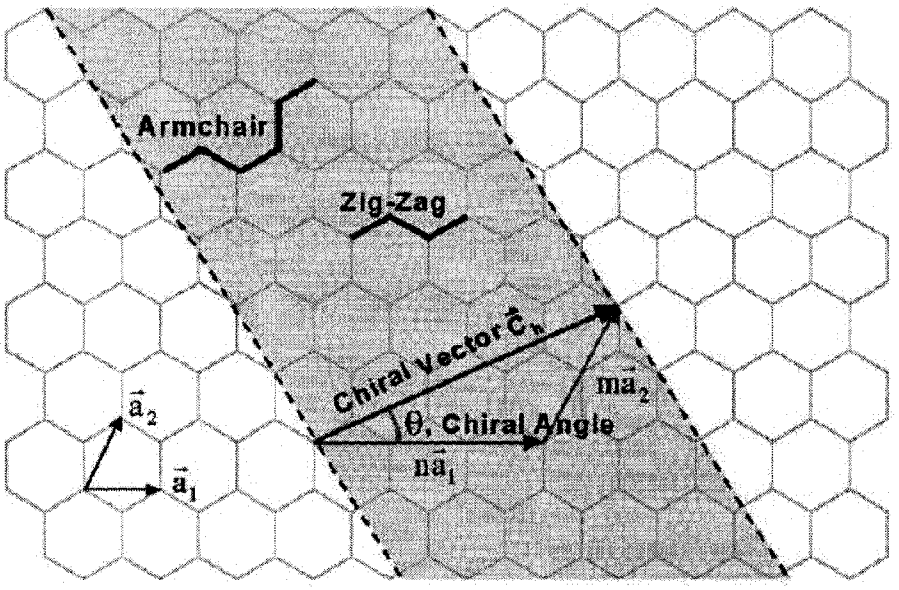

(a)

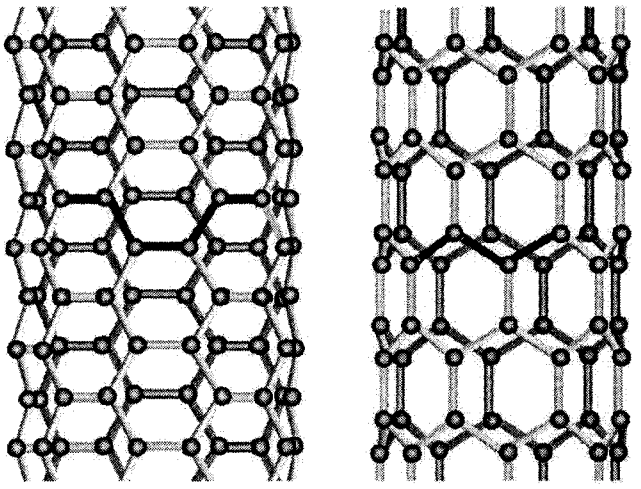

(b) (c)

Figure 1-3 Schematic diagram showing how a hexagonal sheet of graphite is 'rolled' to form a CNT: (a) Graphite sheet, (b) An armchair nanotube, (c) A zigzag nanotube [20]

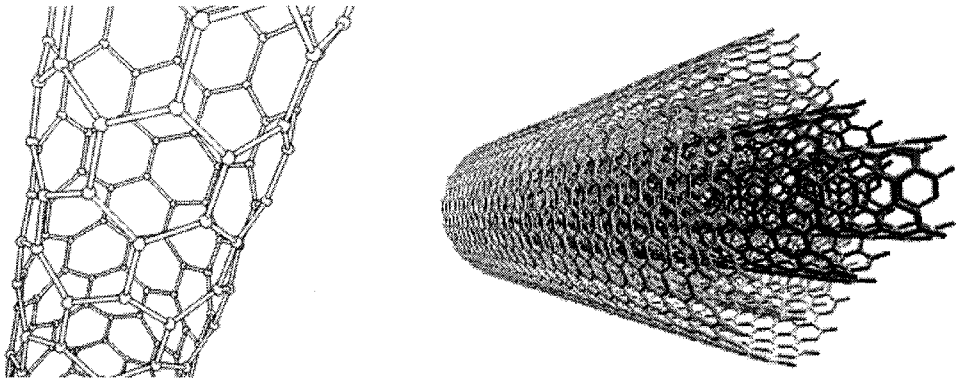

(a) (b)

Figure 1-4 Structure showing CNTs: (a) SWCNTs, (b) MWCNTs [25]

The diameter of CNTs is only a few nanometers according to the name. The lengths of CNTs are from micrometers to millimeters. CNTs have field emission and electronic transport properties, high mechanical strength and special chemical properties. Their strength is one to two orders of magnitude higher and their weight is six times lighter than steels [26]. Many researchers have reported mechanical properties of CNTs that exceed those of any previously existing materials. Although there are varying reports in the literature on the exact properties of CNTs, theoretical and experimental results have shown extremely high elastic modulus, greater than 1 TPa (the elastic modulus of diamond is 1.2 TPa) and reported strengths 10-100 times higher than the strongest steel at a fraction of the weight [20]. The strength of CNTs compared with other materials is shown in Table 1-2 [27]. They have superior thermal and electric properties: thermally stable up to 2800 ^{o}C in vacuum, thermal conductivity about twice as high as diamond, electric-current-carrying capacity 1000 times higher than copper wires [28]. Their excellent chemical, mechanical, electrical, thermal and magnetic properties make the CNTs a promising material in semiconductor, biology,

automobile, chemical, material, medicine, and other industries. There are still a variety of potential applications, such as nano-composite materials, molecular electronic devices, electron field emission, nano-scale transistors, scanning microscopy tips, lithium batteries, mechanical sensors, and gas sensors [29, 30].

Table 1-2 Comparison of Mechanical Properties [31-37]

Material	Yong's Modulus(TPa)	Tensile Strength(GPa)	Elongation at Break(%)
SWNT	~1 (from 1 to 5)	13-53[E]	
Armchair SWNT	0.94[T]	126.2[T]	23.1
Zigzag SWNT	0.94[T]	94.5[T]	15.6-17.5
Chiral SWNT	0.92		
MWNT	0.8-0.9[E]	150	
Stainless steel	~0.2	~0.65-1	15-50
Kevlar	~0.15	~3.5	~2
Kevlar[T]	0.25	29.6	

Note: E – Experimental observation, T – Theoretical prediction

1.4.2 Synthesis of Carbon Nanotubes

The CNTs have been synthesized by many methods such as arc discharge, CVD, PECVD, LPCVD, laser ablation, and plasma deposition. There are two basic types of techniques for CNTs synthesis, namely the vaporization methods (arc discharge, laser ablation) and the catalytic decomposition of hydrocarbons over metal catalyst (CVD). Essentially CNTs structures are all formed in the same way but the processes differ. The arc

discharge technique firstly used to synthesize CNTs is shown in Figure 1-5. After initial synthesis of fullerenes, laser ablation was improved to produce SWCNTs as shown in Figure 1-6. Solar energy was also considered to be used to grow CNTs as shown in Figure 1-7. During the synthesis of CNTs, impurities in the form of catalyst particles, amorphous carbon, and non-tubular fullerenes are also produced. Subsequent purification steps are required to separate the tubes. The gas-phase processes tend to produce nanotubes with fewer impurities and are more amenable to large-scale processing. It was believed that gas-phase techniques, such as CVD, for nanotube growth offer the greatest potential for the scaling-up of nanotube production for the processing of composites [20]. The CVD was one of the most widely used methods for CNTs synthesis because of its high product yield and large-scale capability [24, 38]. Most of the CVD methods, including PECVD, LPCVD and thermal CVD, require high volume of feeding gases, high growth temperature, and additional power sources such as plasma and lasers [39].

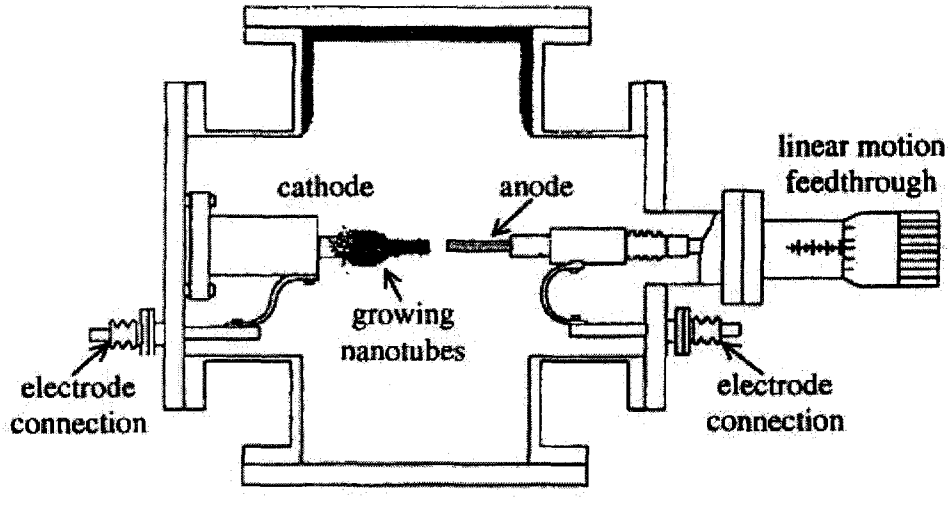

Figure 1-5 Schematic illustration of the arc-discharge technique [40]

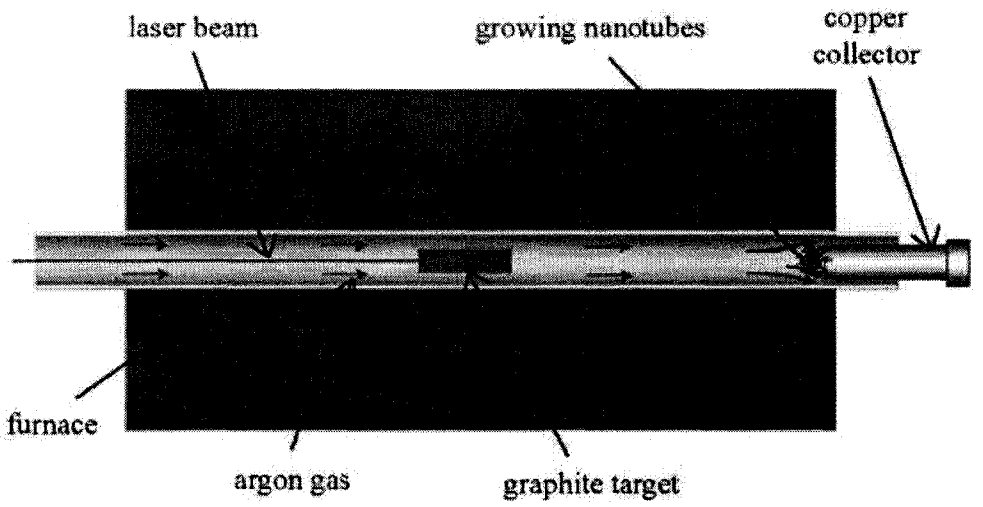

Figure 1-6 Schematic of the laser ablation process [28]

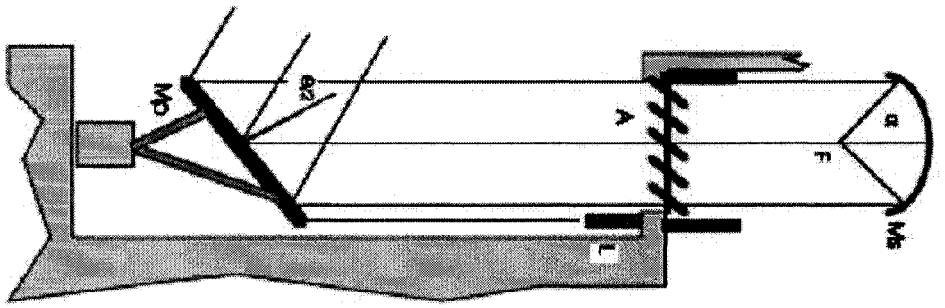

Figure 1-7 Solar furnaces for CNTs synthesis [41]

1.4.3 Synthesis Mechanism of Carbon Nanotubes

An understanding of the growth mechanism of CNTs is essential for material and process design [42-44]. There are two models for the growth of CNT: CNT grows by adding carbon at the top of the tube, as shown in Figure 1-8 (a) [45], and at the bottom, as shown in Figure 1-8 (b) [46].

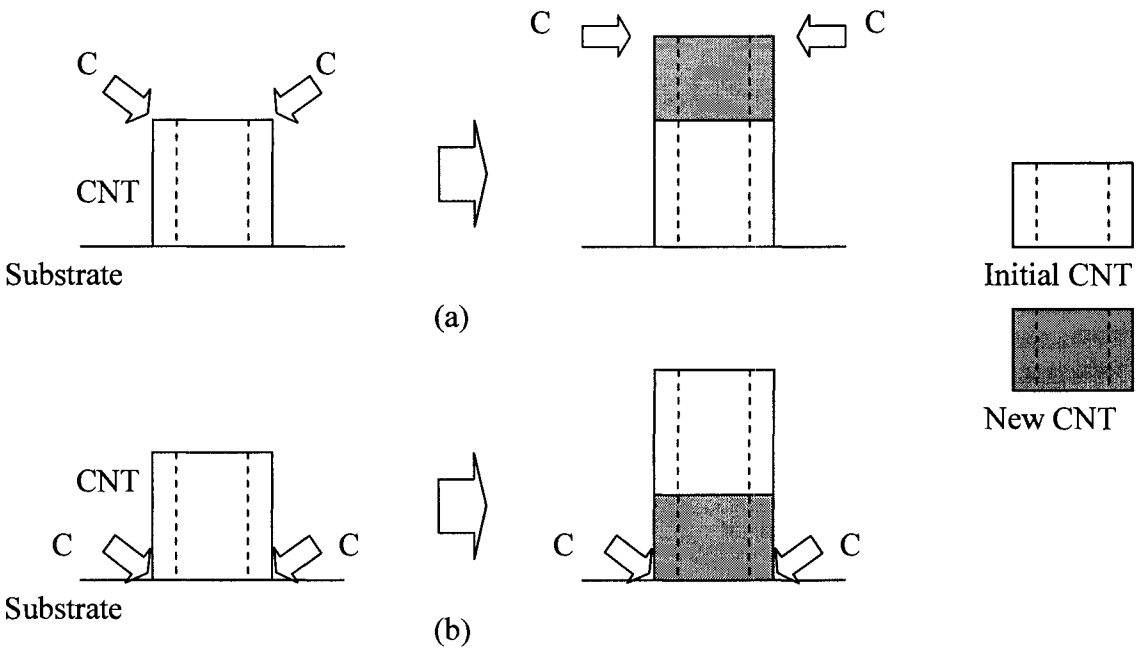

Figure 1-8 Growth models of CNT: (a) add carbon at the top, and (b) add carbon at the bottom

The carbon sources, such as hydrocarbon are decomposed into carbon species at high temperature in CVD as shown in formula (1-1) and (1-2) [47-50]. Those hydrocarbon and carbon species particle are carried to the reaction zone by carrier gas.

$$CH_4 + H\cdot \rightarrow CH_3\cdot + H_2 \tag{1-1}$$

$$CH_4 \xrightarrow{H\cdot} CH_3 \xrightarrow{H\cdot} CH_2 \xrightarrow{H\cdot} CH \xrightarrow{H\cdot} C \tag{1-2}$$

For the catalyst assisted growth of CNTs, the carbon species were dissolved into the metal catalyst droplet because the total energy of carbon-metal bond is lower than separated carbon and metal atoms as shown in Figure 1-9. Then the carbon diffuses through the catalyst particle under an activity gradient. As the CNTs have stable structure and low energy, the

carbon atoms separate out from the catalyst liquid droplet to form CNT. When using iron (Fe) as catalyst, the pure iron is exposed to carbon at high temperature, carbon-containing austenite (γ-Fe) would form, as indicated by the Fe-C phase diagram. As a result, the melting temperature decreases compared with that of pure iron (melting point 1495 °C). At the eutectic point, the melting temperature reached the lowest (1154 °C) with 4.26% of carbon in weight. Therefore some liquid droplets must have been formed at the surface of substrate when it is heated. As the carbon species continue to be dissolved in the liquid droplets, excessive amount of carbon atoms would be driven out to form solid structures outside the droplet, and then the CNT continues to grow with the supply of carbon atoms [51-58].

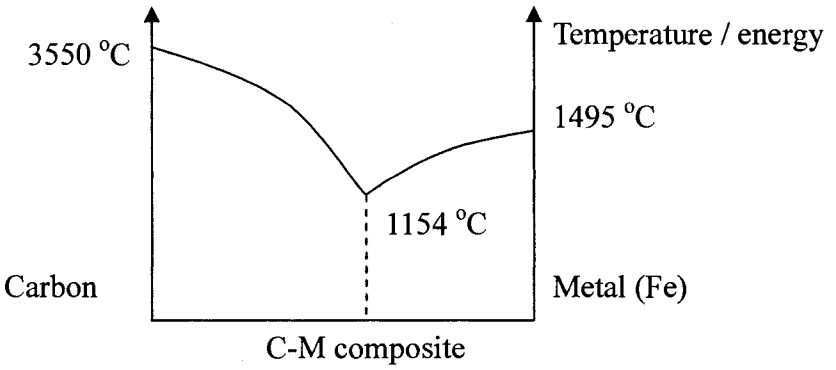

Figure 1-9 Melting temperatures of carbon, metal and carbon-metal composite

For the CVD synthesis process, a possible growth mechanism is explained in Figure 1-10 [59]. The carbon species were carried to reaction zone and dissolved in the liquid droplet of metal catalyst preheated in CVD. As an embryo spindle-like metal particle was formed via pre-treatment process due to the difference of interfacial energies between substrate particle and gas particle, with its catalytic decomposition of hydrocarbon gas to liberate carbon atoms, the first carbon layer was formed on the surface of catalyst metal

particle (Figure 1-10 (a)). The change of surface energy and elastic energy of carbon layer caused the tip radius of curvature of metal particle becoming smaller, and raised the broken bond density (in proportion to the surface energy) on the topside (Figure 1-10 (b)) [59]. Then the rising gradient of surface energy enhanced the surface diffusion of carbon atoms from bottom to top of the metal particle. The top part of graphite was pushed and raised by the carbon atoms coming out from the catalyst metal from the bottom. As the process of hydrocarbon gas adsorbing and dissolving, and carbon atom diffusing repeated, the CNTs continued to grow upward from the metal catalyst.

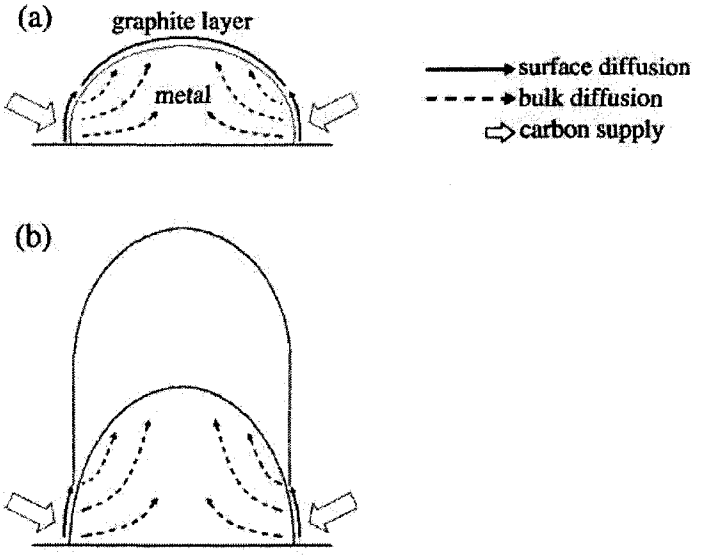

Figure 1-10 The proposed mechanism of CNT growth: (a) Nuclei of graphite formed on the surface of catalyst metal particle, (b) CNT continue to grow upward [59]

1.5 Carbon Nanotube-based Sensors

The CNTs have been proven to have some advantages for sensing applications [4]. Their small size with large surface, high sensitivity, fast response and good reversibility at room temperature enable them as a gas molecule sensor [60]. The enhanced electron transfer

lets them could be used as electrodes in electrochemical reactions [61]. Easy protein immobilization with retention of activity makes them potential biosensors [61]. The main advantages of these sensors are the nano-scale size of the nanotubes sensing element and the corresponding nano-scale size of the material required for a response [62]. Thus, those sensors could be fabricated with fewer materials, and could detect smaller concentrations of object molecules. The mechanical robustness of the nanotubes and the low buckling force increase the probe life along and minimizes damage during repeated hard crashes into substrates [63]. Among all the sensors used in our life, there are two most important and widely used sensors: gas sensors and mechanical sensors. Applying CNTs in gas sensors and mechanical sensors could improve their performance and decrease the cost at the same time. Additional features could be combined to make packaged functional sensors. The electrical resistance of SWCNTs has been found to change sensitively on exposure to gaseous ambient containing NO_2, NH_3, and O_2. By monitoring this change, the presence of gases could be detected. Results showed at least an order of magnitude faster than those currently available and they could be operated at room temperature or at higher temperatures for sensing applications [64].

1.5.1 Gas Sensors

Many materials have been utilized for commercial gas sensors, such as metal oxides, and conducting polymers. The advantage of metal oxides is high sensitivity, but their serious drawback is the high power consumption due to high resistance [65]. Conducting polymers could operate at room temperature with good sensitivity and reproducibility, but the effects of humidity and degradation by ultraviolet irradiation have hindered further practical

applications [66]. The CNT-based gas sensors have been considered because of the high surface ratio of CNTs. Nano-sized CNT-based gas sensors of the field-effect-transistor type have superb sensitivity due to drastic change in the electrical conductivity upon the adsorption of various gases [11]. However the application of CNT-based gas sensors is still limited by long recovery time and complex fabrication processes [67].

Gas sensor is one application of CNTs due to their inherent properties like high specific surfaces area (1580 m^2/g), small size (diameter is 1-100 nm), and good electrical and mechanical properties [68]. The CNT-based gas sensors have received considerable attention because of their distinctive properties such as fast response, high sensitivity, and low operating temperature [69]. The high specific surfaces of CNTs could improve the performance of electrode coated with CNTs [70]. This kind of electrode can be applied in gas sensors.

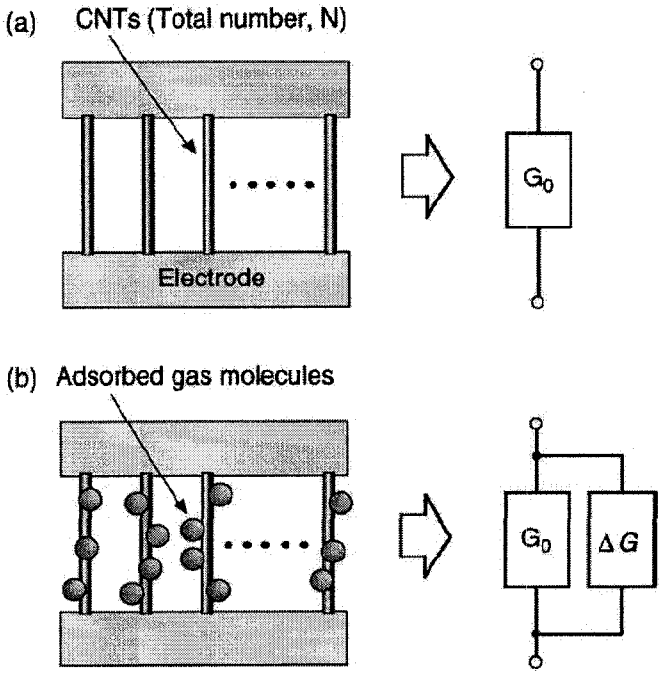

Figure 1-11 Equivalent circuit model of CNT gas sensor: (a) before adsorbing gases, (b) after adsorbing gases [69]

The CNT-based gas sensor structure can be indicated as the Figure 1-11. Many CNTs connect the two electrodes. The initial conductance of the gas sensor is G_o, which depends on the number of CNTs. [69]

$$G_o = N * g_o \quad (1\text{-}3)$$

Where N is the total number of CNTs, and g_o is the average conductance of one CNT. After adsorbing gases, the conductance of individual CNT is changed by Δg. For some oxidative gases, such as O_2, the conductance is increased as the positive-hole density increases due to electron transfer from p-type CNTs to oxidative gases molecules. For the reductive gases, such as H_2, the conductance is decreased due to the electron transfer to CNTs. The whole sensor conductance is changed by ΔG.

$$G = N * \Delta g \quad (1\text{-}4)$$

The total conductance of gas sensor after adsorbing is

$$G = G_o + \Delta G = N * (g + \Delta g) \quad (1\text{-}5)$$

The change of conductance ΔG can be measured for gases detection. The ΔG is dependent on the number of CNTs. This means that the sensor response depends on the amount of CNTs.

1.5.2 Mechanical Sensors

One kind of widely used sensors is mechanical sensors, which are used to measure force, strain, acceleration, and pressure. Those sensors include the accelerometer to control the airbag in automotive, pressure sensor to monitor the tire pressure, strain sensor to measure the strain in some mechanisms. The current widely used pressure sensors were

piezoelectric pressure sensors based on piezoelectric effect, which can be used to measure pressure, acceleration, strain or force by converting them into electrical signal [71]. Some other materials were also used as materials for pressure sensors, such as ceramic pressure sensor [72], semiconductor pressure-pulse sensor [73], and flexible membrane pressure sensor [74]. But those sensors have some drawbacks. The piezoelectric pressure sensors were sensitive and have large measurement range, but they are easy to be interfered by the environment change, such as temperature, humidity, and electric filed.

As CNTs have high strength and superb elasticity at the same time, they are one of the ideal materials to be used in mechanical engineering. The operating temperature and strength of CNTs compared with other materials is shown in Figure 1-12. In mechanical sensors, the resonators are conventionally made of silicon or silicon carbide [75]. For nano-sensors, silicon or silicon-nitride resonators may still be suitable to some extent [76]. However, because of the difficulty in manufacturing defect-free nano-scale resonators, the CNTs may be an ideal candidate material for nano-mechanical resonators [77]. With their ideal smooth surface, naturally large length/diameter ratio, and extraordinary mechanical and physical properties, CNTs offer the most attractive alternative material for nano-mechanical resonators. It was predicted that the fundamental frequencies of cantilevered or bridged SWCNTs could reach the level of 10 – 1500 GHz depending on the nanotube diameter and length [78]. This level of fundamental frequency is much higher than the highest frequency nano-mechanical resonator so far fabricated from silicon carbide using optical and electron-beam lithography [79].

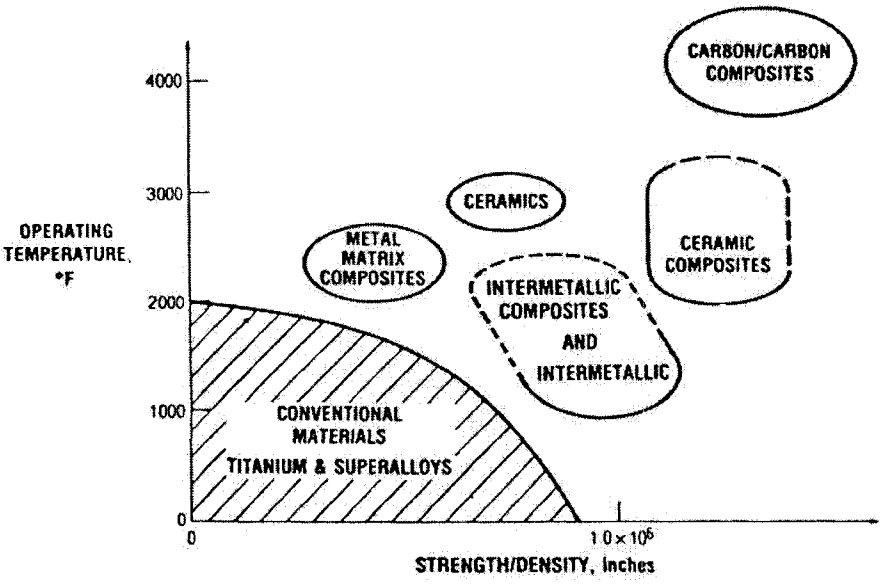

Figure 1-12 The temperature capability and strength of various material classes [80]

Some practical researches on CNT-based mechanical sensors have been performed. The CNTs were integrated in micro-cantilevers for application of tensile strain by positioning individual MWCNT on silicon oxide micro-cantilevers using nano-manipulation tools as shown in Figure 1-13 [81]. The effectiveness of CNT films was investigated in measuring multidirectional strain based on the electrical conductance changes with strains [82]. A CNT strain sensor for structural health monitoring was fabricated by mixing CNTs and polymer to improve the strain transfer, repeatability and linearity as shown in Figure 1-14 [83]. The modeling of CNTs at the atomistic scale was investigated, and cantilevered CNT-based mass sensor was also studied as shown in Figure 1-15. The CNTs are now being researched for use on automotive tires. A tiny sensor is able to monitor and report tire pressure to the driver while being able to withstand extreme temperature and vibrations [83].

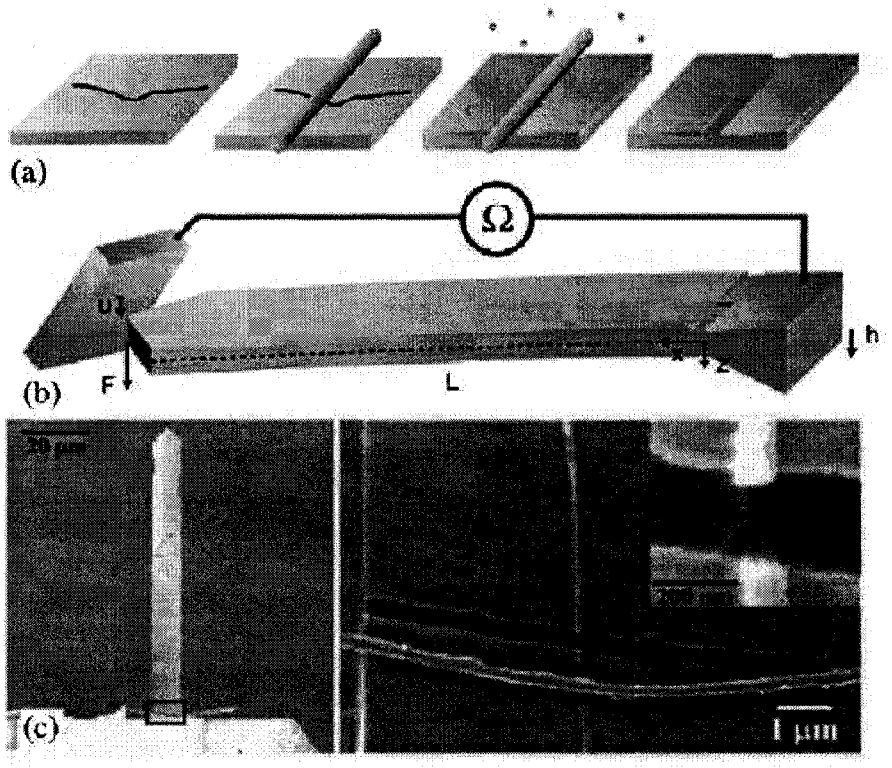

Figure 1-13 Micro-cantilever strain sensors [81]

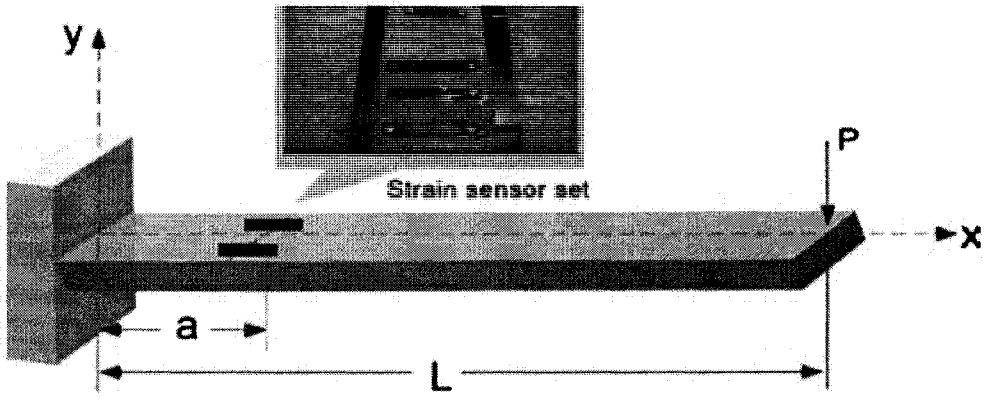

Figure 1-14 Strain sensors on cantilever for structural health monitoring [83]

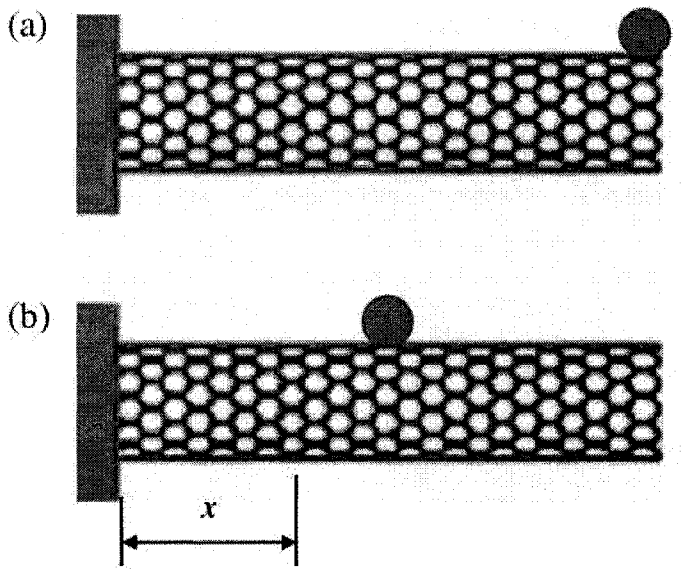

Figure 1-15 Cantilevered CNT resonators with an attached mass: (a) at the free end, and (b) at the middle [71]

1.6 Field Emission Display (FED)

The field emission display (FED) is a type of flat panel display using field emitting cathodes to bombard phosphor coatings as the light emissive medium. The FED is very similar to cathode ray tubes on the method of emission display, however FED is only a few millimeters thick, and instead of a single electron gun, the FED uses a large array of fine tips, with many positioned behind each phosphor dot, to emit electrons through a process known as field emission. Because of emitter redundancy, the FED does not display dead pixels like liquid crystal displays (LCD) even if 20% of the emitters fail. The FED could provide a flat panel technology that requires less power than existing LCD and plasma display technologies because they are energy efficient. They are cheaper to make since they have simpler structure and fewer components [84]. Figure 1-16 (a) shows the functions of the simplest form of a

display pixel. Micro tips are patterned on a matrix of electrodes in a vacuum housing as shown in Figure 1-16 (b) for large area display. The counter electrode is a glass plate coated with a conducting but transparent layer (conductive glass) and a phosphor layer. A voltage difference of a few kilovolts between the micro tips cathode and the glass plate results in field emission and the generation of light through excitation of the cathodoluminescent phosphor. An image can be obtained by addressing selectively the difference positions of the matrix [85]. The structure of FED is shown in Figure 1-17 [86].

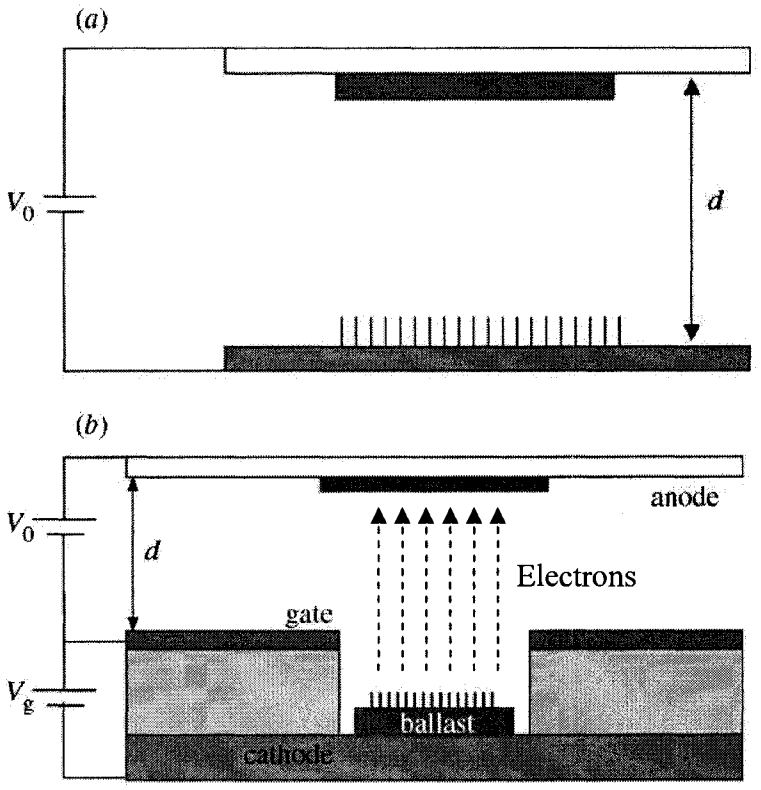

Figure 1-16 Schematic of the working principle of a field-emission display pixel: (a) diode structure, (b) triode structure with emitter tips array [85]

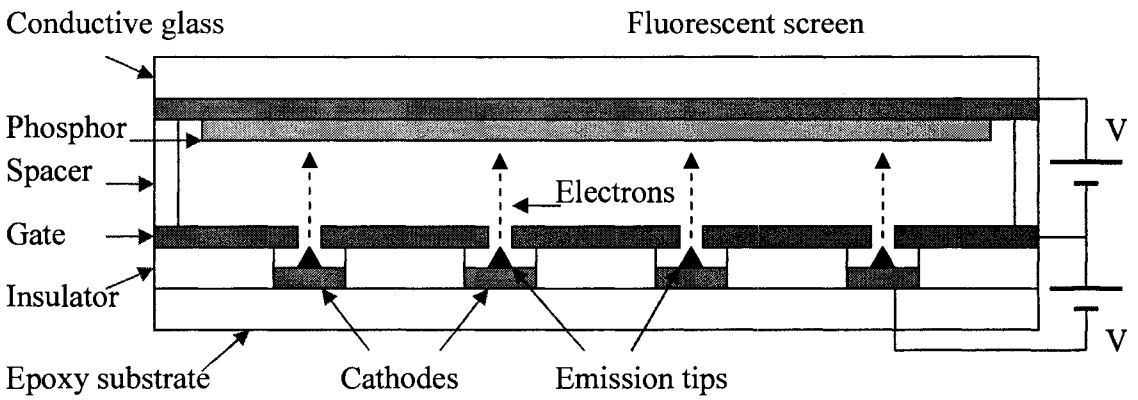

Figure 1-17 Schematic diagram of the field emission display structure

In conventional FEDs, micro tips made of refractory metals such as molybdenum have usually served as emission sources. When a voltage is applied between a gate electrode and a micro tip emitter, a strong electric field is generated at the apex of a micro tip. Such a high electric field induces electron emission from the micro tip. Emitted electrons are accelerated towards an anode and hit phosphor surface, giving rise to visible light illumination. Even the FEDs with micro tip possesses CRT-like display performances as well as well-established fabrication processes, they have been carped at a fault by their investment and production costs as high as those of thin film transistor liquid crystal displays since field emitter arrays are fabricated by conventional semiconductor processes [87]. Many kinds of materials have been tried to make the micro emitter, such as ZnO nanopins [88], amorphous diamond films [89], silicon tip arrays with diamond coating as shown in Figure 1-18 (a) [90], metal oxide semiconductor as shown in Figure 1-18 (b) [91], Si-doped AlN as shown in Figure 1-18 (c) [92]. Smaller emitter tips require lower voltage to send out electrons, so more research have been done to find proper materials to make small and sharp tips.

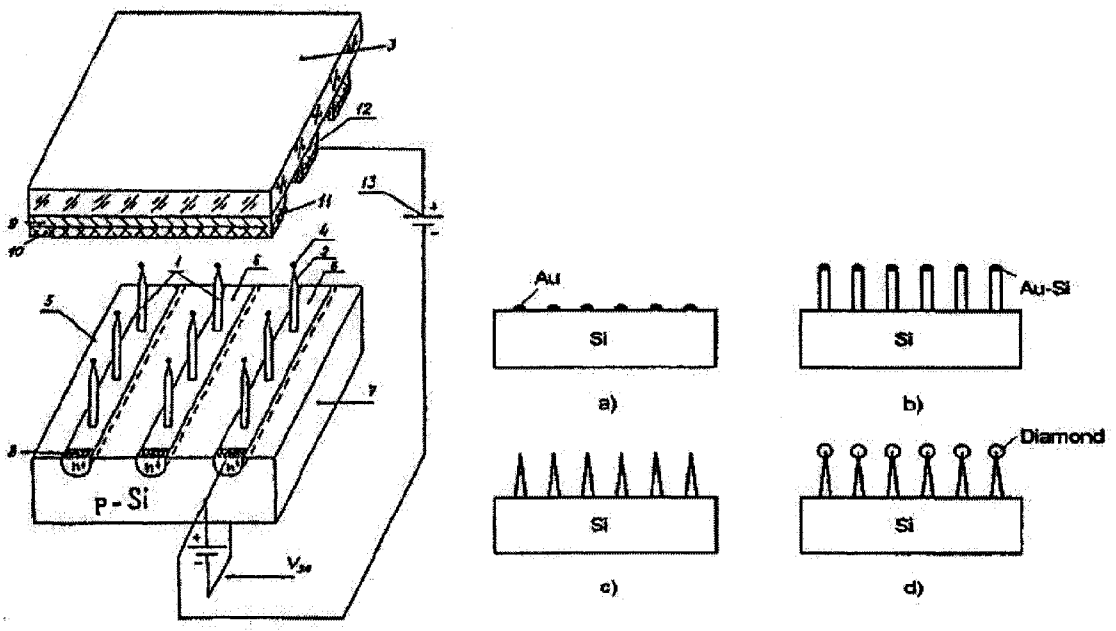

(a)

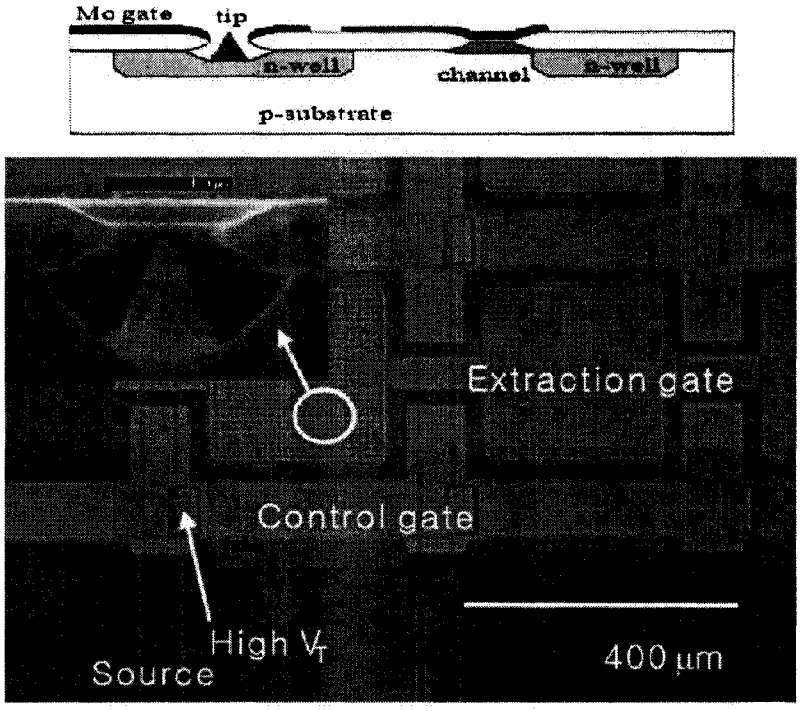

(b)

Figure 1-18 Schematic diagram of the field emission display structure using: (a) array of diamond-coated Si tips [90], (b) metal oxide tips [91]

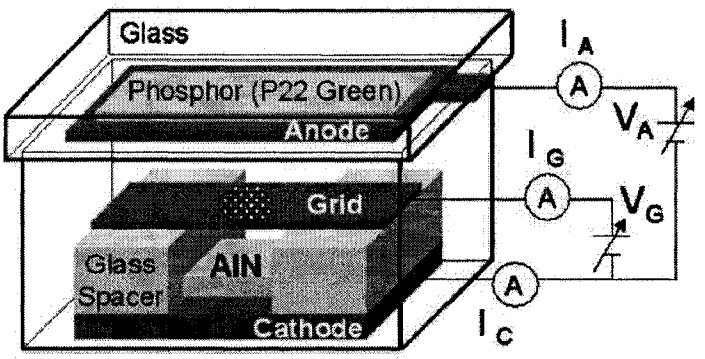

(c)

Figure 1-18 continued: (c) the heavily Si-doped AlN [92]

Recently, the CNTs have been spotlighted as one of promising alternatives for new electron emission sources due to their superior emission properties and simple fabrication processing. The CNTs are expected to make it possible to produce FEDs with low cost, low power consumption, scalability, etc [93-100]. The CNTs have several advantages over other field-emitting materials. In contrast to commonly used emitters such as tungsten, the CNTs are built by covalent bonds. Each carbon atom is bond to three other carbon atoms by a covalent sp^2 bond. As a result, the activation energy for surface migration of the emitter atoms is much larger than tungsten electron source. Therefore, the tip can withstand the extremely strong fields (several V/nm) needed for field emission. When compared with other film field emitters such as diamond or amorphous carbon structures, the CNTs show high aspect ratio, small radius of curvature of the cap and good conductance. Moreover, the CNTs are chemically inert, and react only under extreme conditions or at very high temperature. Besides, carbon has one of the lowest sputter coefficients, which is an advantage since an electron source is usually bombarded by positive ions. All of above, CNTs are proper materials for emitter tips of field emission displays.

Basically, there are three methods for building field-emission devices from CNTs: CNTs can be mounted by means of nano-manipulation, devices can be made from bulk samples of CNTs, and CNTs can be grown directly on desired positions [86]. The mounting CNTs was performed under high resolution microscope such as scanning electron microscope, thus it is difficult to produce a batch of tips on large scale area. The second approach is to realize films either by pressing, printing or spraying CNTs powder on a support, and the CNTs can be fixed tightly using carbon glue or paste. Even though this technique is simple, the field emission is often dominated by a few CNTs, and the emission site density is very low. This is a drawback for display application. The third way is to grow CNTs directly on patterned metallic catalyst using chemical vapor deposition. This means that patterned CNTs films can be formed directly from growth, and the morphology of the film can be controlled to a great extent. The density of CNTs can be adjusted with the amount of catalyst on the substrates. The diameter of the CNTs depends directly on the diameter of the catalyst particle that seeds the growth. The diameter can be controlled by dispersing particles of well-defined size into an inert matrix (such as Al). But the current techniques to grow CNTs all require high temperature which may damage the epoxy substrates of cathode plate. Some other methods were also tried to make CNTs tips, such as electrophoresis deposition of CNTs as shown in Figure 1-19 [101]. But the CNTs cannot adhere on the electrodes very well and more techniques were needed for post-process.

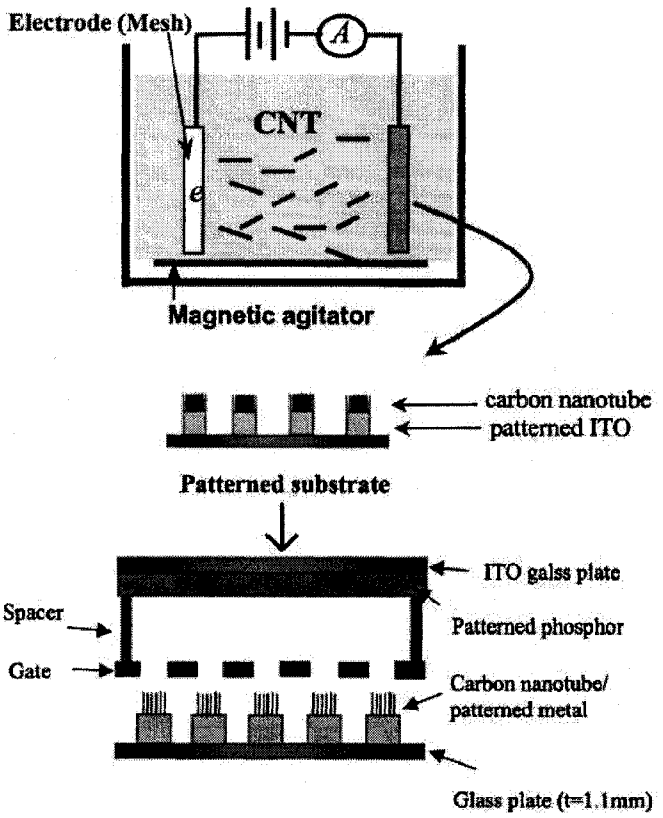

Figure 1-19 Schematic diagram of the electrophoresis process for the selective deposition of CNTs [101]

The assembled FED unit is shown in Figure 1-20. The display unit was assembled using two printed circuit boards as shown in Figure 1-20 (a). One board was etched to leave some copper strips as cathode electrodes, so it may be called the cathode plate. The micro emitter tips, such as CNTs, were grown on the cathode electrodes. On another board, holes were drilled to form extracting aperture gate, so this board may be called the gate electrode plate. The cathode plate was separated from the gate electrode plate using an insulating spacer with thickness of 200 μm. The phosphor screen was placed about 3.5 mm away from the gate electrode plate. Sometimes, a third plate made of metal with apertures for focusing was inserted between the gate electrode plate and the phosphor screen [86].

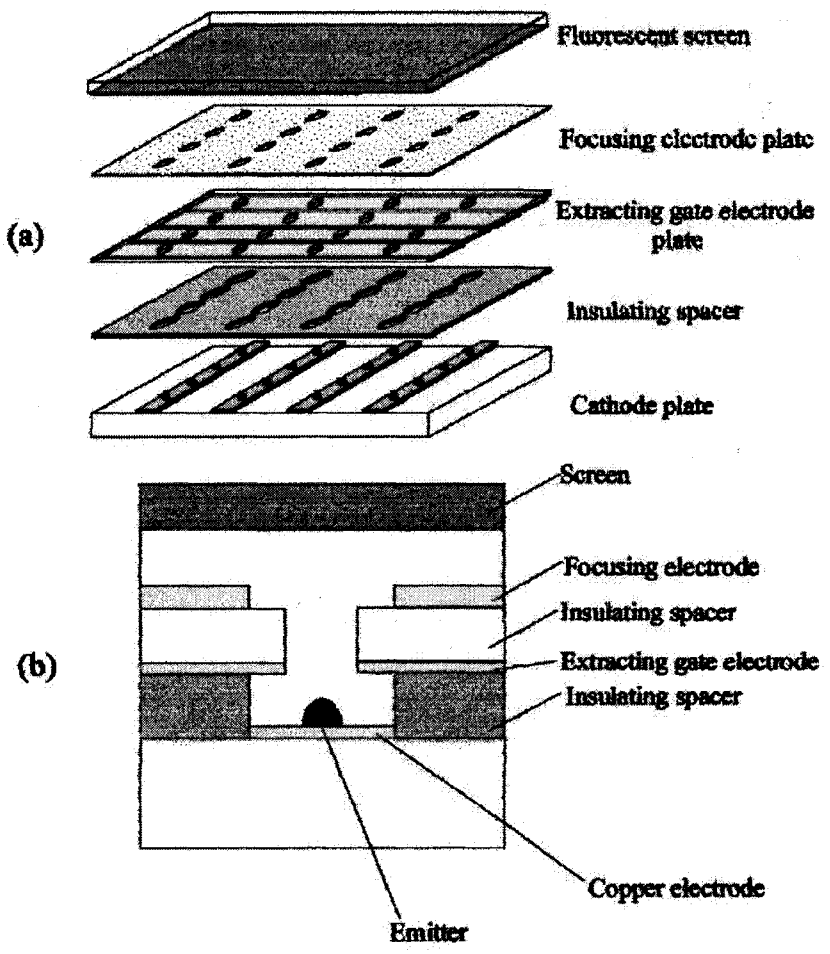

Figure 1-20 Assembled FED display unit: (a) components used to assemble the FED unit, (b) cross-section of a pixel of the FED unit [86]

1.7 Nano-Electro-Mechanical System (NEMS)

Nanotechnology is the science and technology dealing with the world of nano-scale objects. A nanometer is, by definition, 10^{-9} of a meter. A nanometer is equal to the length of 10 hydrogen atoms in a line. Nanotechnology is applied to fabricate devices with atomic or molecular scale precision. Devices with minimum feature sizes less than 100 nanometers (nm) are considered to be products of nanotechnology. The nano-scale marks the nebulous

boundary between the classical and quantum mechanical worlds; thus, realization of nanotechnology promises to bring revolutionary capabilities. Fabrication of nano-machines, nano-electronics and other nano-devices will undoubtedly solve an enormous amount of the problems faced by mankind today. Nano-science is an interdisciplinary field that seeks to bring about mature nanotechnology. Focusing on the nano-scale intersection of fields such as physics, biology, engineering, chemistry, computer science and more, nano-science is rapidly expanding [102]. The Figure 1-21 shows molecular gears - two "Fullerene Nano-gears" with multiple teeth from a NASA computer simulation.

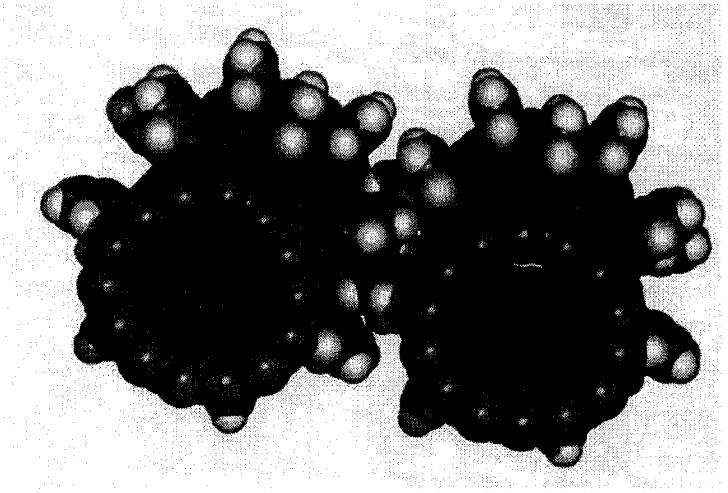

Figure 1-21 Fullerene molecular gears from a NASA computer simulation [103]

In fact, nanotechnology was used long before it was defined. One example is carbon black, which was produced by Degussa and used as the substance that makes car tires black and improves the wear resistance of the rubber, since the 1920s. Of course they were not aware that they were using nanotechnology as they had no control over particle size and even any knowledge of the nano-scale. Many of the working with nanotechnology is simply

applying knowledge of the nano-scale to existing industries, whether it is improved drug delivery mechanisms for the pharmaceutical industry, or producing nano-clay particles for the plastics industry. Nanotechnology is an enabling technology rather than an industry in its own right. Nanotechnology is a fundamental understanding of how nature works at the atomic scale. New industries will be generated as a result of this understanding. [104]

With nanotechnology, a large set of materials and improved products rely on the change in the physical properties when the feature sizes are shrunk. Nano-particles take advantage of their dramatically increased surface area to volume ratio. When brought into a bulk material, nano-particles can strongly influence the mechanical properties, such as the stiffness or elasticity. Traditional polymers can be reinforced by nano-particles resulting in novel materials such as lightweight replacements for metals. Therefore, an increasing societal benefit of such nano-particles can be expected. Such nanotechnology-enhanced materials will enable a weight reduction accompanied by an increased stability and an improved functionality. Now, nanotechnology has been widely applied in the following fields: medicine (diagnostics, drug delivery, tissue engineering), chemistry and environment (catalysis, filtration), energy (reduction of energy consumption, increasing the efficiency of energy production, the use of more environmentally friendly energy systems, recycling of batteries), information and communication (novel semiconductor devices, novel optoelectronic devices, displays, nano-logic, quantum computers), consumer goods (food, household, optics, textiles, cosmetics) [105].

Nano-science and nanotechnology only became possible in the 1910's with the development of the first tools to measure and make nanostructures. But the actual development started with the discovery of electrons and neutrons that showed scientists that

matter can really exist on a much smaller scale than what we normally think of as small. The Atomic Force Microscope (AFM) and the Scanning Tunneling Microscope (STM) are two early versions of scanning probes that launched nanotechnology [106]. More powerful inspection tools such as SEM and TEM have been developed to show clearer images of smaller nano-particles of nanometers size.

MEMS is the micromachining techniques initially developed in the Integrated Circuit (IC) industry. Many MEMS processes have been developed to produce complex structures, devices and systems on the scale of micrometers and even smaller. Those MEMS techniques combine mechanisms, electronic circuit, and other structures such as optical component into very small devices. At the same time, cost per unit was decreased because of applying well-developed IC techniques and manufacturing batch production. Specifically, MEMS technology has enabled many types of sensors, actuators and systems to be reduced in size by orders of magnitude, while often even providing improved sensor performance (e.g. inertial sensors, optical switch arrays, biochemical analysis systems etc) [10].

Photolithography is the single most important process that enables ICs and MEMS to be produced reliably with microscopic dimensions and in high volume. The essentials of the photolithographic processes are illustrated in Figure 1-22. MEMS have also driven the development and refinement of other micro-fabrication processes such as surface micromachining (sacrificial layer) and bulk micromachining (deep reactive-ion etching (DRIE)). Figure 1-23 illustrates a typical surface micromachining process removing the underlying film by sacrificial layer. DRIE is a dry etch process that can be used to etch deeply into a silicon wafer while leaving vertical sidewalls and is independent of the crystallographic orientation as shown in Figure 1-24.

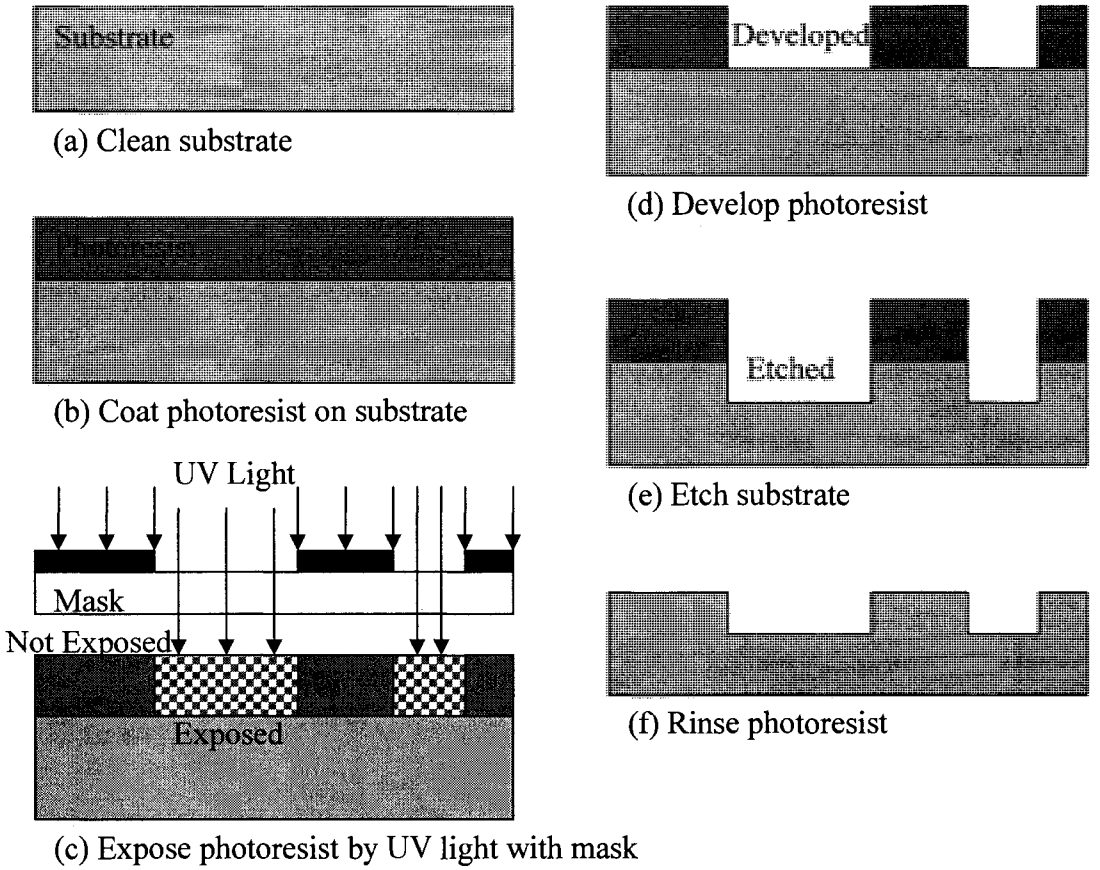

Figure 1-22 Photolithographic process

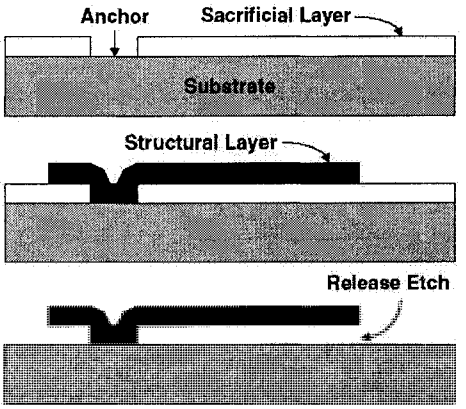

Figure 1-23 Surface micromachining and the sacrificial layer technique [106]

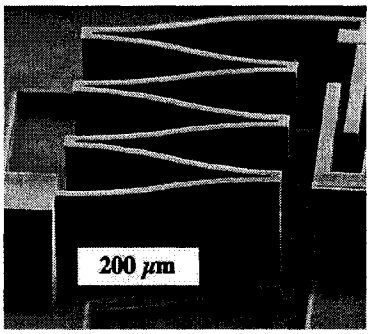

Figure 1-24 Micro-flexure created by vertical etching through a wafer with DRIE [107]

Some gas-sensitive materials can react with some kinds of gases very easy and fast. By applying those materials with electronic circuit, special gases can be detected when they react. Figure 1-25 shows an example of a polymeric impedance-based gas sensor that uses an SU-8 micro-well structure. In order to decrease prices, some micro-fabrication facilities provide service to fabricate many devices from different customers on one wafer as shown in Figure 1-26.

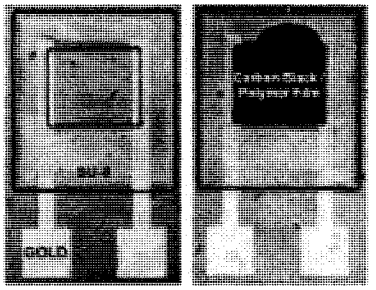

Figure 1-25 Micro-fabricated polymer carbon-black gas sensor with SU-8 micro-well [108]

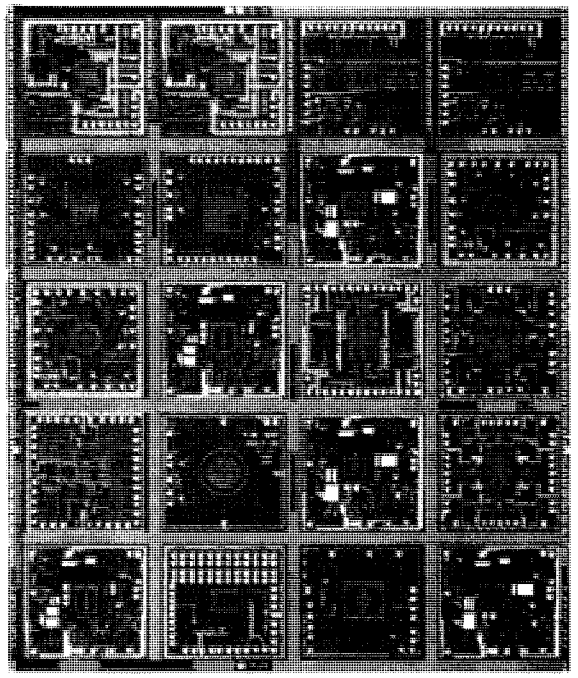

Figure 1-26 Several dice produced with the Analog Devices iMEMS foundry process [109]

There is a continuing demand for reducing the size of MEMS devices. The significance of the miniaturization goes well beyond just smaller size and reduced weight. Miniaturization also enables increasing robustness, reducing energy consumption, and integrating more functions in even smaller packages. With the advancements in fabrication technologies, the components of devices can now be downsized to the nanometer scale, and thus NEMS can be developed. The core parts of NEMS were nanometer scale. While design and fabrication capabilities are still primitive from the applications perspective, NEMS has become a major alternative in the development of nanotechnology [75].

Chapter Two

2 Synthesis of Carbon Nanotubes

The synthesis of CNTs by hot filament assisted CVD system is discussed in this chapter. The hot filament CVD system is illustrated in detail. The growth processes of CNTs are described step by step. The samples of CNTs are characterized by SEM, TEM, RAMAN and XRD, and the results are analyzed for optimization. The growth conditions, such as temperature, catalyst, gases, and substrates, are discussed.

2.1 Introduction

CNTs have been synthesized by many methods such as arc deposition, CVD, laser ablation and plasma deposition. The CVD method is possibly one of the most widely used methods for CNTs synthesis because of its high product yield and large-scale capability [24, 25]. Most of the CVD methods including plasma-enhanced CVD and thermal CVD synthesizing CNTs require a high feeding rate of source gases, high pre-heating temperature, and additional power sources such as plasma and lasers [68]. In this research, the CNTs were synthesized using a hot filament assisted CVD system at low gas flow rate, low temperature and atmospheric pressure. Methane was used as the source of carbon because it can be decomposed into carbon radical species effectively using the hot filament. In this research,

the effects of many conditions on the growth of CNTs by the above hot filament CVD system were investigated.

The whole process to synthesize CNTs is shown in Figure 2-1: prepare the substrates (coate catalyst on substrates and make pattern of catalyst for application), and grow CNTs by CVD.

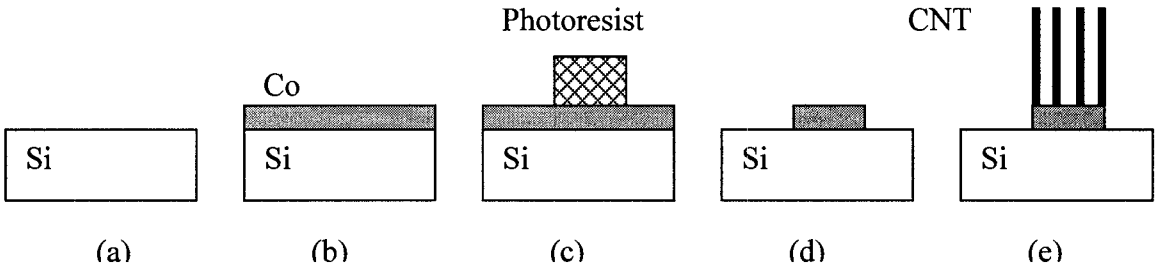

Figure 2-1 Processes to grow CNTs: (a) Si substrate, (b) Si coated with Co by PVD, (c) Photolithography, (d) Catalyst pattern made by etching Co, and (e) Grow CNTs by CVD

The first step of experimental is to prepare substrates for growing CNTs. The silicon wafer and glass coated with catalyst were used as the substrates. The metallic catalyst, such as Co, Ni or Fe, was coated on the silicon wafer or glass by PVD. Depending on the amount of catalyst wire used in PVD and the distance between silicon wafer or glass substrates and filament of PVD, the thickness of catalyst film coated on substrates range from 0.5 nm to 50 nm. By photolithography and etching, some catalyst patterns were made on the substrates. Sometimes the CNTs were grown directly on the catalyst without pattern.

2.2 Experimental

The CNTs were deposited with carbon source (CH_4) brought by carrier gas (Ar or 5% H_2 in Ar) to the reaction zone on catalyst (Co, Ni or Fe) by thermal CVD with hot filament. The metallic catalysts were coated on silicon substrates by PVD. Tungsten filaments were used in the CVD tube to achieve high temperature up to 2000 ^{o}C to decompose CH_4 into carbon species. The CNTs were analyzed by SEM, TEM, Raman spectroscopy and XRD.

2.2.1 Hot Filament Assisted CVD System

The hot filament CVD system is made up of a quartz tube, a furnace with three heating coils, a hot filament, and the power supply. The CVD system with filament was shown in Figure 2-2. A Lindberg/Blue 3-Zone Tube Furnace consisted of a quartz tube surrounded by three groups of heating coil is used to contain and heat the substrates. The diameter of the quartz tube is 7 cm. The length of the quartz tube within heating zones is 120 cm. The furnace can be programmed to heat the samples step by step using UP150 Program Temperature Controller. Two kinds of gas CH_4 and Ar (or 5% H_2 in Ar) were mixed and passed through the quartz tube. The filament made of tungsten wire was shaped into a coil. The diameter of tungsten wire is 0.5 mm. The filament in the 100 W bulb was also used directly. The voltage of 10 - 30 V was applied on the filament.

The CH_4 and Ar (or H_2) gases were mixed and passed into the quartz tube. When the gases passed through the hot filament, the CH_4 was decomposed into carbon radical species and hydrogen at around 2000 ^{o}C temperature. The Ar (or H_2) carried the carbon radical species to the substrates, and the CNTs were grown on the catalyst on the substrates with those carbon species.

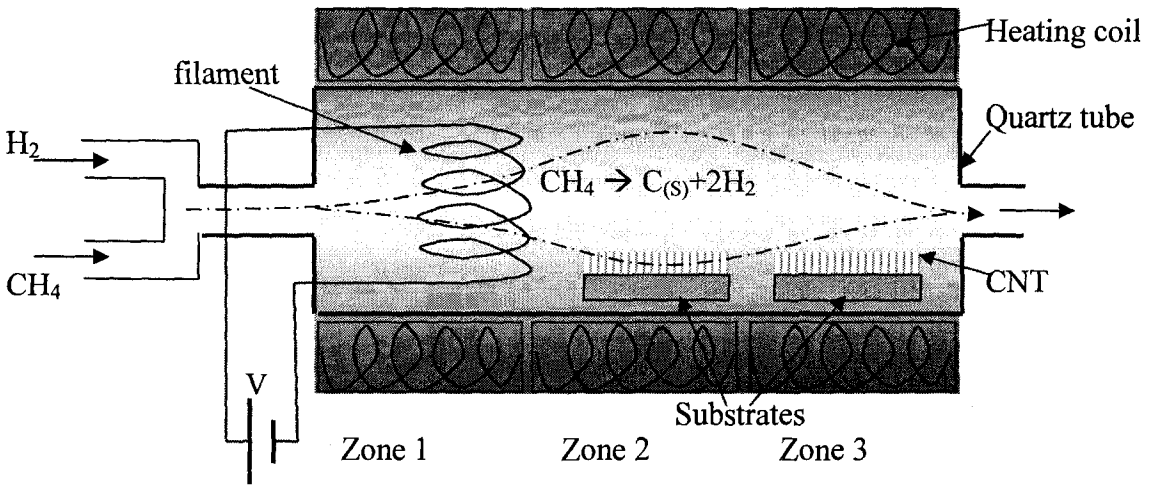

Figure 2-2 Schematic diagram of the CVD system with hot filament for CNTs growth

2.2.2 Preparation of Substrates

The substrates were prepared by coating Co, Ni and Fe metal or their oxide and salt as catalyst on silicon wafer or glass. Co, Ni and Fe were selected as catalyst because of their high yields of CNTs [110]. The catalyst metal was coated on the silicon or glass by PVD. Their oxides were coated by applying their nitride on substrates and then being annealed to get oxides. The substrates were rinsed by acetone and distilled water and dried before coating. Some catalyst films coated on substrates were etched to get micro pattern or gas sensor pattern as shown in Figure 2-3. The length of micro-pattern in Figure 2-3 is 2 micrometer. The CNTs were grown on those micro patterns. Some substrates with catalyst were treated with plasma etching, hydrochloric acid, hydrofluoric acid, and then rinsed by distilled water and dried.

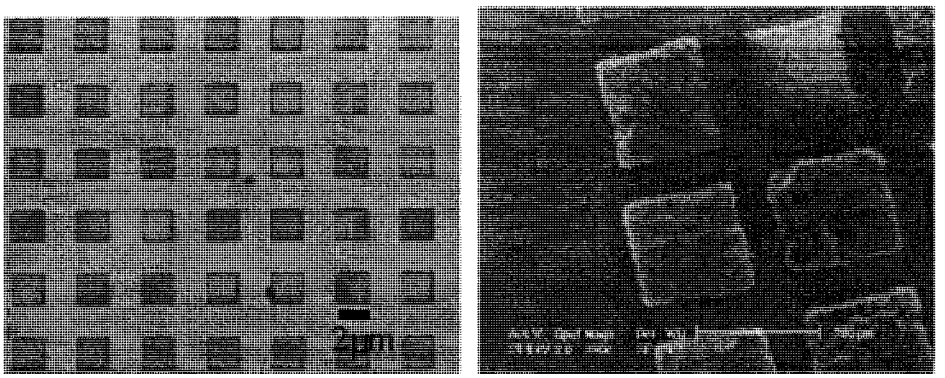

(a) (b)

Figure 2-3 (a) micro patterns array on substrate, (b) CNTs grown on patterns

The thickness of the catalyst thin film coated by PVD can be explained by Figure 2-4 (a) and calculated by formula 2-1, 2-2, 2-3 and 2-4. The length of catalyst wire to be coated is l, and the diameter is d. The distance between the substrate and catalyst is D. The thickness of the thin film is t. So the volume of catalyst wire is given as

$$V = \frac{\pi d^2 l}{4} \tag{2-1}$$

By assuming the catalyst wire is coated on a ball with diameter of D/2, the volume of the thin film is calculated as

$$V_2 = 4\pi D^2 t \tag{2-2}$$

As the catalyst is all coated to form the thin film, their volumes are equal

$$V = V_2 \tag{2-3}$$

By combining equation 2-1, 2-2 and 2-3, the thickness is given as

$$t = \frac{d^2 l}{16 D^2} \tag{2-4}$$

The diameter of catalyst wire is 0.25 or 0.5 mm. By changing the length of catalyst

wire, and distance between catalyst and substrates, the thin film thickness can be controlled. The thickness of the catalyst film can be measured by AFM to scan the edge area of the catalyst film as shown in Figure 2-4 (b). The typically used thickness is listed as table 2-1.

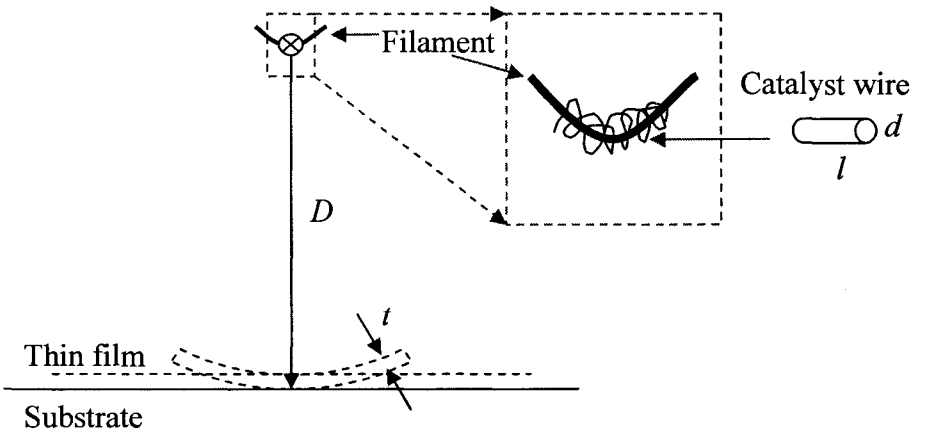

(a)

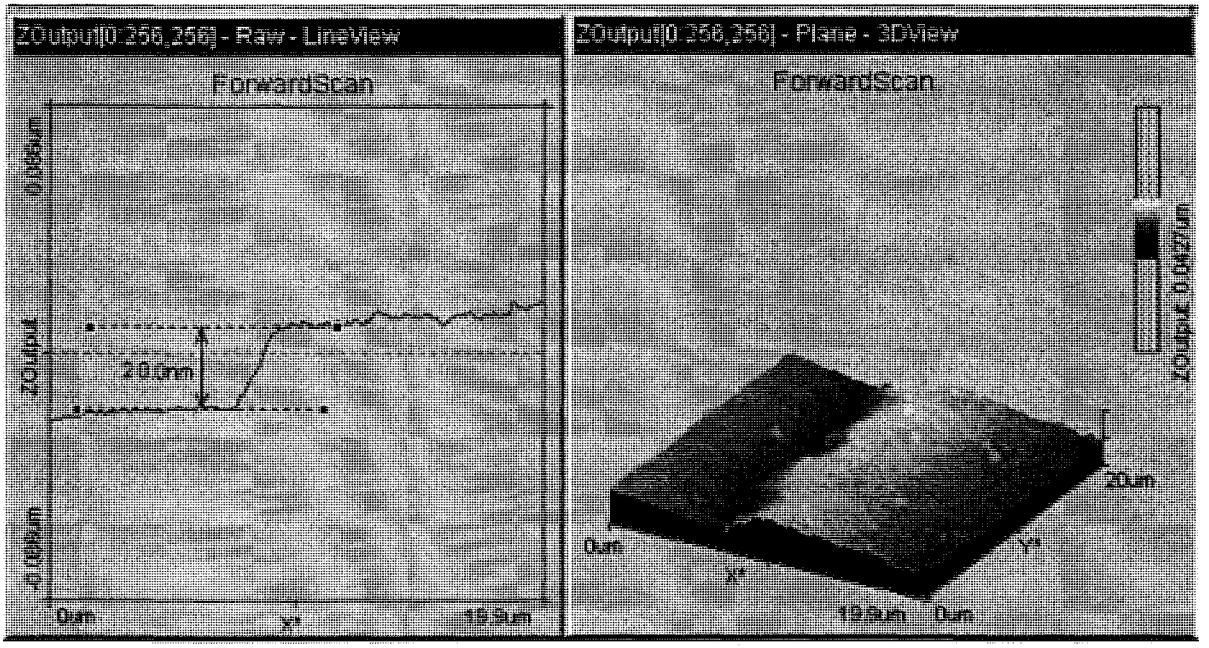

(b)

Figure 2-4 Catalyst film thickness: (a) calculate thickness of Co film coated by PVD, (b) AFM image to measure thickness of Co film (the left image shows the thickness of 20 nm)

Table 2-1 Thickness of catalyst film coated on substrates by PVD

Catalyst diameter - *d* (mm)	Catalyst length - *l* (mm)	Distance - *D* (cm)	Film thickness - *t* (nm)
0.25	5	5	7.8
0.25	10	10	3.9
0.25	10	15	1.7
0.25	20	10	7.8
0.25	20	15	3.5
0.5	20	10	31.2
0.5	10	10	15.6
0.5	10	15	6.9
0.5	10	20	3.9

2.2.3 Synthesis Processes of Carbon Nanotubes

The substrates were placed at the center (zone 2) and end (zone 3) of the quartz tube in the CVD. The temperatures of zone 1 and 2 were raised to 400 - 900 °C, and the temperature of zone 3 was 100 °C lower than zone 1 and 2 or the same. The sequences to grow CNTs are shown in Figure 2-5.

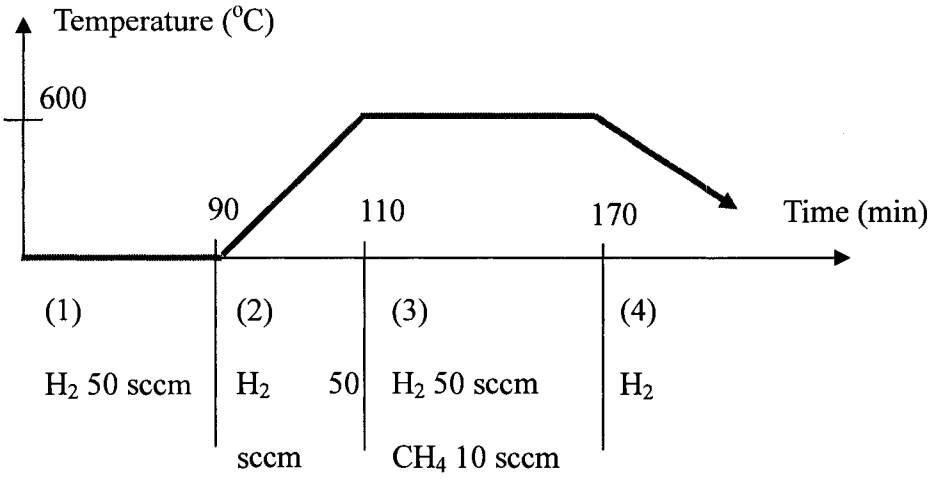

Figure 2-5 Sequences to synthesize CNTs

Sequences:

(1) Pass CH_4 at flow rate of 50 standard cubic centimeters per minute (sccm) for 5 min and H_2 (or Ar) 50 sccm for 60 min; (exhaust air from pipes to clean gas pipes, and clean CVD quartz tube)

(2) Pass H_2 (or Ar) 50 sccm, turn on CVD and run the program to heat furnace to growth temperature (400 - 900 °C); (take about 30 min, preheat substrates)

(3) Apply 10 - 30 V voltage on filament until it was red and approached white color (filament temperature was about 1500 °C ~ 2000 °C), pass H_2 (or Ar) 50 sccm and CH_4 5 sccm, maintain furnace at growth temperature (400 - 900 °C), keep those conditions for 0.5 - 1.5 hrs;

(4) Turn off filament and furnace, close CH_4, and pass H_2 (or Ar) until the system cool down to room temperature.

In order to compare the synthesis of CNTs at low temperature with that at high temperature, the experiment was repeated at the same condition by changing only the temperature of the reaction area (zone 3) to 450 °C, 500 °C, 600 °C, 700 °C, 800 °C and 900 °C. Fe, Ni and Au were also used as catalyst for growing CNTs.

2.3 Characterization and Discussions

After the CVD synthesis, the samples grown with CNTs were characterized by SEM (Philips XL30 FEG SEM), high-resolution TEM (JEOL 3011 High Resolution Electron Microscope), Raman spectroscopy and XRD. SEM was used to analyze the samples morphology, and HR-TEM was used to inspect the CNTs nanostructure. Raman and XRD were used to determine the CNTs.

The CNTs were found on the samples coated with Co, Fe, Ni and Au at low and high temperature. It was found that the CNTs could be formed at as low as 450 °C.

2.3.1 Scanning Electron Microscope (SEM)

With the SEM (Philips XL30 FEG SEM), the samples can be magnified up to 100,000 times. The range of object size is from 5 nm to 100 micron. The SEM specimens were prepared by mounting the silicon wafers coated with CNTs on the support with carbon tape.

The CNTs were found on some samples, but sometimes there was nothing deposited when the substrates position, furnace temperature or filament voltage were changed. There was no CNTs grown on the substrates put at the center (zone 2) of the quartz tube under temperature 900 °C whether it was coated with Co, Ni or Fe as shown in Figure 2-6. There was only catalyst particles left on the silicon wafer surface. At the same conditions as stated

above, the CNTs were found on the samples kept at the end (zone 3) of the quartz tube under 800 °C temperature as shown in Figure 2-7. These samples were made under the same conditions: Ar 50 sccm, CH_4 5 sccm, and the filament voltage of 10V for 0.5 hr. When the temperatures of zone 1 and 2 were changed to 800 °C and the temperature of zone 3 was changed to 700 °C, CNTs were grown on all samples at both positions. Figure 2-8 is the SEM image of CNTs grown on Ni catalyst at the center of quartz tube under 800 °C. The Ni catalyst substrate was treated with plasma etching. When the temperatures were decreased to under 500 °C, it was difficult to deposit CNTs. The CNTs grew faster at the end of the quartz tube than at the center. When the CH_4 flow rate was increased to 10 sccm, CNTs also grew faster but more amorphous carbon was found. It was also observed that the CNTs on the Ni catalyst (Figure 2-7 (b)) were longer than those on the Co catalyst (Figure 2-7 (a)) when substrates were put at the same position. So under the same conditions and position, CNTs grow faster on the Ni catalyst than Co catalyst at temperature 800 °C with a hot filament.

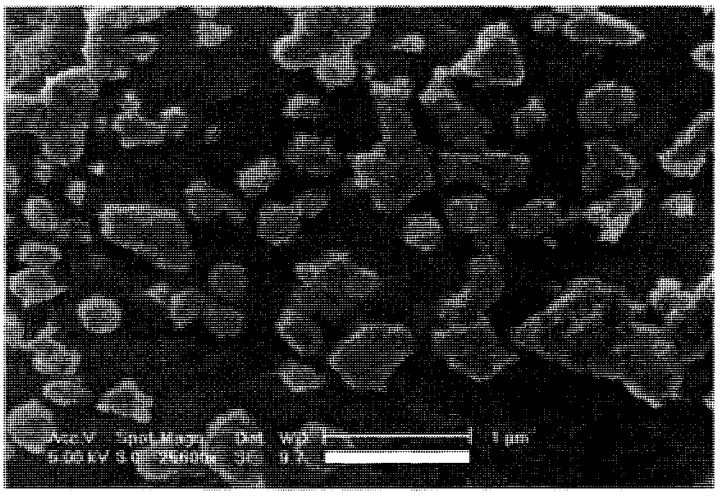

(a)

Figure 2-6 SEM images: catalyst (without CNTs) on the samples at the center of quartz tube under 900 °C: (a) Co catalyst

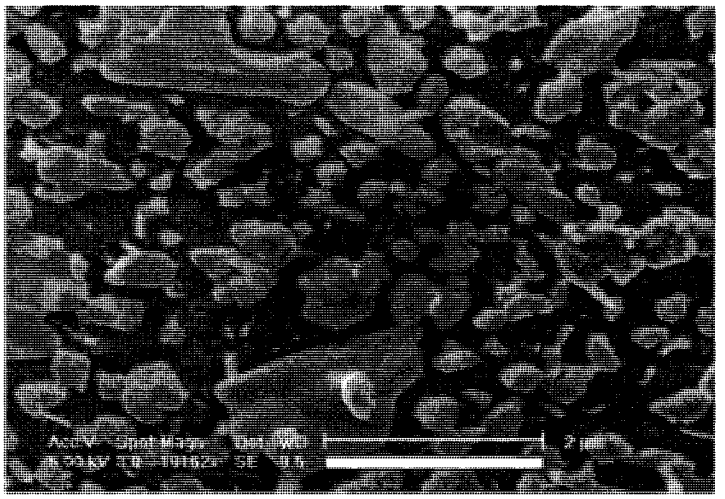

(b)

Figure 2-6 continued: (b) Ni catalyst

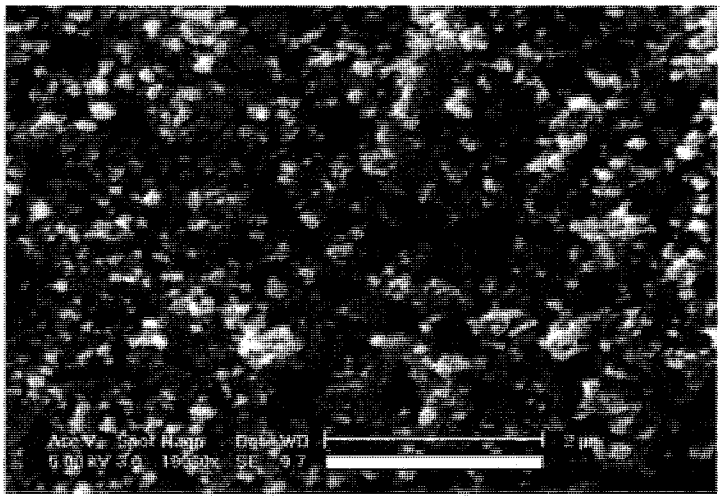

(a)

Figure 2-7 SEM images of CNTs on the samples at the end of quartz tube under 800 °C: (a) Co catalyst

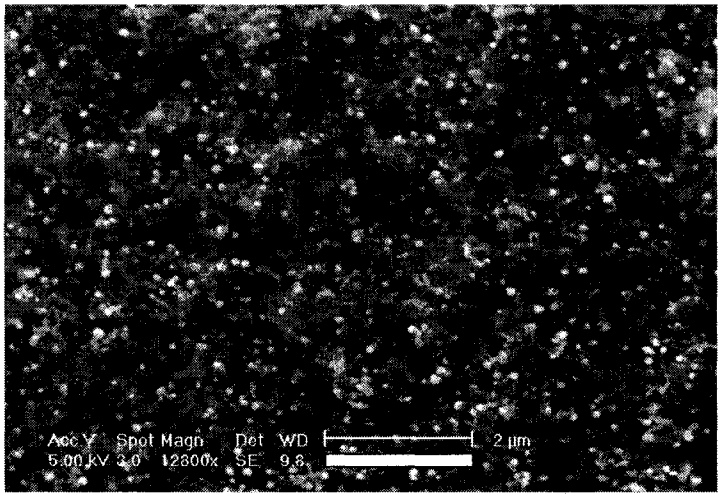

(b)

Figure 2-7 continued: (b) Ni catalyst

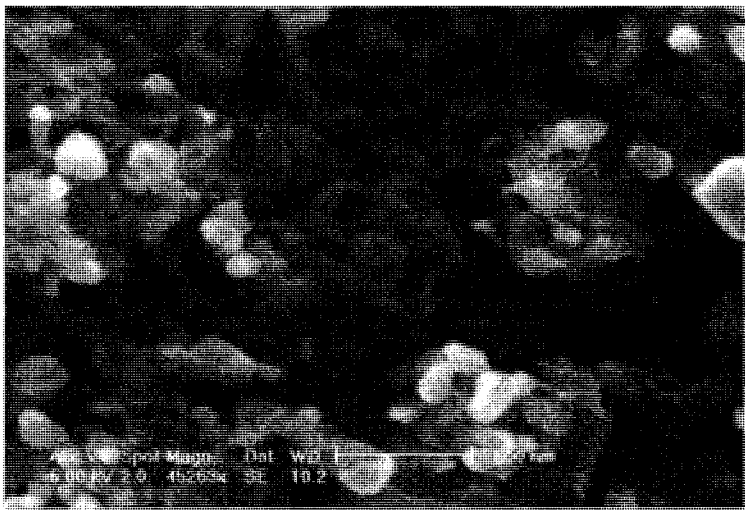

Figure 2-8 SEM images of CNTs on the Ni catalyst substrates treated with plasma and kept at the center of quartz tube under 800 °C

The SEM pictures in Figure 2-9 show the CNTs grown on cobalt catalyst pattern as shown in Figure 2-3 for 1 hr at the conditions: Ar 55 sccm, CH_4 5 sccm, filament voltage of 12V, furnace at 800 °C, and kept at the end of the quartz tube. When the filament voltage was increased, the color of filament changed from red to white, and the temperature was

increased accordingly up to 2000 °C. The filament with a higher temperature can decompose more CH_4 into carbon, and the CNTs can grow longer and faster with sufficient carbon source. Some CNTs observed from Figure 2-9 (a) were as long as 12 μm. Some amorphous carbon besides CNTs was also found in Figure 2-9 (b). As observed from Figure 2-9 (c), the diameters of CNTs were from 10 nm to 150 nm. The catalyst particles were found at the top of CNTs, and some of them were a little bigger than the diameters of CNTs. By changing the filament voltage and deposition time, the growth of CNTs can be controlled. By synthesizing the CNTs on the catalyst pattern, the CNTs bridged over the metal electrodes connected to the external measuring instruments [111]. The CNT-based sensors can utilize the electrical conductance change caused by the gas adsorption or mechanical deformation as the electrical readout. This means that the sensor response is dependent on the amount of CNTs. More CNTs provide higher sensitivity. [30]

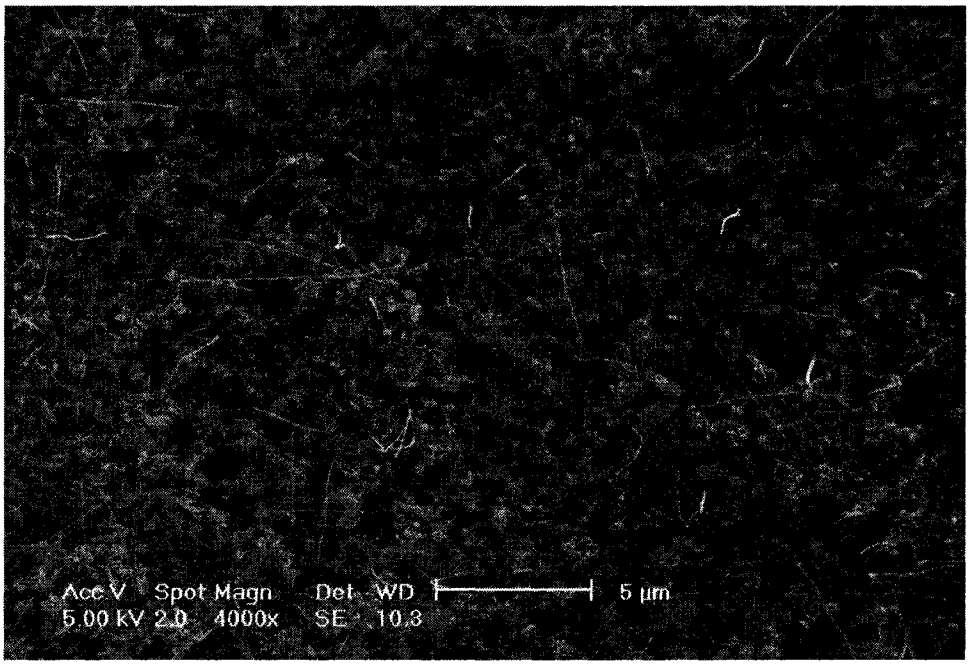

(a)

Figure 2-9 SEM images of CNTs on Cobalt catalyst pattern at different magnification

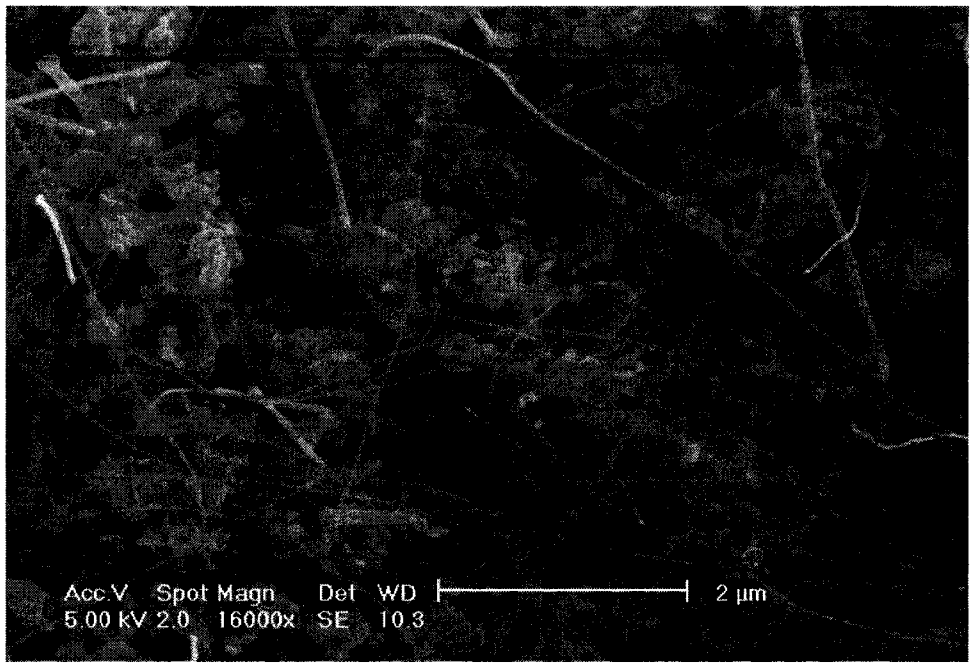

(b)

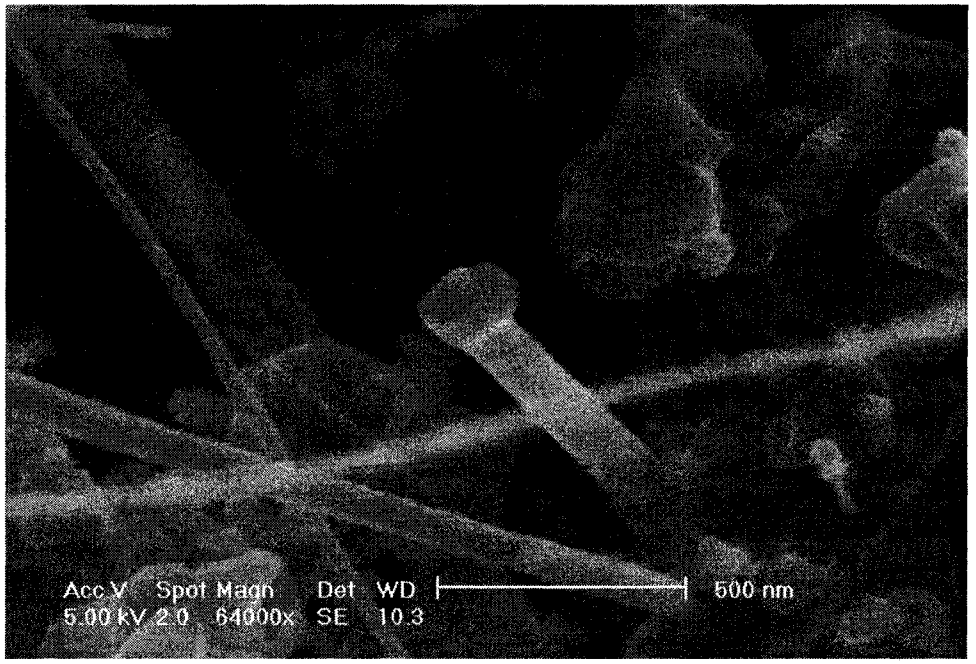

(c)

Figure 2-9 continued

Figure 2-10 is the SEM picture taken from the top of CNTs array. The diameters of those CNTs are uniform. They are perpendicular to the substrate. Figure 2-11 is the SEM

picture showing CNTs grown on micro pattern. The smallest width of the micro pattern is about 1 micron.

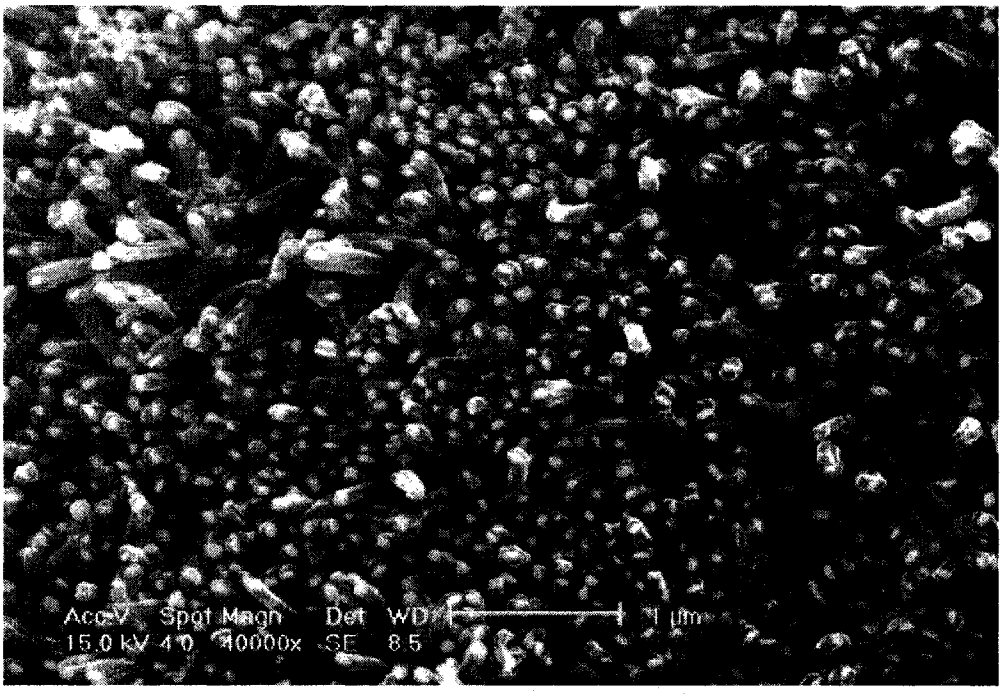

Figure 2-10 SEM image of top view of CNTs array

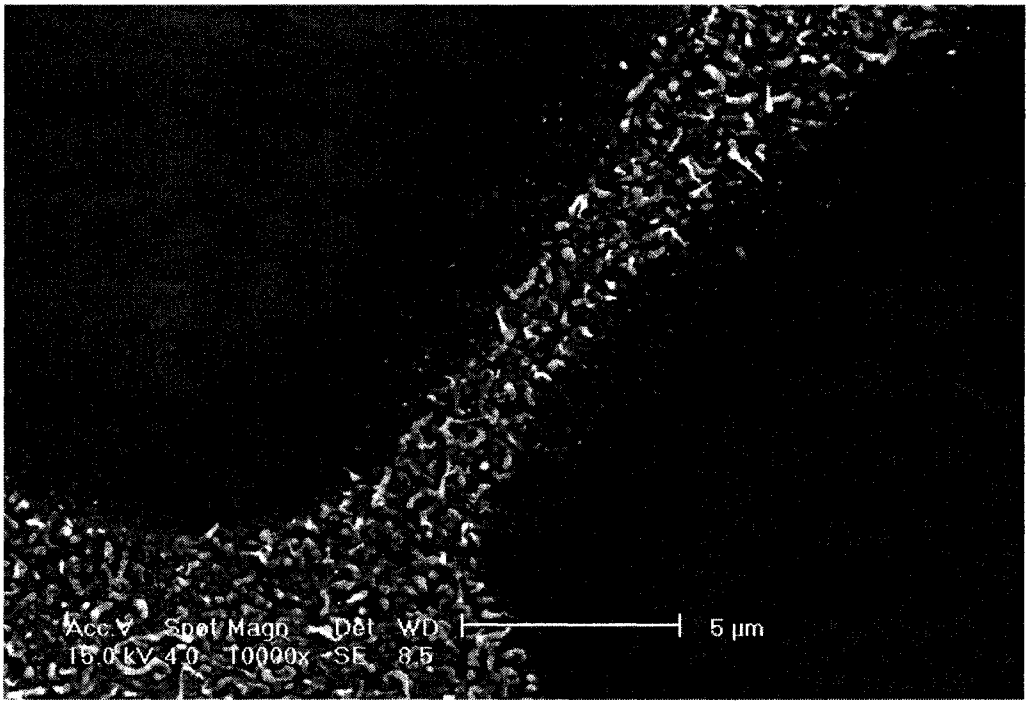

Figure 2-11 SEM image of CNTs grown on micro pattern

2.3.2 Transmission Electron Microscope (TEM)

The high-resolution TEM (HR-TEM) was used to inspect the nanostructure of CNTs. The TEM specimens were prepared by detaching the CNTs from the substrates and putting a few CNTs onto a micro grid. Figure 2-12 (a) shows a CNT grown on silicon substrate at 500 °C, and its diameter is 20 nm. There is no catalyst seed on the top of CNT. It was found in Figure 2-12 (b) that the CNTs grown at 500 °C have about 8~10 parallel layers, and the thickness of whole wall is about 6nm, so each layer is about 0.6nm. Figure 2-12 (c) shows the multi-layers CNT grown at 450 °C. Among the CNTs grown at 600 °C, double-walled CNTs were also observed as shown in Figure 2-12 (d).

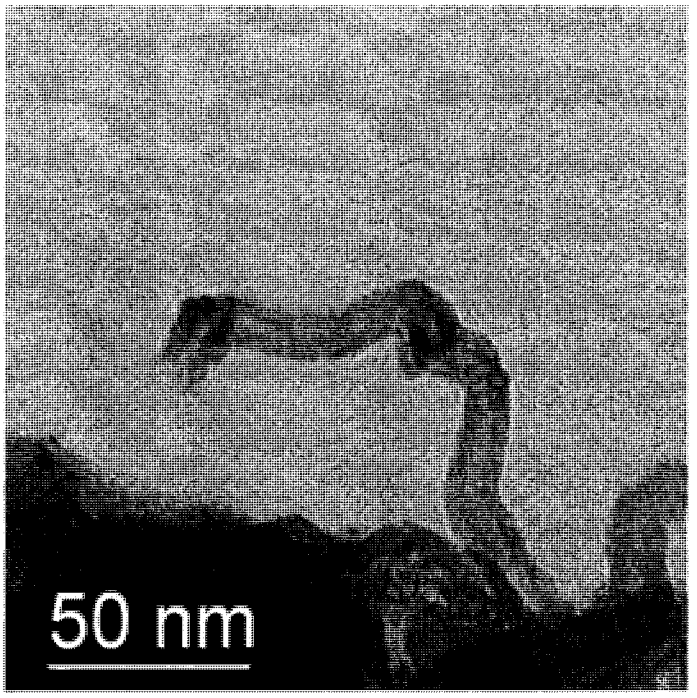

(a)

Figure 2-12 TEM images of CNTs grown with Co on silicon: (a) CNT grown at 500 °C

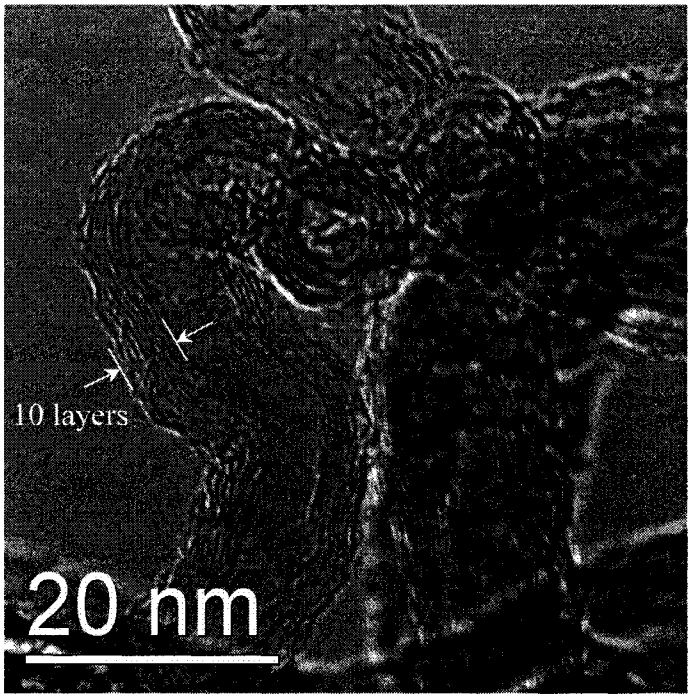

(b)

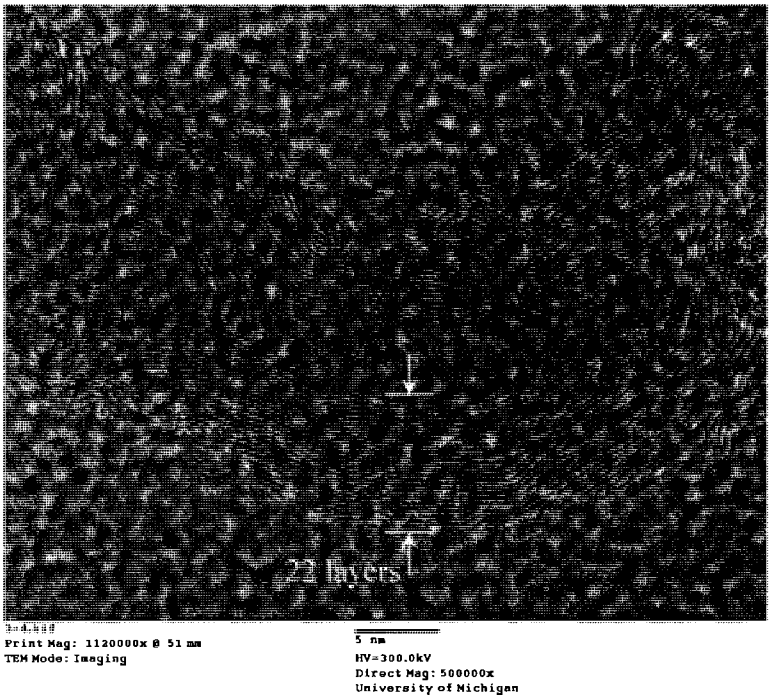

(c)

Figure 2-12 continued: (b) 10-layers CNT grown at 500°C, (c) multi-layers CNT grown at 450°C (the scale bar is 5 nm)

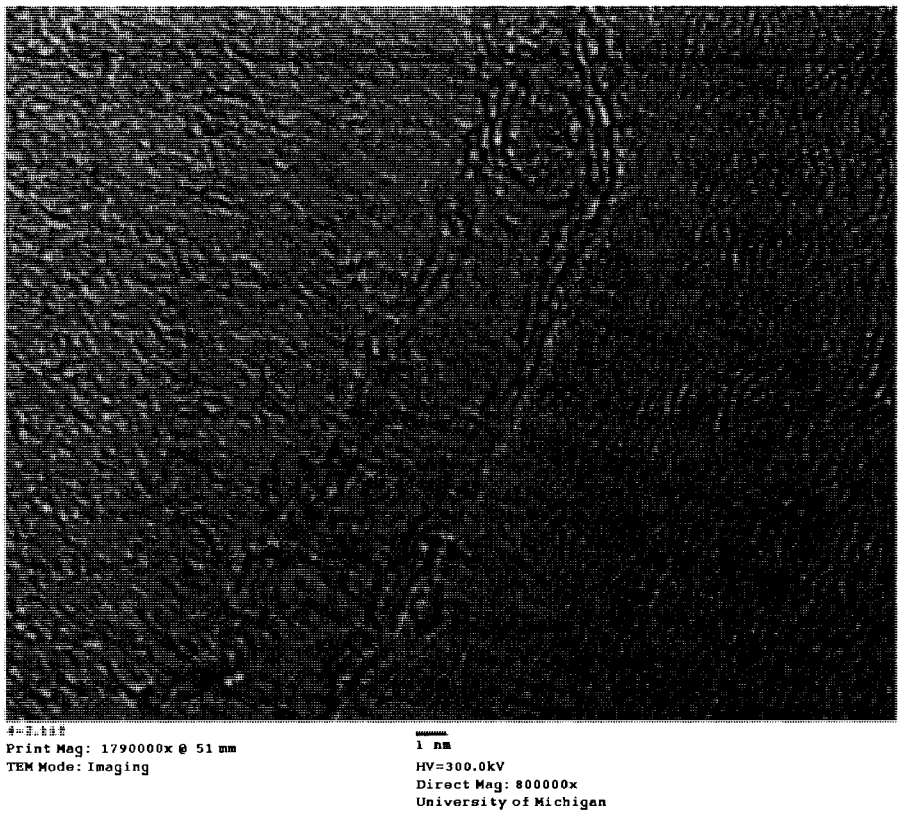

(d)

Figure 2-12 continued: (d) double-walled CNT grown at 600°C (the scale bar is 1 nm)

2.3.3 Raman Spectroscopy

The CNTs were also characterized by Raman spectroscopy (Jobin Yvon Horiba LabRam confocal Raman microscope with 785 nm and 633 nm excitation). Raman gives information on the average properties of the material in a sample volume within the diameter of the laser beam. The positions and relative intensities of the G mode (for "graphite") and D mode (for "disorder-induced") give much information about the structure and domain size of a carbon material. The strength of the D band relative to the G band is a measure of the amount of disorder in the CNTs [112]. The samples of CNTs on substrates were placed under the lens for measuring. The excitation source was 785 nm laser and the exposure time used

was 60 s totally. Two peaks were observed at almost the same Raman shift on the CNTs films deposited on Co, Ni and Fe catalyst as shown in Figure 2-13. One peak at about 1330 cm^{-1} corresponds to the disorder of the graphite structure (D-band). The other strong peak at about 1600 cm^{-1} is related to the high-frequency E_2g first-order mode of carbon structure (G-band). Those two strong peaks could determine the CNTs as shown in Figure 2-13 (a). The two peaks become stronger and shaper from Co to Ni and Fe catalyst as shown in Figure 2-13 (e), which indicate the increase of the disorder of carbon structure and higher crystalline quality [24, 113].

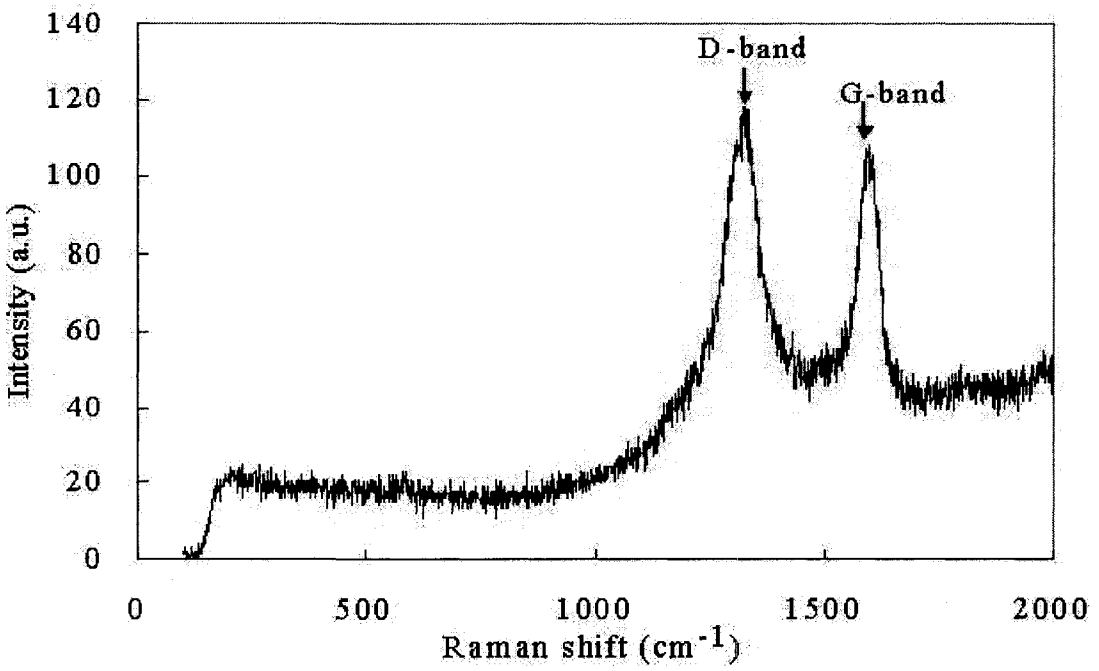

(a)

Figure 2-13 Raman spectroscopies of CNTs: (a) D-band and G-band of CNTs

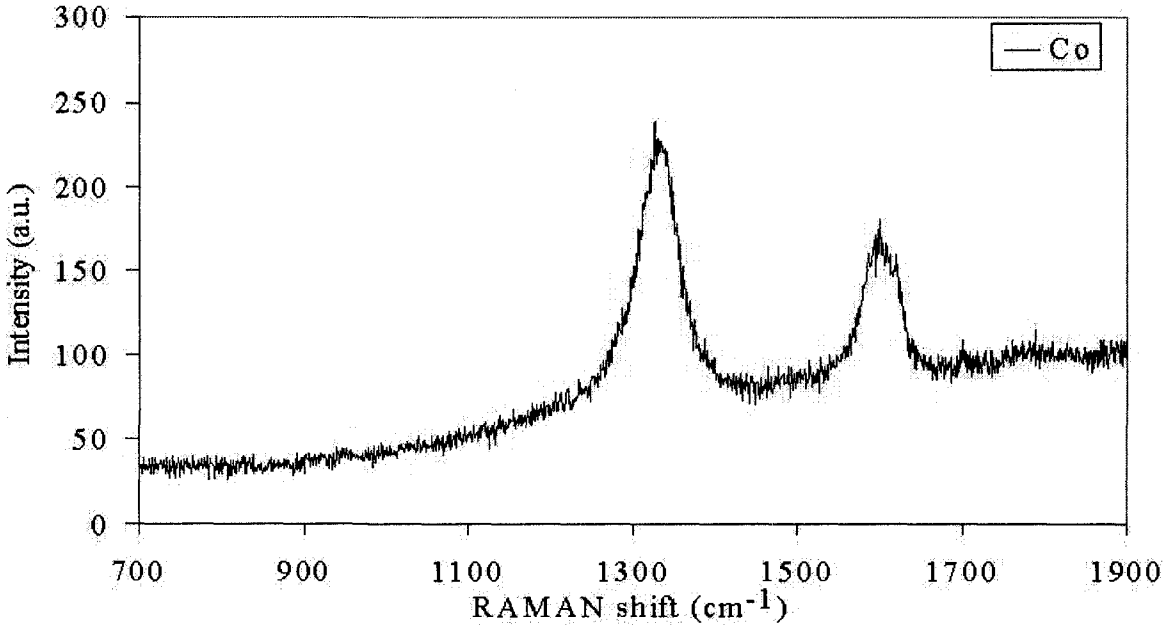

(b)

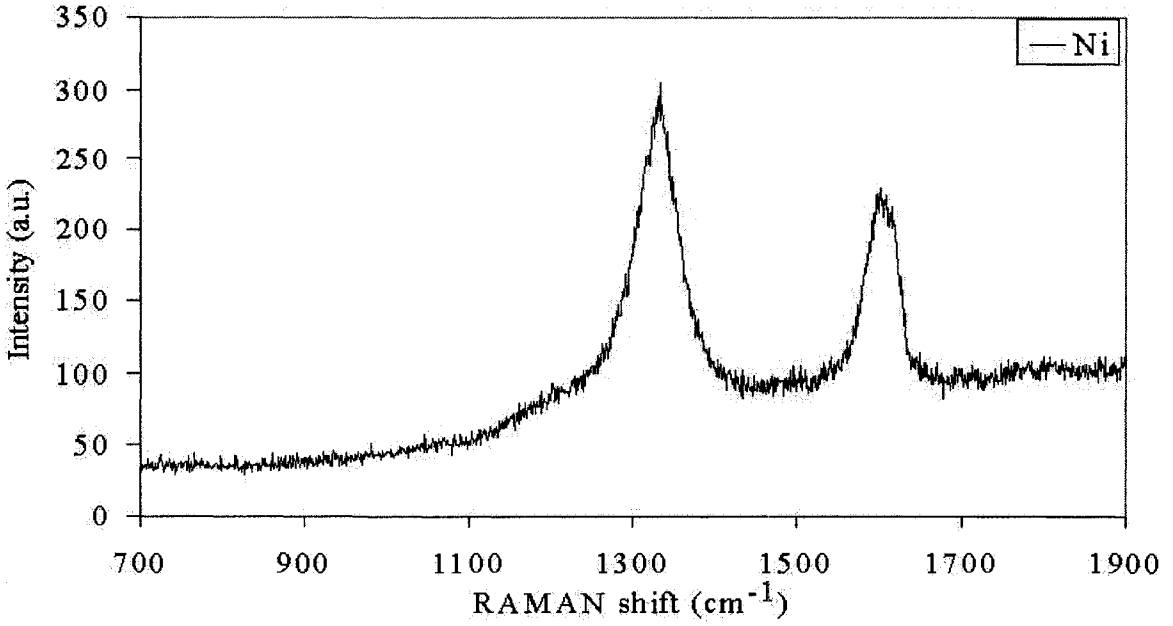

(c)

Figure 2-13 continued: (b) Co catalyst, (c) Ni catalyst

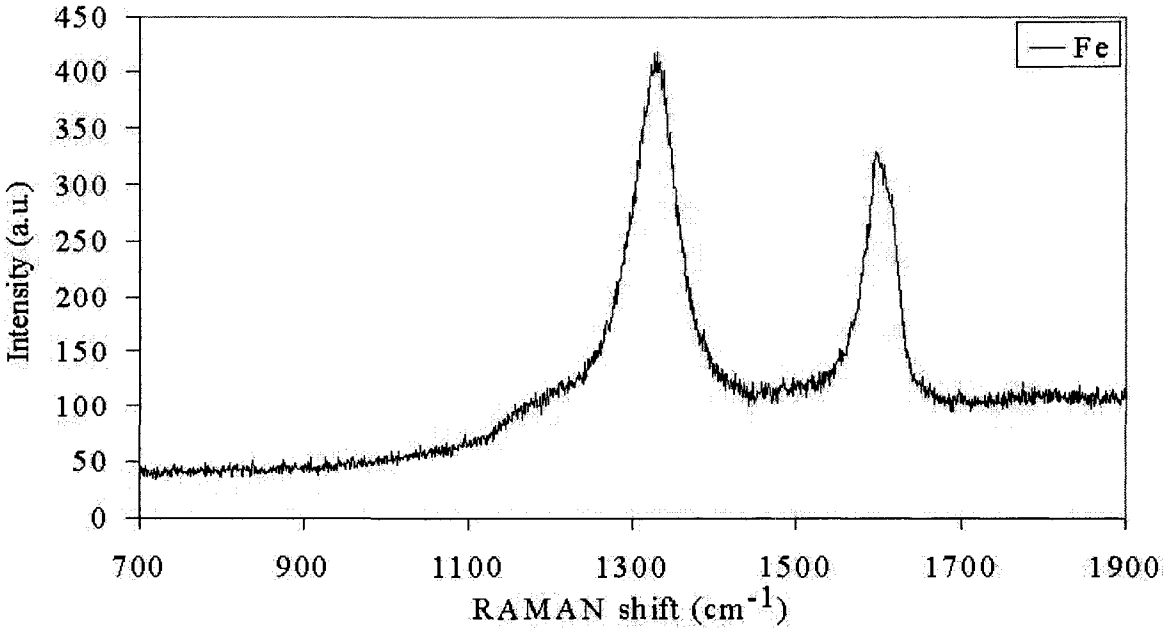

(d)

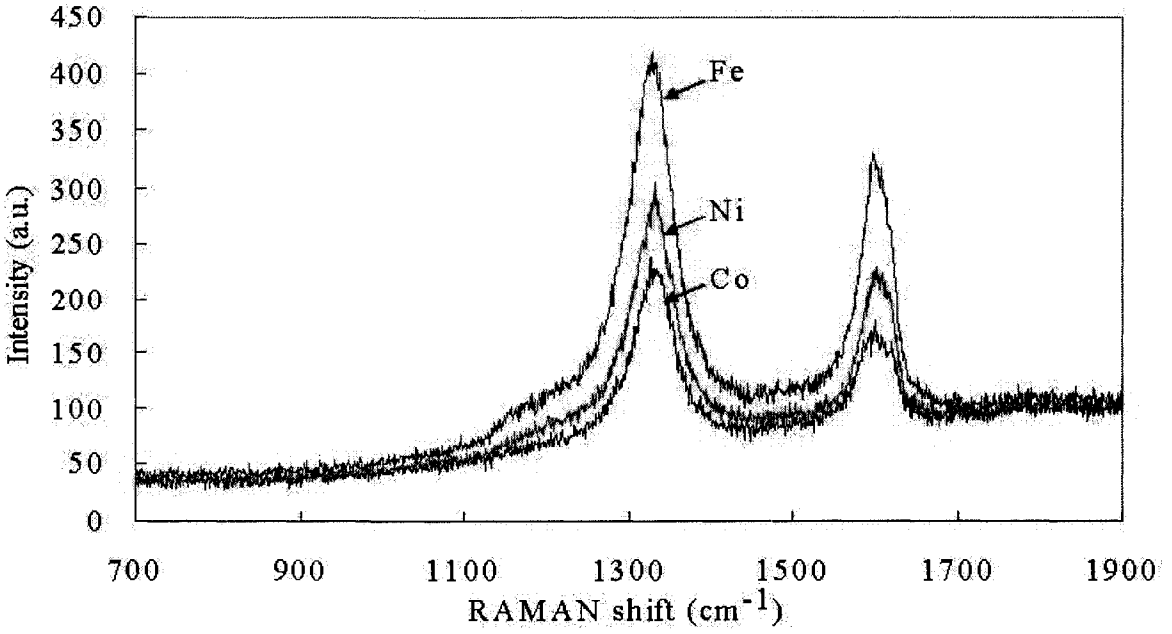

(e)

Figure 2-13 continued: (d) Fe catalyst, (e) Co, Ni, Fe catalyst

2.3.4 X-ray Diffraction (XRD)

The CNTs samples were also characterized by X-ray diffraction. The X-ray diffraction intensities of CNTs were recorded on a PANalytical X'Pert Pro X-ray Diffractometer with a X'Celerator high speed detector. It scans the samples with Cu $K\alpha_1$ radiation (λ = 1.541874 Å). The CNTs samples synthesized on glass substrates were placed on the X-ray diffractometer. The scanning angle (2θ) is from 20° to 55°. The X-ray diffraction patterns of the CNTs sample was shown in Figure 2-14. The peaks (002) (101) indicated the graphite structure. [114-116]

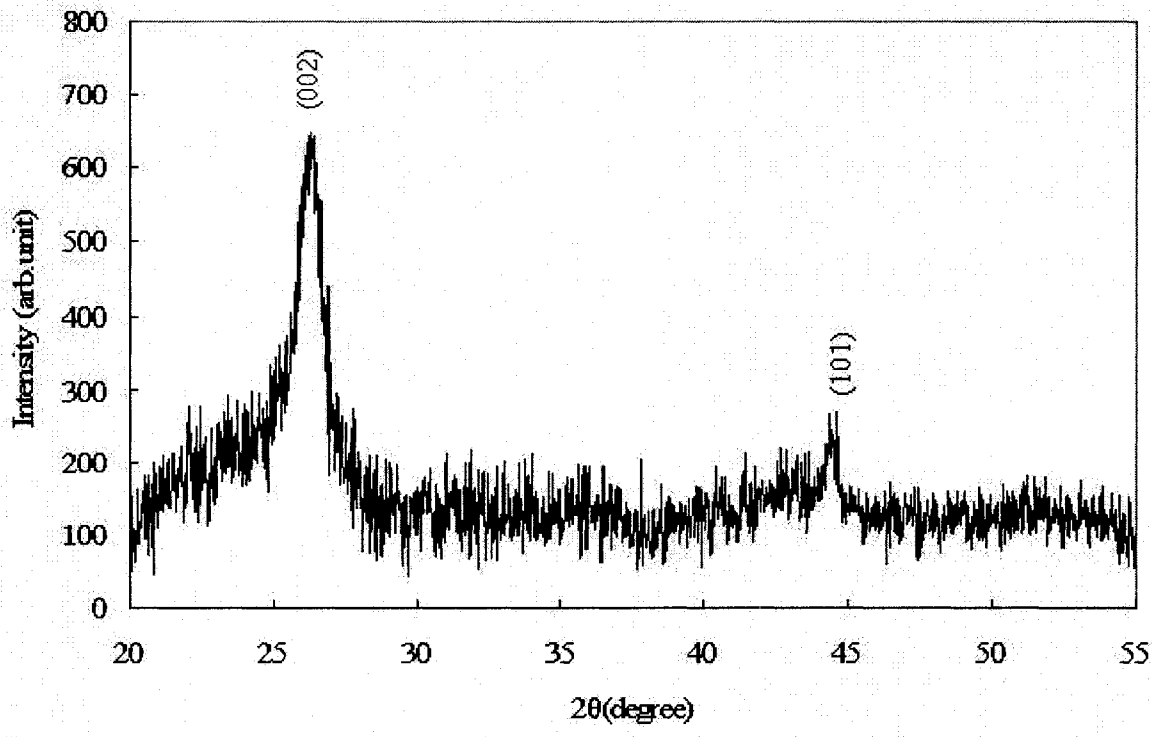

Figure 2-14 X-ray Diffraction patterns of MWCNTs

2.4 Synthesis Conditions and Discussions

The CNTs were characterized by many inspection methods. The influences of filament, temperature, catalyst and substrates on the synthesis of CNTs are discussed by analyzing those results.

2.4.1 Filament

Without the hot filament, the CVD system requires a higher temperature to grow CNTs, otherwise it is hard to synthesize CNTs, and sometimes no CNTs could be grown. The normal CVD system without the hot filament can grow CNTs at temperature higher than 700 °C, and normally 800 °C is better. The hot filament CVD system can grow CNTs at the temperature as low as 450 °C, and usually at 500 ~ 600 °C. So using the filament can reduce the temperature requirement significantly.

2.4.2 Temperature

It was found that CNTs can be formed at as low as 450 °C by this hot filament CVD system, which is the lowest temperature recorded to grow CNTs. The SEM picture of CNTs grown at low temperature 450 °C is shown in Figure 2-15. It was synthesized with the Co catalyst on silicon substrate. Measured from Figure 2-15 (b), the diameters of CNTs are about 20 nm.

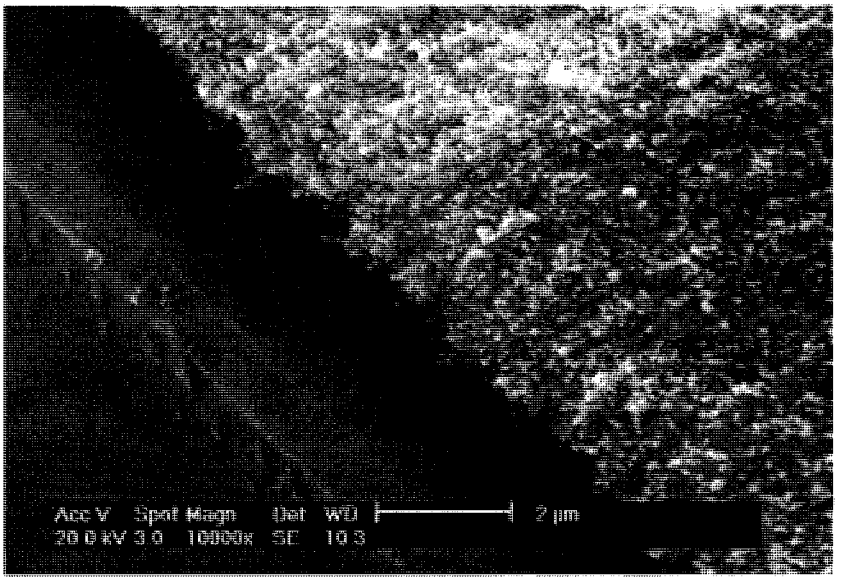

(a)

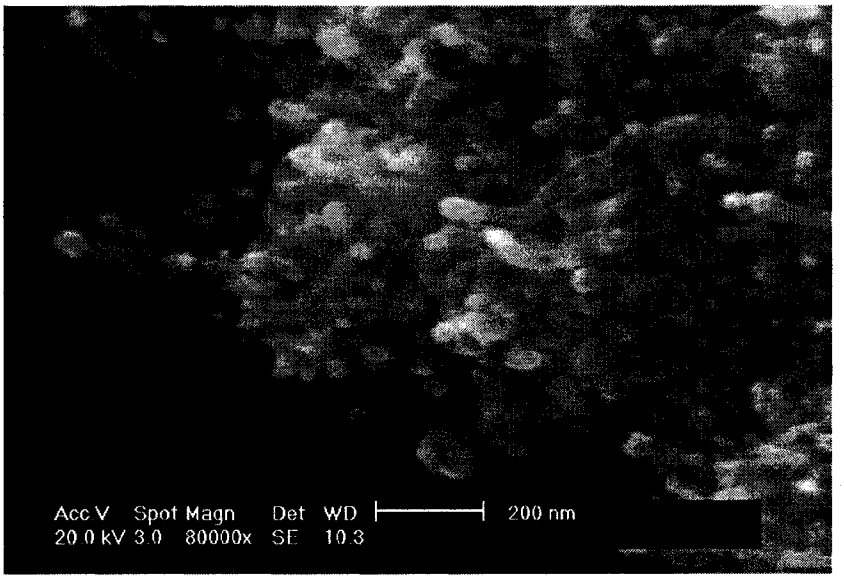

(b)

Figure 2-15 SEM images of CNTs synthesized with Co on silicon at 450 °C: (a) large view, (b) high resolution

The CNTs were also synthesized at 500 °C, 600 °C, 700 °C, 800 °C and 900 °C as shown in Figure 2-16. The CNTs grew faster and longer but more solid carbon particles were also deposited as the temperatures were changed from 500 °C to 900 °C. There were few CNTs grown on the substrate at 500 °C as shown in Figure 2-16 (a) because very thin Co catalyst was coated on the silicon substrate. Figure 2-16 (b) is the CNTs grown at the edge of Co catalyst pattern on silicon substrate. When the temperature was raised to 700 °C, the catalyst was melted and merged to form bigger particle, and small and big CNTs was grown at the same time as shown in Figure 2-16 (c). After the temperature approached 800 °C and 900 °C, the CNTs were grown faster and longer, but more amorphous carbon was also deposited as shown in Figure 2-16 (d) and Figure 2-16 (e).

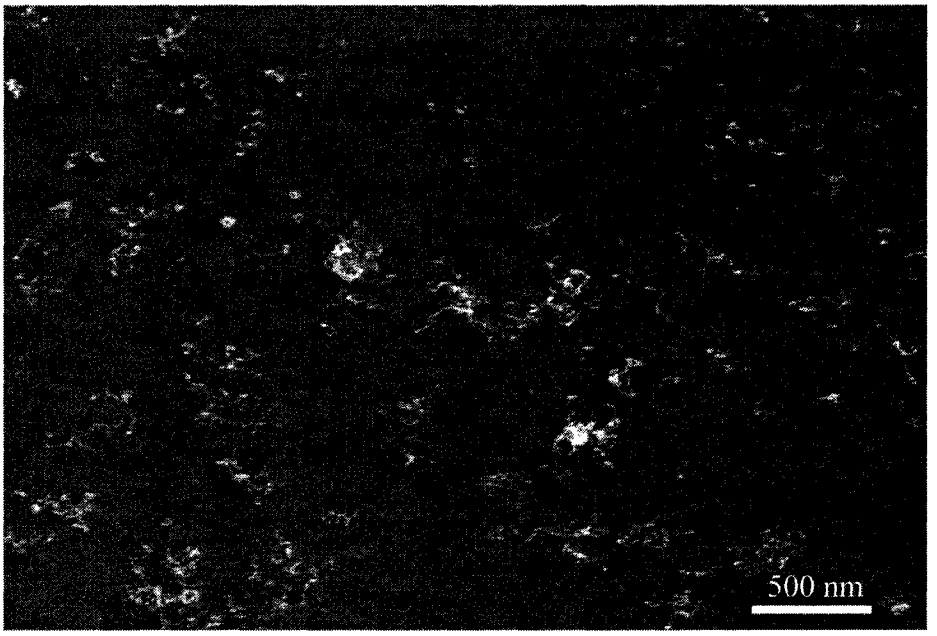

(a)

Figure 2-16 SEM images of CNTs synthesized at: (a) 500 °C

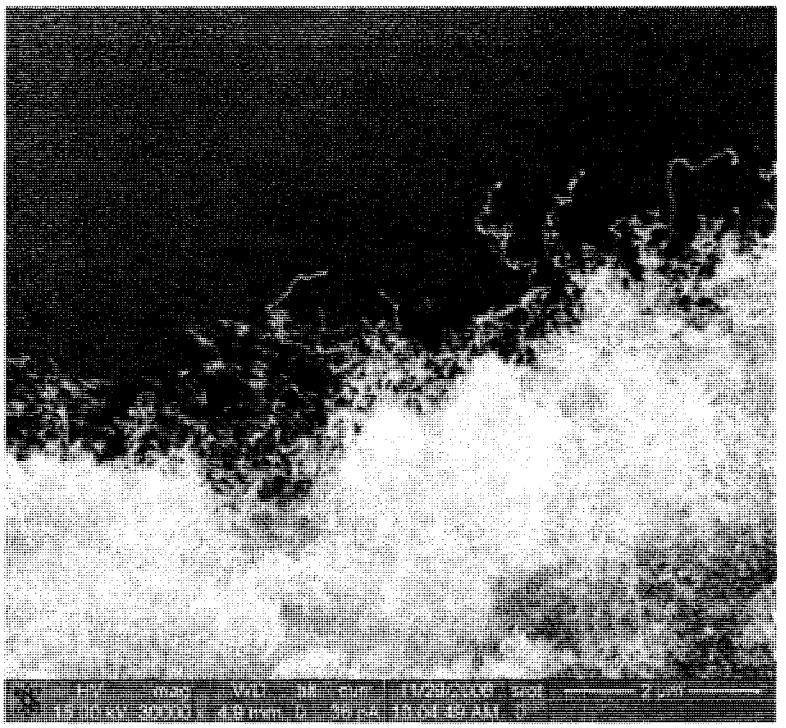

(b)

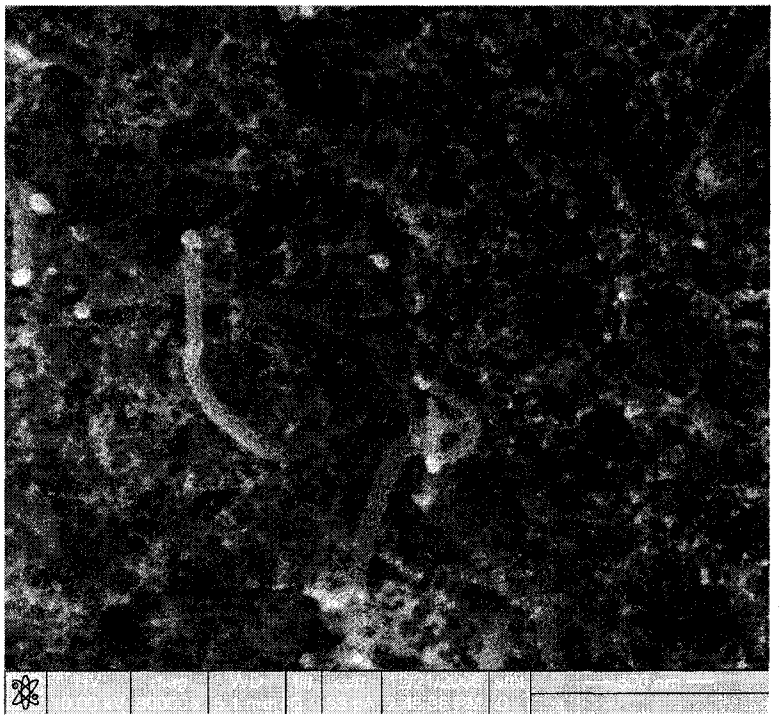

(c)

Figure 2-16 continued: (b) 600 °C, (c) 700 °C

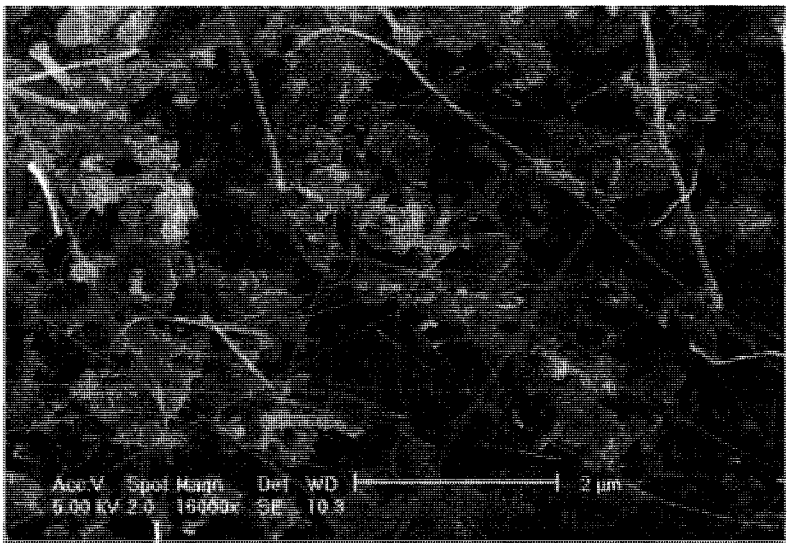

(d)

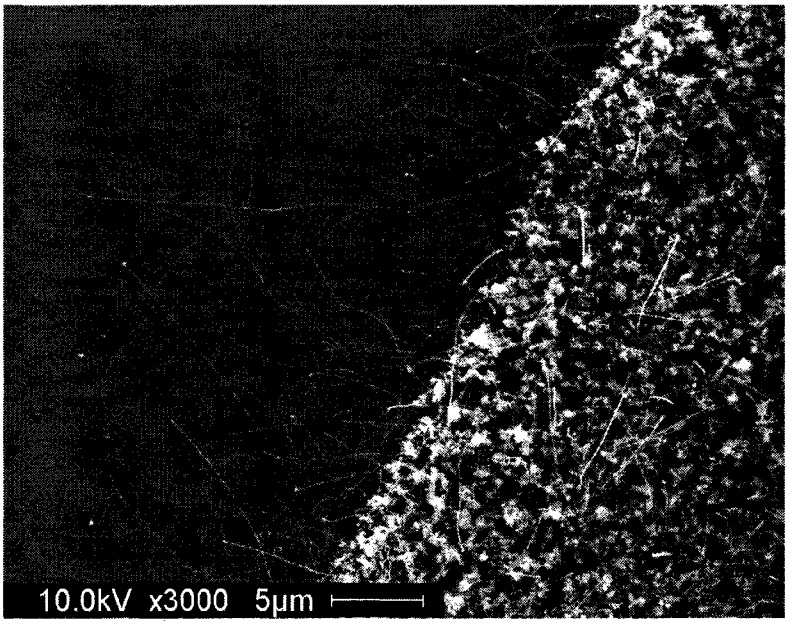

(e)

Figure 2-16 continued: (d) 800 °C, (e) 900 °C

2.4.3 Catalysts

Many catalysts such as Co, Ni, Fe, and Au were used for synthesizing CNTs. The alloy of Co and Ni was used as catalyst to grow CNTs on silicon substrate at 600 °C as shown in Figure 2-17. Sometimes, the catalyst metal was used directly for synthesis. Sometimes, their nitrides were used instead, and post-annealing was done to transfer nitrides to oxides before synthesis.

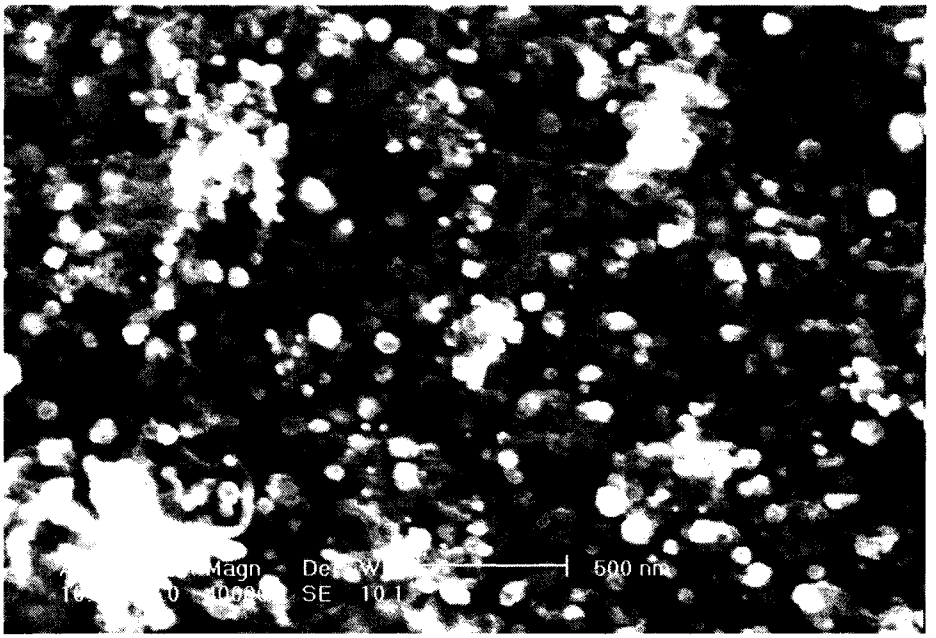

Figure 2-17 SEM image of CNTs synthesized with Co and Ni on silicon at 600 °C

Gold solution (colloidal gold) was also used as catalyst to grow CNTs. The colloidal gold was dropped and coated on silicon substrates using a spin coater. The colloidal gold coated silicon substrates were annealed in an oven at 400 °C for 1 hr in air. Then the silicon substrates were put in the hot filament CVD system to grow CNTs at 600 °C, with CH_4 10 sccm and H_2 50 sccm, for 1 hr. The CNTs were characterized by SEM as shown in Figure 2-18. The diameters of CNTs were about 10 nm.

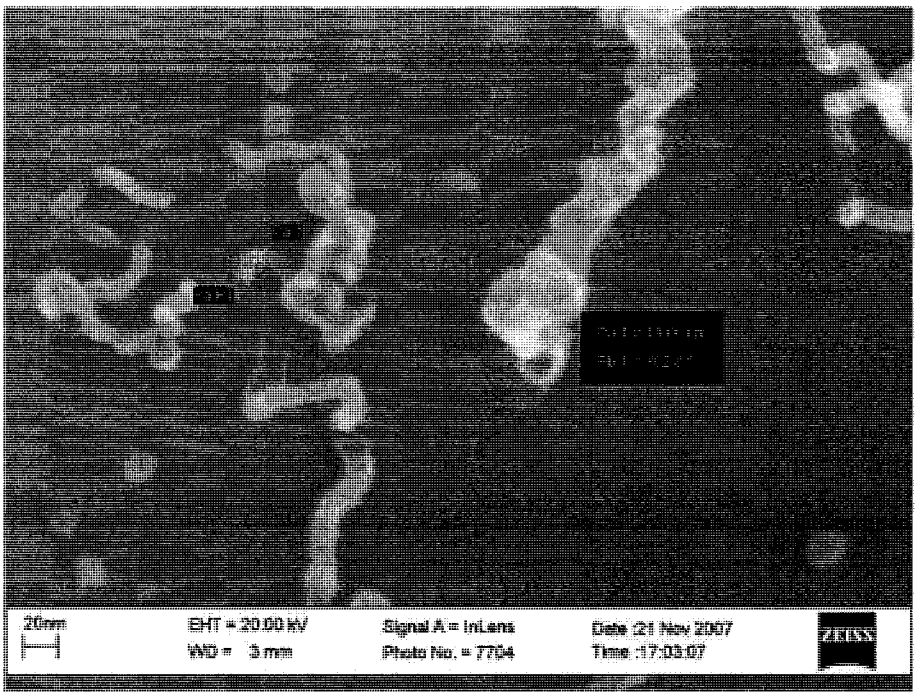

(a)

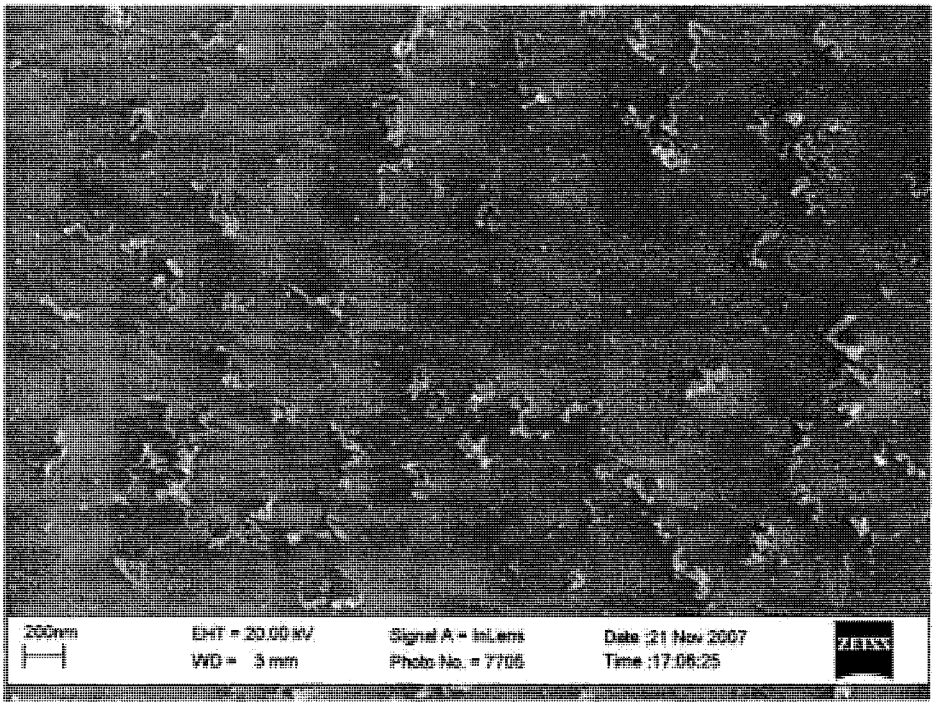

(b)

Figure 2-18 SEM images of the CNTs grown with gold catalyst: (a) CNTs grown with Au, (b) Large view of CNTs grown with Au

Sometimes, the catalysts were mixed with other metals when making the catalyst substrates and growing CNTs. Those metals, such as Cu (used as electrodes) and W (used as filament), influence the synthesis of CNTs. The effect can be appeared in several ways: (i) no nanotube was grown on the catalyst; and (2) formation of carbon nanofibers. The formation of nanofibers was observed as shown in Figure 2-19.

(a)

Figure 2-19 TEM image of Carbon Nanofibers synthesized at: (a) 400°C (the scale bar is 5 nm)

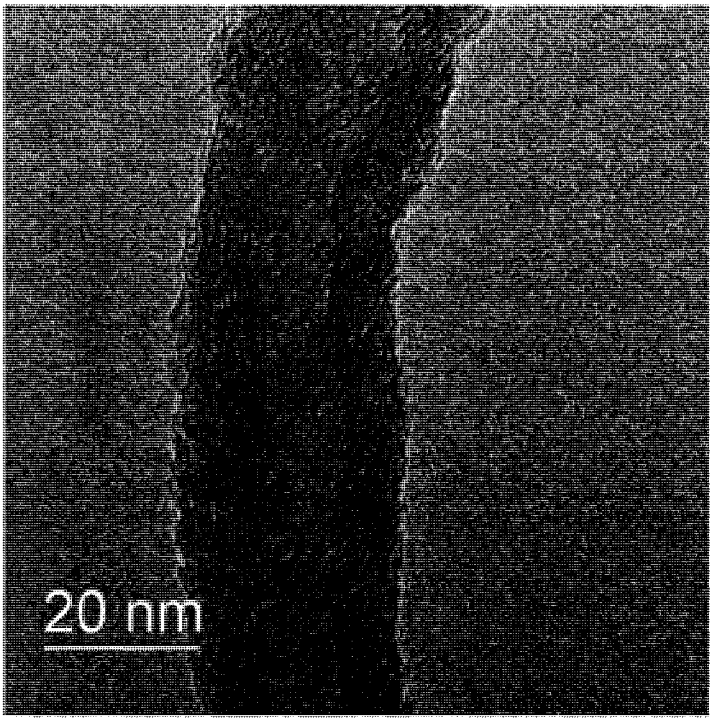

(b)

Figure 2-19 continued: (b) 500°C

2.4.4 Substrates

It is difficult to synthesize CNTs on glass substrates using traditional methods since glass can be melted when temperature is higher than 560 °C (strain point). Using this hot filament CVD system, it is possible to synthesize CNTs on glass substrates because CNTs can be grown at temperatures lower than 500 °C. Figure 2-20 is the SEM image of CNTs synthesized with Co catalyst on glass substrate at 500 °C. The diameters of CNTs are very small. Figure 2-21 is the RAMAN of CNTs synthesized with Co catalyst on glass substrate at 500 °C. The D-band (1324 cm^{-1}) and G-band (1598 cm^{-1}) indicated that they are CNTs.

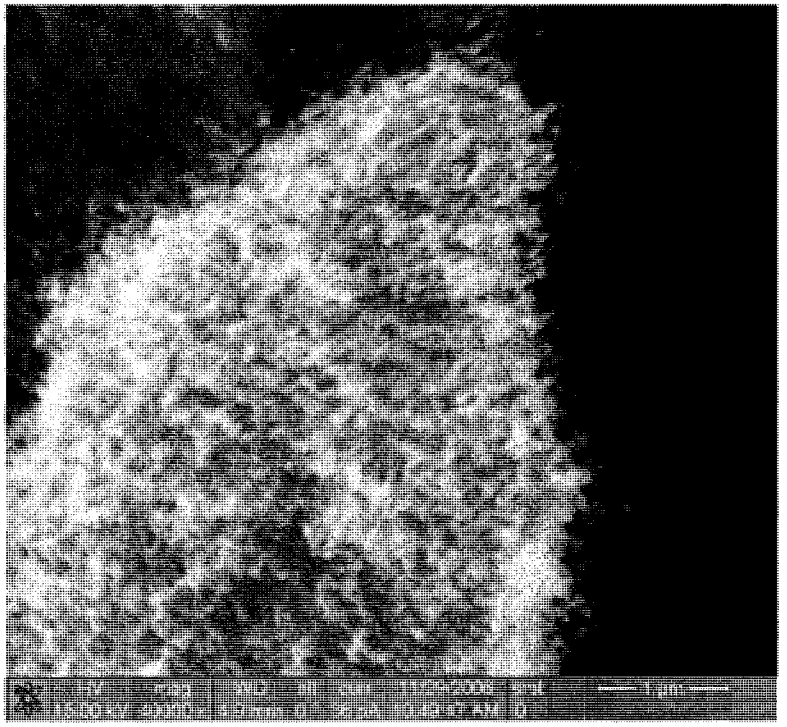

Figure 2-20 SEM image of CNTs synthesized with Co on glass at 500 °C

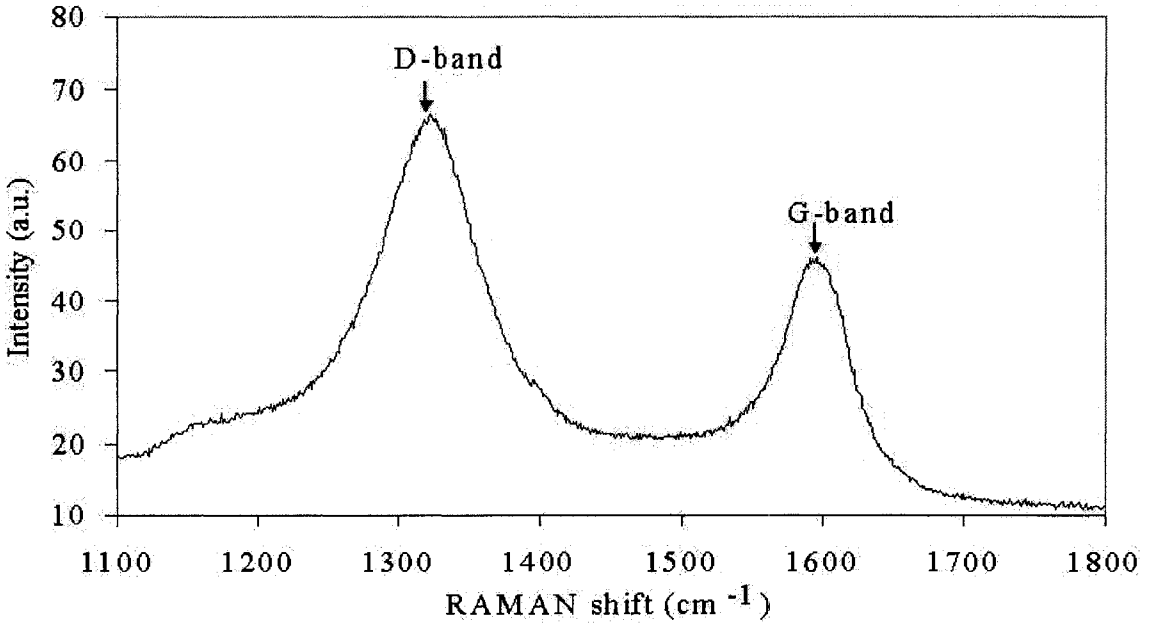

Figure 2-21 RAMAN spectrum of CNTs synthesized with Co on glass at 500 °C

The cobalt nitrate [$Co(NO_3)_2$] was also used as catalyst to grow CNTs on glass substrates. Different amount of $Co(NO_3)_2$ were dissolved into 1 ml alcohol and 1 ml diethanolamine to make different concentration solution. The amount of $Co(NO_3)_2$ were 5 mg, 50 mg, and 200 mg. The $Co(NO_3)_2$ solution were dropped on glass substrates rotating on spin coater. The glass substrates coated with $Co(NO_3)_2$ solution were annealed in oven at 400 °C for 1 hr to transfer $Co(NO_3)_2$ into CoO. The glass substrates with CoO were put in hot filament CVD system to grow CNTs with CH_4 10 sccm and H_2 50 sccm at 500 °C for 1 hr. After the synthesis, all samples of different concentrations were characterized by RAMAN. As shown in Figure 2-22, the D-band and G-band become sharper from samples of 5 mg to 200 mg $Co(NO_3)_2$, and D-band become stronger. These indicate that the increase of disorder of CNTs synthesized with $Co(NO_3)_2$ from 5 mg to 200 mg.

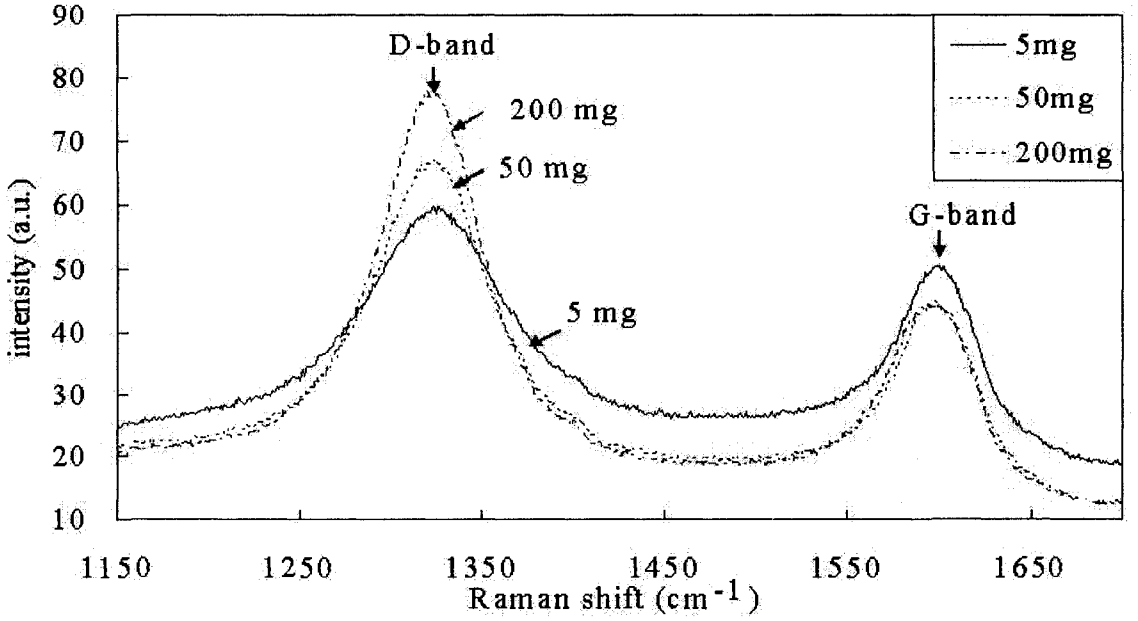

Figure 2-22 RAMAN spectrum of CNTs synthesized with different concentration of $Co(NO_3)_2$ solution on glass at 500 °C

Including the filament, temperature, and catalyst, there are some other parameters that can influence the synthesis of CNTs, such as gases flow rate, voltage applied on filament, and substrates treating.

2.4.5 Advantages of the Hot Filament Assisted CVD system

This hot filament assisted CVD system has several advantages compared with other synthesis methods and other CVD systems as following.

a) Low temperature (450 ^{o}C)

The hot filament CVD system could synthesize CNTs at the low temperature: 450 ^{o}C.

b) More types of substrates (glass)

Since the hot filament CVD system can synthesis CNTs at low temperatures, some substrates that can not sustain high temperatures, such as glass and epoxy, may be used. The common substrates, such as silicon, metal can certainly be used.

c) More types of catalysts

Using this hot filament CVD system, the CNTs have been synthesized with many types of catalyst, such as Co, Fe, Ni, and Au.

d) Simple equipment, less usage of gas source and energy

The hot filament CVD system is made of normal CVD system plus a filament with power supply. It is very simple and easy to be operated. With the assistant of a hot filament, this CVD system requires less energy and less carbon source because of high efficiency of decomposing hydrocarbon.

2.5 Synthesis Mechanism of CNTs in Hot Filament CVD

In this hot filament CVD system, the carbon source, CH_4, is decomposed into carbon species when they pass through the hot filament at 2000 °C as shown in following formula (2-1) and (2-2). The solid carbon species particles are carried by H_2 (or Ar) to reaction zone at lower temperature. The metal catalyst, Co, has been preheated by the CVD furnace to form small liquid droplets. The carbon species particles are dissolved in the catalyst liquid droplets and then separate out to form CNTs.

$$CH_4 = CH_2 + H_2 \quad (2\text{-}1)$$

$$CH_2 = C\ (solid) + H_2 \quad (2\text{-}2)$$

From the SEM and TEM pictures of CNTs synthesized by this hot filament system, two models of growth were found as shown in Figure 2-23. Figure 2-23 (a) and (b) show the catalyst seed on the top of CNT. The carbon species were dissolved by the catalyst seed on the top and then separated out from the catalyst, so those CNTs continued to grow by adding carbon at the top of CNT and pushed the catalyst seed to move forward as shown in Figure 2-24 (a). Figure 2-23 (c) shows the CNT without catalyst seed on the top. Those CNTs grew from the catalyst substrate by adding carbon at the bottom that separated out from the catalyst substrate and pushing the top part of CNT move upward as shown in Figure 2-24 (b).

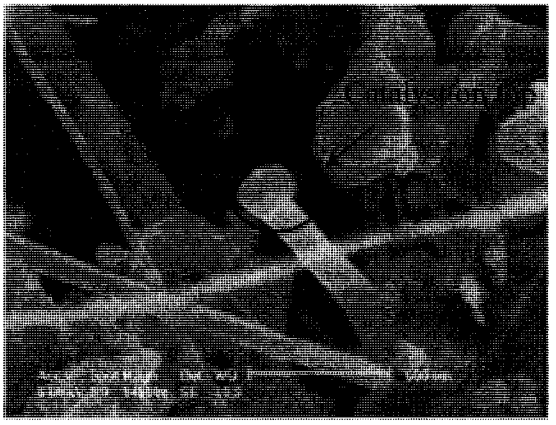

(a)

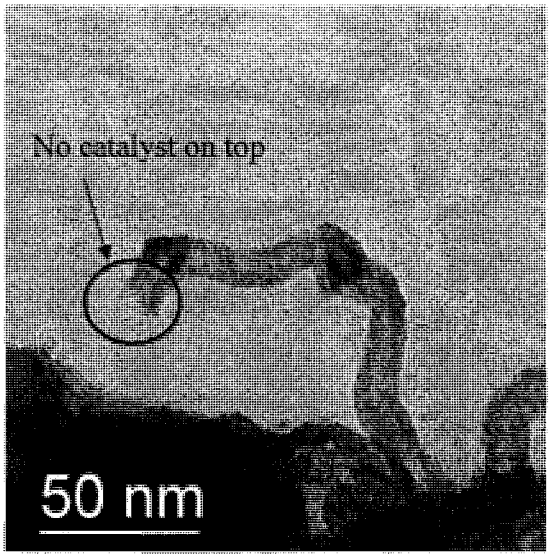

(b)

Figure 2-23 SEM/TEM images of CNTs: (a) SEM of CNT with catalyst seed on top, (b) TEM of CNT without catalyst on top

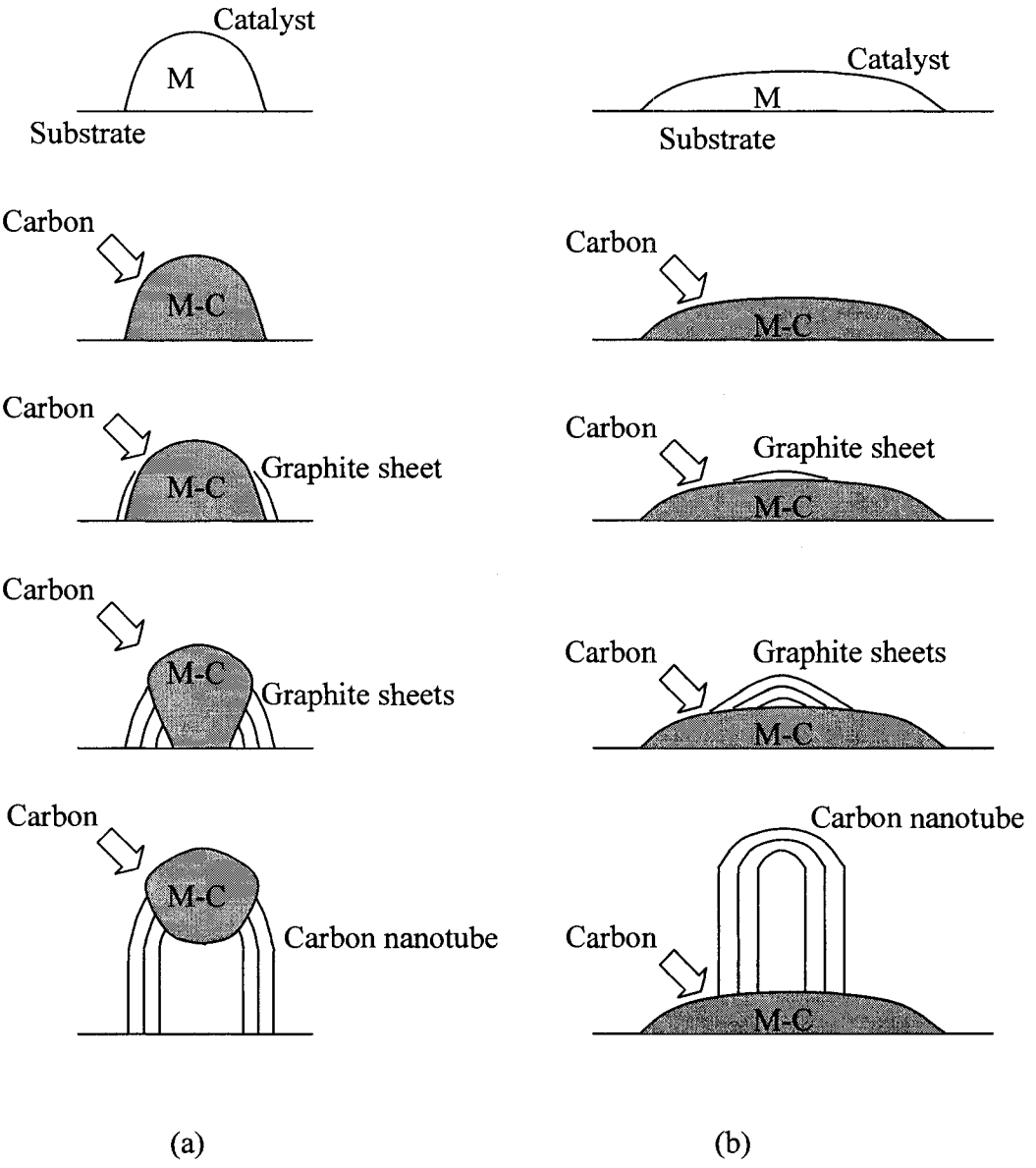

Figure 2-24 Schematic diagram of two models of CNT growth: (a) add carbon at the top, and (b) add carbon at the bottom

2.6 Synthesizing Smaller Carbon Nanotubes

The tiny size is one of the important reasons that the CNTs have so many unique

properties. The effort to grow smaller CNTs has never stopped. Growing small CNTs by this hot filament CVD system was also investigated. The size of CNTs could be influenced by the size of catalyst and the synthesis process.

Smaller CNTs can be grown on smaller catalyst particle. When using PVD to coat catalyst on the substrates, less catalyst wire is used to get thinner catalyst film. When using $Co(NO_3)_2$ solution, lower concentration lead to smaller catalyst particle on the substrates. The smallest diameter of the CNTs grown by this hot filament CVD system was about 4 nm as shown in Figure 2-25. The CNTs in Figure 2-25 (a) and (b) were grown with Co coated by PVD, and the thickness of Co thin film was less than 10nm. The diameter of small CNTs shown in Figure 2-25 (a) was about 4 nm. The CNTs in Figure 2-25 (c) and (d) were grown with $Co(NO_3)_2$ solution, which was made by dissolving 1 mg $Co(NO_3)_2$ in 5 ml alcohol. The diameter of small CNTs shown in Figure 2-25 (c) was about 4.5 nm. Those small CNTs were grown at 600~700 °C, with 10 sccm CH_4 and 50 sccm H_2.

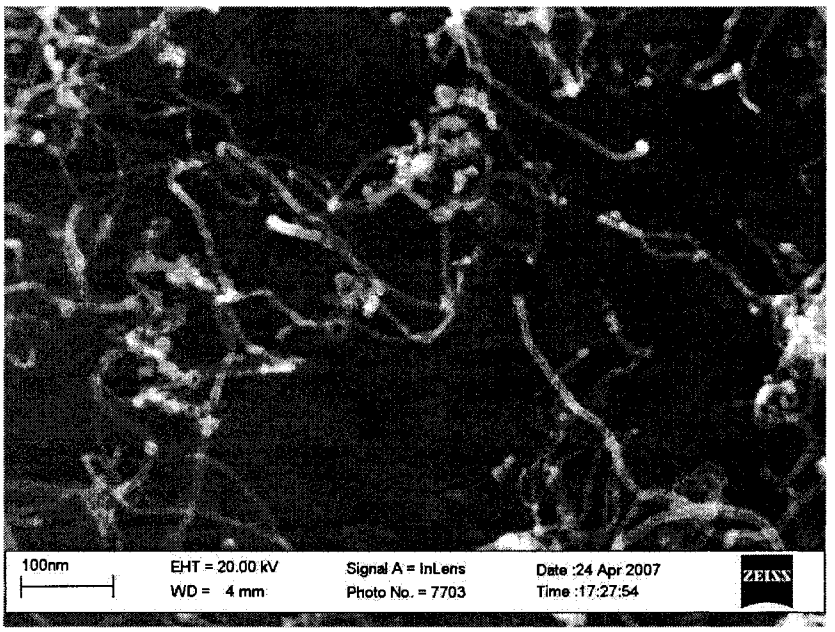

(a)

Figure 2-25 SEM images of small CNTs: (a) 4 nm CNTs synthesized with Co coated by PVD

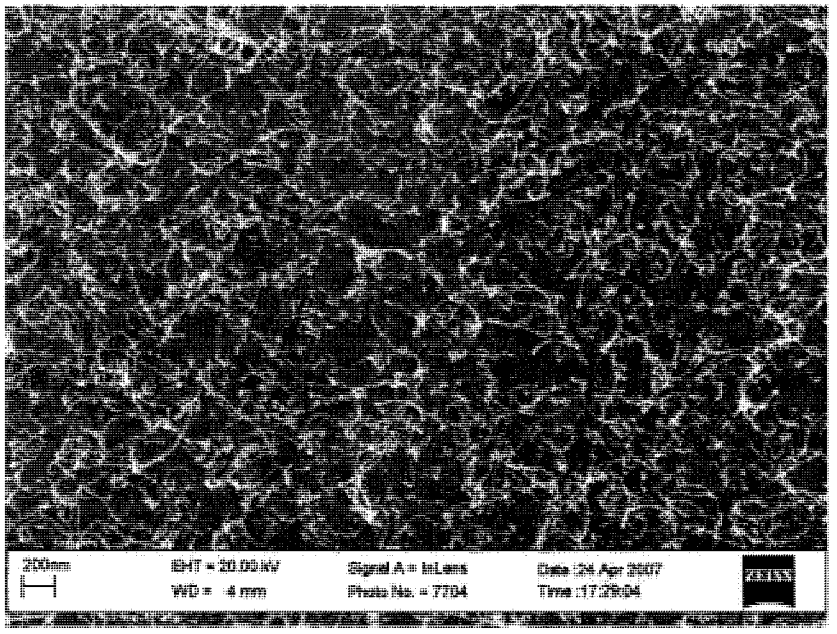

(b)

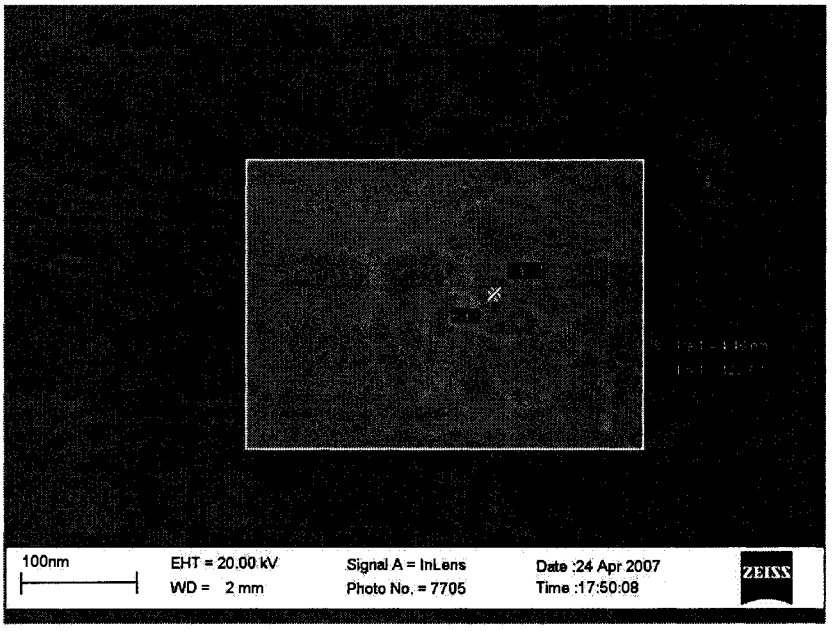

(c)

Figure 2-25 continued: (b) large view of CNTs synthesized with Co coated by PVD, (c) 4.5 nm CNTs synthesized with $Co(NO_3)_2$

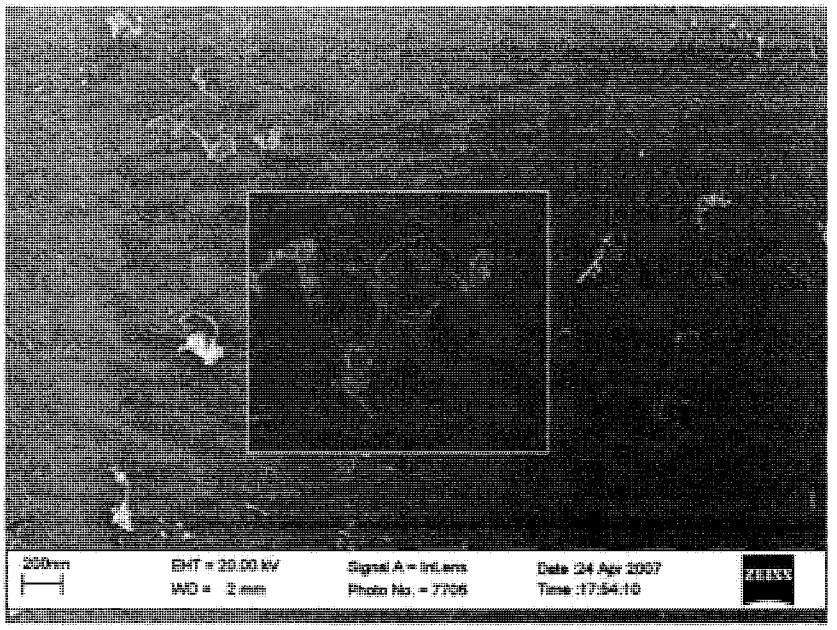

(d)

Figure 2-25 continued: (d) large view of CNTs synthesized with $Co(NO_3)_2$

2.7 Conclusions

The CNTs were synthesized by hot filament CVD system with a gas mixture of H_2 and CH_4 on Co, Ni and Fe catalyst coated on silicon and glass substrates at temperatures from 450 °C to 900 °C. When the temperature was raised, CNTs grew faster and longer but more amorphous carbon was deposited too. By optimizing the catalyst, filament and gases flow rate, the CNTs may be grown at lower temperature than 450 °C. Further research of synthesizing CNTs for gas sensors, mechanical sensors and measurement are discussed in the later. All achievement of synthesis of CNTs can be concluded as following:

1) Growing CNTs at low temperature 450 °C;

2) Growing CNTs on glass substrates;

3) Growing small CNTs of 4 nm in diameter;

4) Controlling the growth by adjusting catalyst, filament, gas flow rate and furnace temperature.

Chapter Three

3 Application of Carbon Nanotubes in Gas Detectors

The fabrication and testing of CNT-based gas detectors are discussed in this chapter. The principle of CNT-based gas detector is described. The fabrication processes, including catalyst pattern preparation, the CNTs synthesis, electrodes coating, gas detector assembling, are illustrated step by step. The testing setup of CNT-based gas detector and test results of some gases such as H_2 and NO_2 are described.

3.1 Introduction

Traditionally metal oxides are utilized as commercial gas sensor materials. Metal oxides sensors are least expensive and high sensitive. However, they have many drawbacks, such as high power consumption due to high resistance [67]. More new materials were considered as gas sensor materials, such as conducting polymers. CNTs were also considered because of the large surface area which can increase the interface with gases.

Presently in this research project, the CNTs can be grown longer than 10 microns on silicon substrates by controlling the conditions such as catalyst, gas flow rate, furnace

temperature, filament, and growth time. In this part of the research, application of CNTs in gas detectors was investigated. The CNTs were grown on across patterned electrodes on substrate. The CNTs should grow from the edge of pattern electrode toward another electrode, and connect them as shown in Figure 3-1 (a). The gas sensor can also be made by synthesize CNTs on patterned catalyst and then coat electrodes on both ends of the pattern as shown in Figure 3-1 (b).

Then the electric current passing through CNTs can be measured when the voltage is applied on electrodes. When the CNTs adsorb gases, the conductivity of CNTs changes, and accordingly the electric current will change.

The normalized sensitivity of the SWCNTs sensor is higher than that of the MWCNTs sensor, probably because SWCNTs contain more semi-conductive tubes [69]. But the synthesis of SWCNTs requires higher conditions than MWCNTs, and SWCNTs are more expensive than MWCNTs. Sometimes their properties on some applications are approximate, so MWCNTs are selected as the materials to fabricate gas detectors.

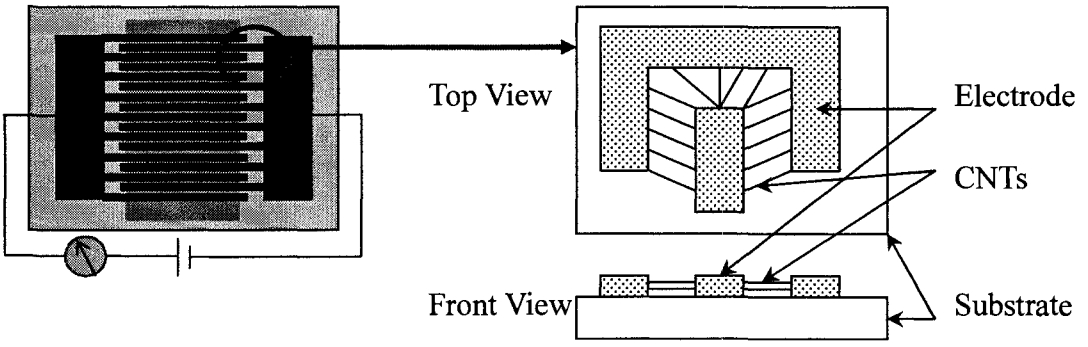

(a)

Figure 3-1 CNT-based gas sensors: (a) Schematic of gas sensor with CNTs bridging electrodes

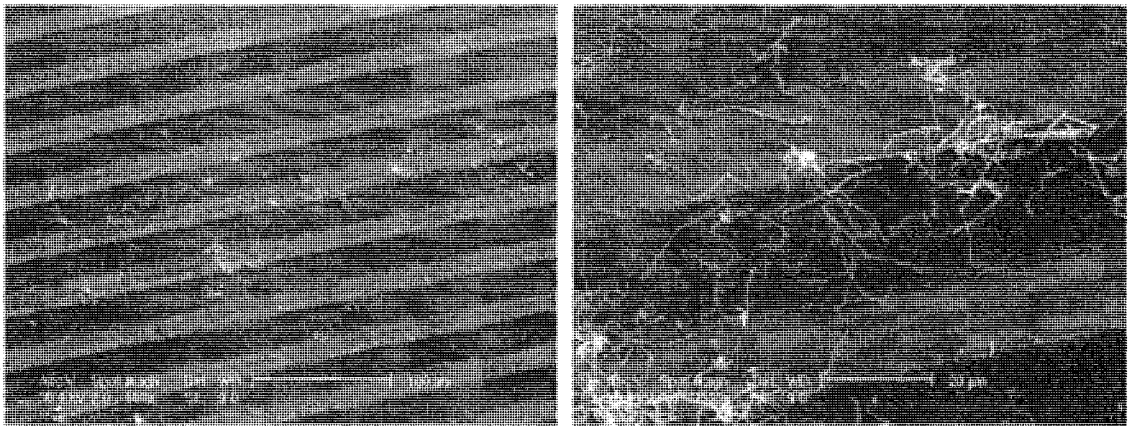

(b)

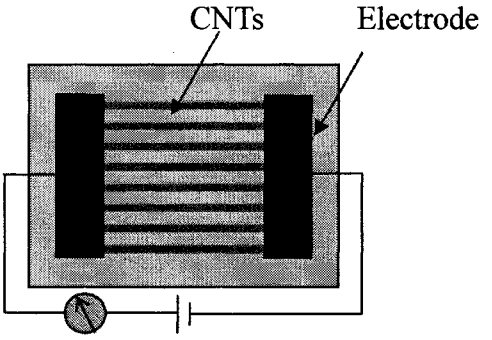

(c)

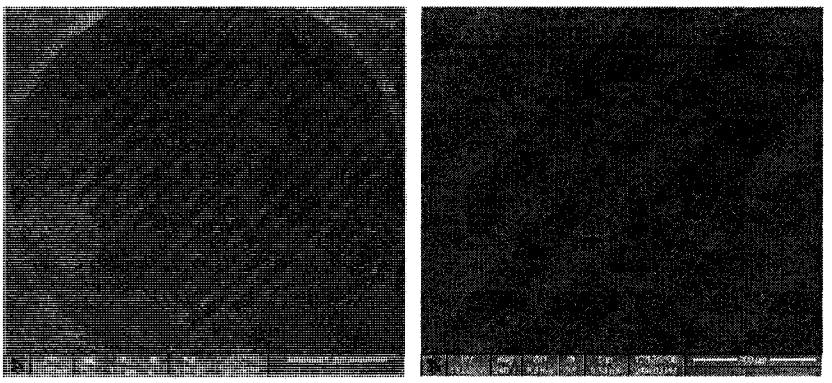

(d)

Figure 3-1 continued: (b) SEM images of CNTs bridging electrodes, (c) Schematic of gas sensor with CNTs film grown on pattern, (d) SEM images of gas sensor pattern

3.2 Principle of CNT-based Gas Detectors

The CNT-based gas sensors have received considerable attention because of their outstanding properties, such as faster response, higher sensitivity, lower operating temperature, and a wider variety of detectable gas than other types of gas sensors [117]. The CNT-based gas sensing utilizes the electrical impedance change of the CNTs due to adsorption of gas molecules as the electrical readout. As the dielectrophoretically trapped CNTs bridge over the electrode gap, the electrical connection, which provides a way to measure the CNTs impedance by using an external measuring circuit, can be readily achieved [69].

3.3 Fabrication of CNT-based Gas Detectors

The CNTs were grown on the patterned catalyst coated on the Si/SiO_2 substrates, and the samples with CNTs were assembled with electrodes to fabricate the gas detectors.

3.3.1 Preparation of Catalyst Patterns

In order to control the contact surface of CNTs and gases and the length of CNTs film, catalyst was etched to make special pattern on the substrates. The PVD was used to coat catalyst thin film on substrates, photolithography was used to make mask pattern of photoresist on the catalyst, and plasma etching and wet etching were used to etch the catalyst to make the pattern.

The Co was used as catalyst to be coated on substrates of silicon wafer with SiO_2 layer by PVD. The CNTs film, for gas detector, cannot be too thin to connect each other, otherwise the current will not pass through the CNTs film and no signal can be detected. The CNTs film

is not necessary to be so dense. Otherwise the CNTs film would not be smooth and easy to be peeled off the substrates. Usually, a Co wire of 10 - 20 mm in length and 0.25 mm in diameter was used to be coated on silicon, the distance between catalyst/filament and substrates was 15 - 20 cm, and the thickness of catalyst was controlled at range of 0.5 - 10nm for gas detectors. After PVD coating, the silicon wafer was cut into small pieces to make single pattern, or big pieces to make arrays of patterns.

Photolithography was done in the clean room to make mask of photoresist for etching the catalyst. First, MICROPOSIT S1813 positive photoresist was coated on the silicon substrates by spin coater. The rotate speed of spin coater was 4000 rpm, and the thickness of photoresist was about 100 micron. Sometimes negative photoresist was also used to get reversal patterns. The silicon substrates coated with photoresist were soft baked at 80 ^{o}C for 20 min in the oven. After that, the silicon substrates were taken out from oven and put on the exposure plate, and the mask with the selected pattern was placed on the silicon substrates. The silicon substrates with photoresist were exposed for 20 s under UV light. The silicon substrates were placed in the oven to be baked at 80 ^{o}C for 5 min. Then the silicon substrates with photoresist were dipped into MICROPOSIT MF–319 developer solution to be developed for about 30 - 40 s. Sometimes, distilled water was added to dilute the developer to slow down the development. After the unexposed photoresist was removed, the silicon substrates were rinsed with distilled water to remove the developer and clean the silicon surfaces. Then the silicon substrates were firstly placed on the spin coater to throw off the water and then in the oven to be hard baked at 100 ^{o}C for 20 minutes. The patterns of photoresist were checked under optical microscope.

The cerium (IV) ammonium sulfate [$(NH)_4Ce(SO_4)_4 \cdot 2H_2O$] solution was used to wet

etch the cobalt catalyst. Normally, 5 - 20 mg cerium (IV) ammonium sulfate was dissolved into 5 - 20 ml distilled water to make the etching solution. The silicon substrates with photoresist pattern and Co film were dipped into the cerium (IV) ammonium sulfate solution for 10 - 60 s. After the Co uncovered by photoresist was etched totally, the silicon substrates were rinsed with distilled water. Then the photoresist was removed by acetone. At last, these samples were rinsed with distilled water and dried. The substrates were ready for growing CNTs. The pictures of some gas sensor patterns are shown in Figure 3-2

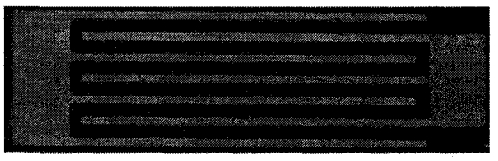

(a)

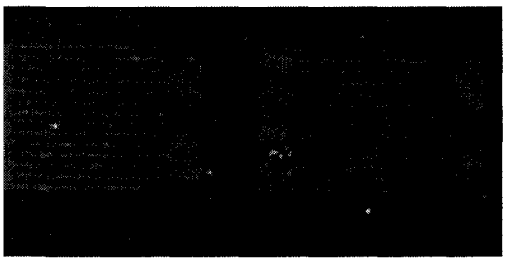

(b)

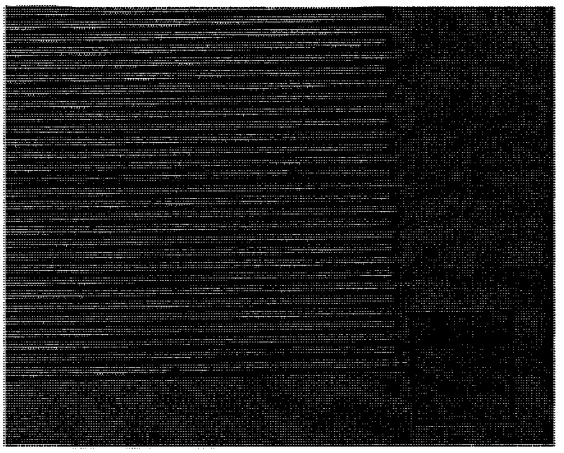

(c)

Figure 3-2 Gas sensor patterns: (a) one pattern, (b) pattern array, (c) another pattern

3.3.2 Synthesis of Carbon Nanotubes

After the catalyst patterns were made on the silicon substrates, they were put into the CVD system to synthesize CNTs. The silicon substrates were put on the quartz base frame, and the quartz base frame was placed at the center (zone 2) or the end (zone 3) of quartz tube of CVD system. A tungsten wire (15 - 20 cm in length, 0.25 or 0.5 mm in diameter) was coiled to be used as filament to decompose the CH_4. The filament was attached at the end of two copper electrodes that were fixed on the aluminum cap at one end of quartz tube. The copper electrodes went through the holes on the aluminum cap and were connected to power regulator, which can adjust the AC voltage applied on electrodes from 0 to 110 V. The electrodes were insulated from the cap by ceramic, and the holes were sealed well. Then the bolts of cap were tightened to seal the end of quartz tube.

The H_2 and CH_4 gases were opened for a moment to clean pipes first. The H_2 was kept passing at flow rate of 50 sccm for 1 – 1.5 hrs to press out the air in the CVD quartz tube. The CVD furnace was turned on to heat the quartz tube. The temperature was raised to 400 ^{o}C and kept for 1 hr to pre-heat the substrates and transfer the metal oxide into metal in hydrogen environment. Then it was ready to grow CNTs: temperature of CVD furnace was raised to 500 - 900 ^{o}C, H_2 flow rate was kept at 50 sccm, CH_4 was open and kept at flow rate of 10 sccm, and voltage of 10 - 15 V was applied on the filament to heat it to 1500 - 2000 ^{o}C. The color of filament changed from dark red to orange, and then almost white. Those conditions were kept for 1 - 2 hrs to grow CNTs. After that, voltage on filament was turned off, CVD furnace was turned off, CH_4 was closed, and H_2 was kept passing until the CVD furnace was cooled down to room temperature or lower than 100 ^{o}C.

After the CVD furnace was cooled to room temperature, the silicon substrates with CNTs

were taken out from the quartz tube for next processing. The Figure 3-3 show some pictures of CNTs grown on patterns.

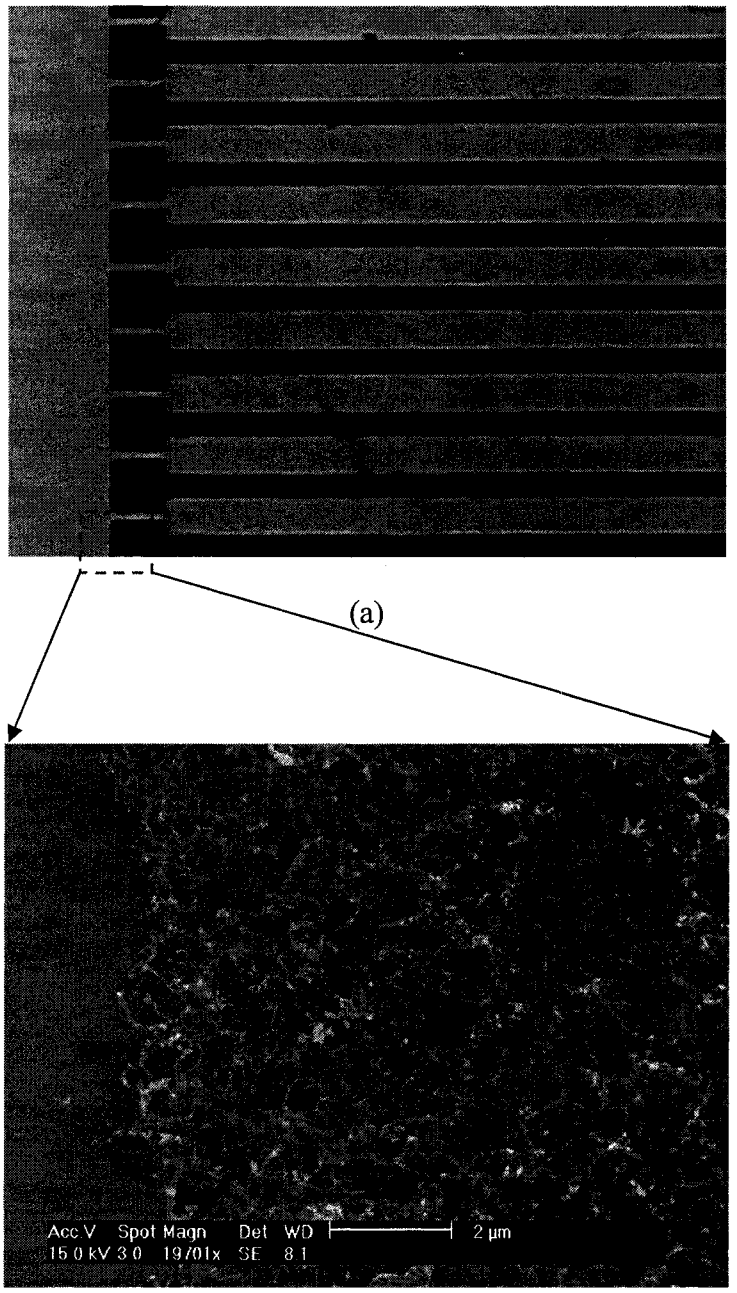

(b)

Figure 3-3 CNTs synthesized on patterns: (a) picture of one pattern, (b) SEM image of CNTs on one pattern

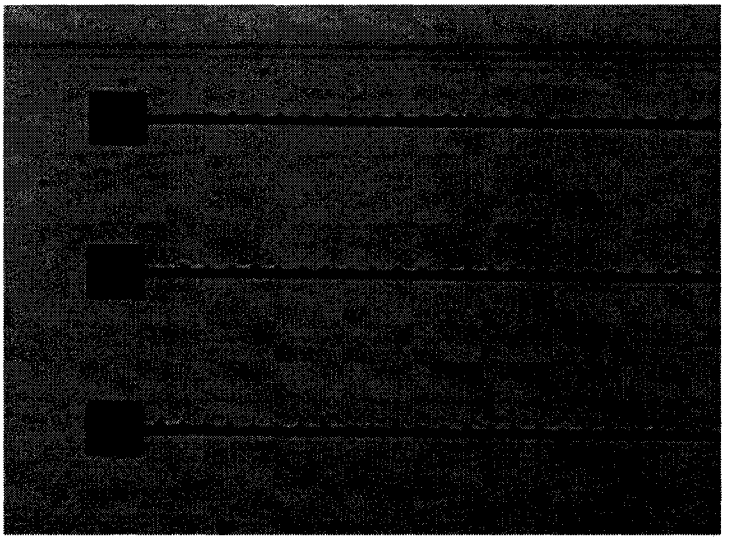

(c)

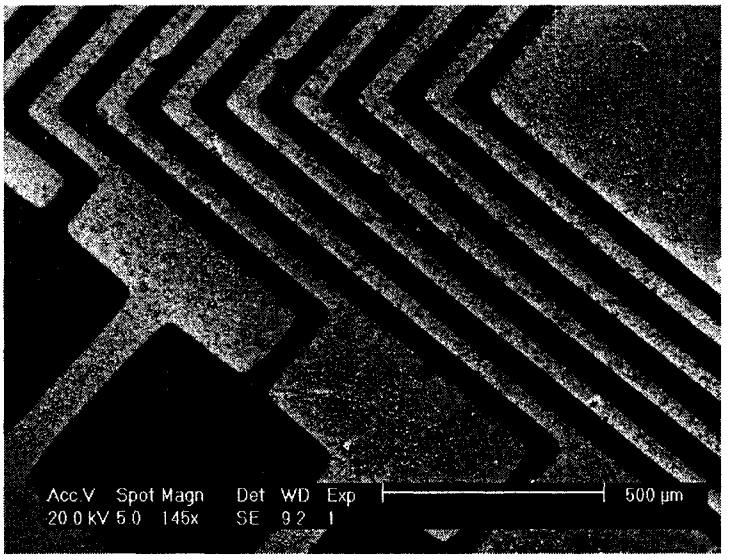

(d)

Figure 3-3 continued: (c) picture of another pattern, (d) SEM image of the third pattern

3.3.3 Assembling of CNT-based Gas Detectors

The gold electrodes were fabricated on the substrates to make a circuit to connect CNTs film. Firstly, an aluminum film was cut to cover the center part of CNTs pattern on the silicon substrates, and small areas at the two ends of CNTs pattern were not covered. The

samples were kept in the PVD chamber to coat gold at the two ends of the CNTs patterns through the holes on the aluminum film. A gold wire (10 - 15 mm in length, 0.5 mm in diameter) was used for coating. After PVD coating, the aluminum film was removed. Gold was coated on the CNTs and silicon substrates at two ends of the samples. Electrodes can be connected to the gold coated on the silicon substrates to connect the CNTs to a multimeter for measuring the resistance of CNTs. The finished gas detector is shown in Figure 3-4.

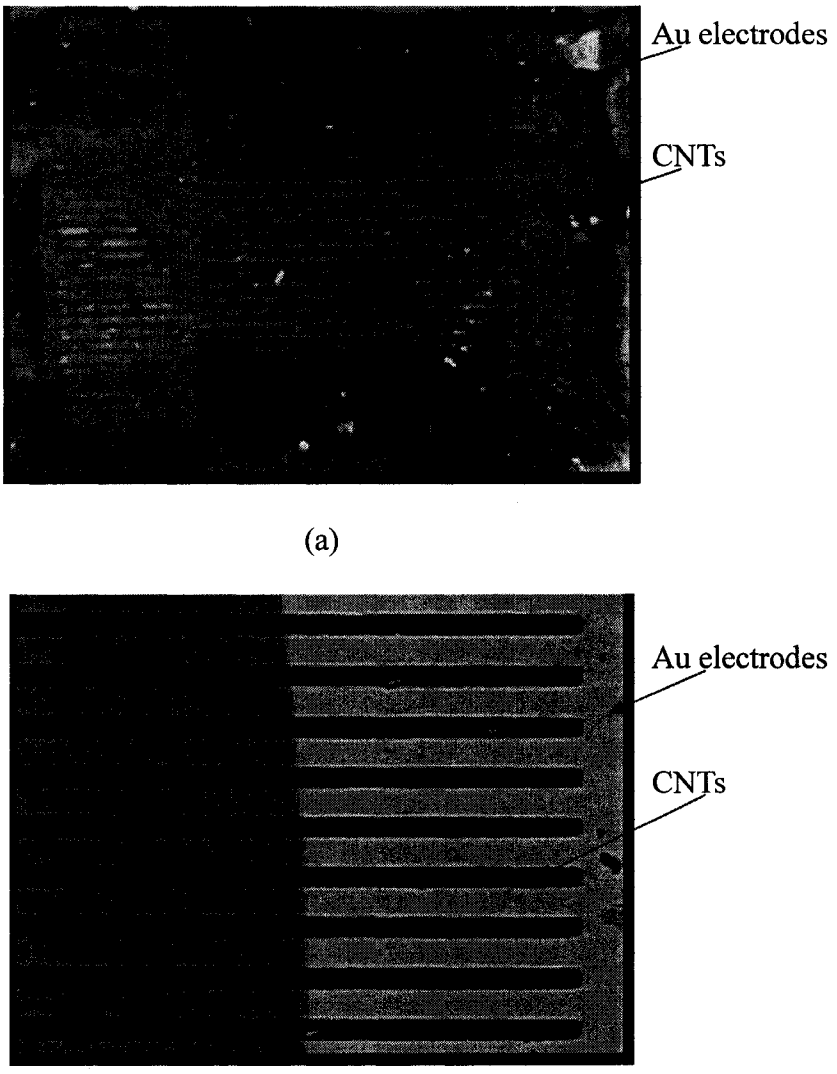

Figure 3-4 CNT-based gas sensor patterns coated with Au electrodes: (a) whole view of gas sensor (b) CNTs (black lines) and Au electrodes (right half area)

3.4 Testing of CNT-based Gas Detectors

The CNT-based gas detectors were installed on the testing setup to test the properties for several gases. The gas sensitivity of the CNTs was determined by measuring the resistance of the CNTs between Au substrate using a high mega ohm multimeter (Keithly Model: 22-816).

3.4.1 Testing Setup

The testing setup for CNT-based gas detector is shown in Figure 3-5. A tungsten wire was shaped into coil and filled with ceramic paste to make a heating base for the CNT-based gas detectors. Two pieces of quartz glass were adhered at both sides of the heating base to insulate it from the CNT-based gas detectors and other bases. The tungsten wire in the heating base was powered by a regulator that can adjust voltage and current. The gas detectors were fixed on the quartz glass of the heating base. Two tungsten wires were connected to the gold film coated on both ends of the gas detectors, and connected to a multimeter at the other end. The probe of the thermometer was touched on the heating base quartz glass and connected to the electronic temperature meter outside the glass bottles. All those units were put into two glass bottles that were sealed together by O-ring and bolt. All wires went through the glass bottle wall and connected units inside and outside. There were one inlet and one outlet pipe for gases on those glass bottles. The gas inlet was connected to the gas bottle and the gas outlet was connected to exhaust system.

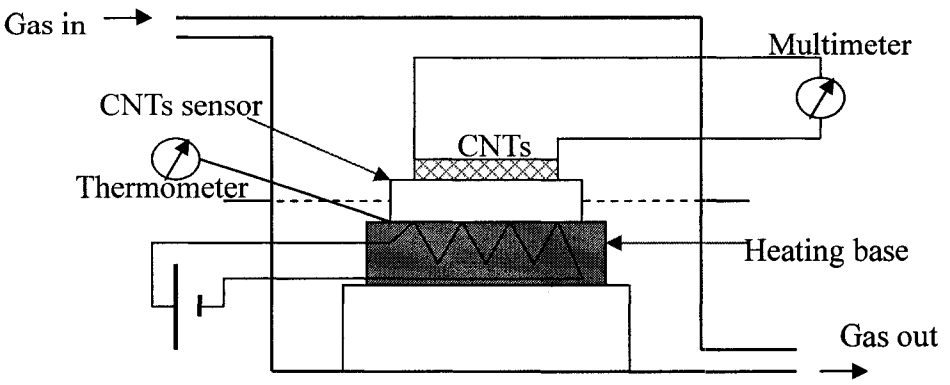

Figure 3-5 Testing setup of CNT-based gas detector

3.4.2 Testing Processes

After the testing setup was connected and ready, the processes of testing were: applying voltage on the heating coil to pre-heat the gas detectors, turning on Keithly high mega ohm multimeter to record resistance, opening the gas, recording the resistance by the multimeter and the time, closing the gas and opening the air (or inert gas Ar), recording the resistance and time, and repeating opening and closing the gas if needed. The gas detector was tested mainly with H_2. Several kinds of gases were also used to test the gas detectors, such as CH_4, N_2, CO and so on.

The gas flow rates entering into the measuring glass chamber were controlled by means of needle valves coupled to digital displays. The ratio between the particular gas and Ar (or air) inside the chamber was controlled by varying the ratio between gas flow rates entering into the chamber. The sensitivity (S) of these CNTs films were defined by the ratio of resistance change, shown as

$$S = 100 \times \left(\frac{R_{H2} - R_{Air}}{R_{Air}} \right) \tag{3-1}$$

Through the sensor testing chamber with a volume of 500 cm^3, the Ar (or air) was passed at a continuing flow rate of 150 cm^3/min. 5% H_2 in Ar was passed into the system through a mass flow controller. The flow rates were changed to see the variation of sensitivity with different concentration of H_2.

3.5 Results and Discussions

Figure 3-6 shows the Raman spectrum obtained for this CNTs sample. The Raman spectrum has two peaks corresponding to D-band (~1332 cm^{-1}) and G-band (~1580 cm^{-1}) of graphite. The G-band is sharper and has higher intensity than D-band indicating that the Raman spectrum is clear evidence for existence of MWCNTs.

Figure 3-7 shows the SEM images of CNTs grown on gas sensor substrate. It can be seen that the nanotubes are randomly distributed all over the place. The diameter of nanotubes is around 4 nm (Figure 3-7 (b)). These nanotubes were in contact with gold electrodes and the resistivity between two electrodes was 400 Ω. During the heating process, the resistance of nanotubes was clearly reduced. In fact these sensors were highly sensitive to small changes in temperature. Though not given in this picture, TEM images indicated that these nanotubes were made of 8 - 10 graphitic layers.

Figure 3-8 shows the response curve for H_2 (5% H_2 in Ar) and air at two different temperatures of 150 °C and 300 °C. The resistance of sensor film was decreased when H_2 gas was introduced into the chamber. The catalytic coated films were measured after being treated at the same temperature. For such ultra thin films of metal, no signal can be obtained for a measurement rage of 1 G Ω. Thus, any sensing characteristics associated with CoO film was ruled out. The sensitivity at 150 °C and 300 °C are about 25 and 60, respectively. At 150

°C, response was lower than 300 °C. The recovery time was faster for 150 °C than 300 °C case. Similar sensors were operated at 400 °C to detect H_2. However, no clear signals were detected for any concentration of H_2. While resistance of CNTs film was reduced when the temperature was increased from 300 °C to 400 °C, it did not exhibit the sensitivity for H_2 at 400 °C. Also, at 350 °C, sensitivity was quite degraded compared with 150 - 300 °C range. It was reported that for MWCNTs, desorption of hydrogen is high at temperatures above 350 °C. Thus, at these temperatures (350 ~ 400 °C), hydrogen absorption did not occur in CNTs hence, and the change of resistance was not observed. [118-120]

Figure 3-9 shows the response curve for passing H_2 (5% H_2 and 95% Ar) and Ar turn by turn at 80°C. The resistance (sensitivity) of gas detector was increased when H_2 was introduced into the chamber. The resistance pulled back when H_2 was stopped and Ar was introduced into the chamber. The sensitivity was lower at 80°C compared with at higher temperature. [121-127]

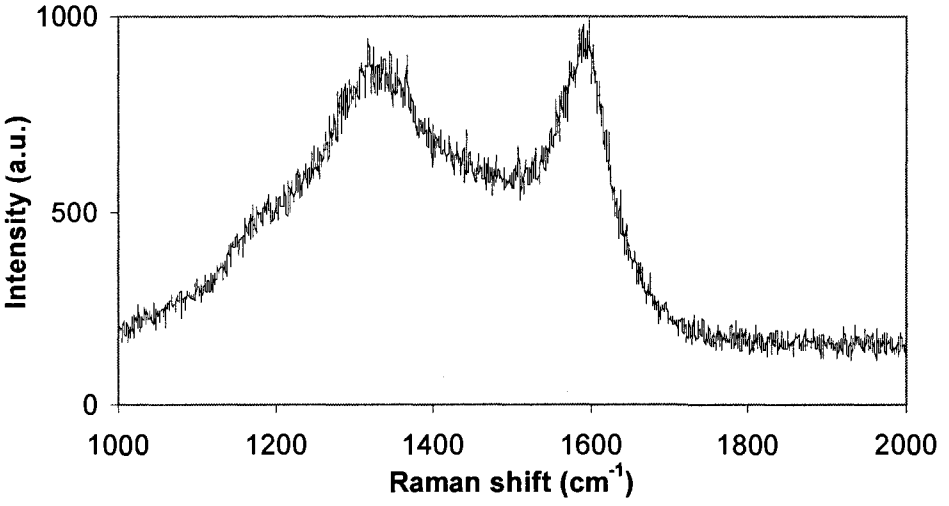

Figure 3-6 Raman spectroscope of CNTs grown on SiO_2 substrate

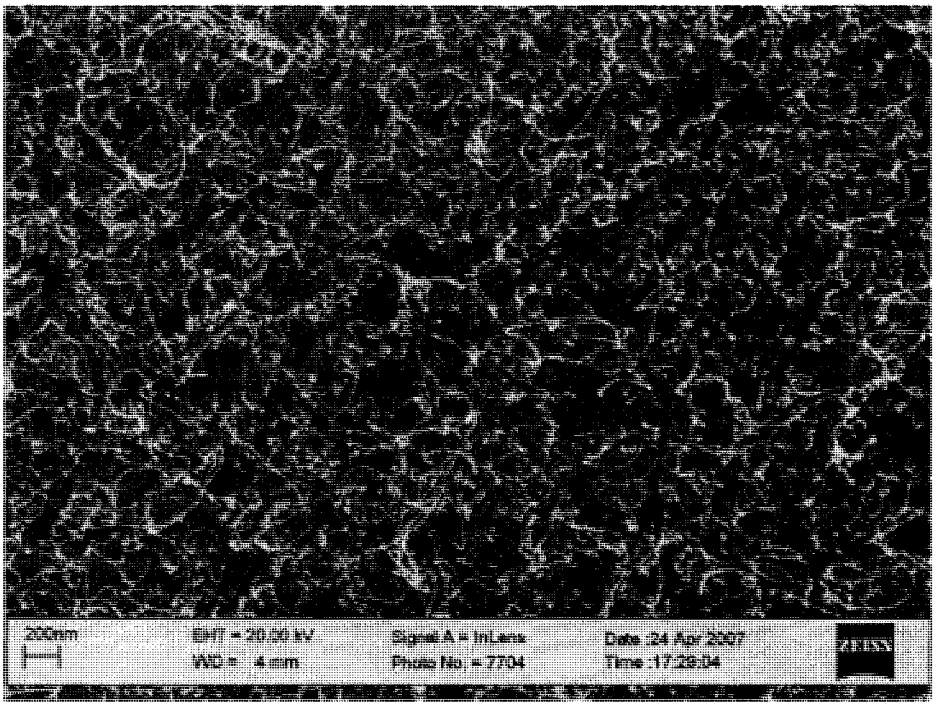

(a)

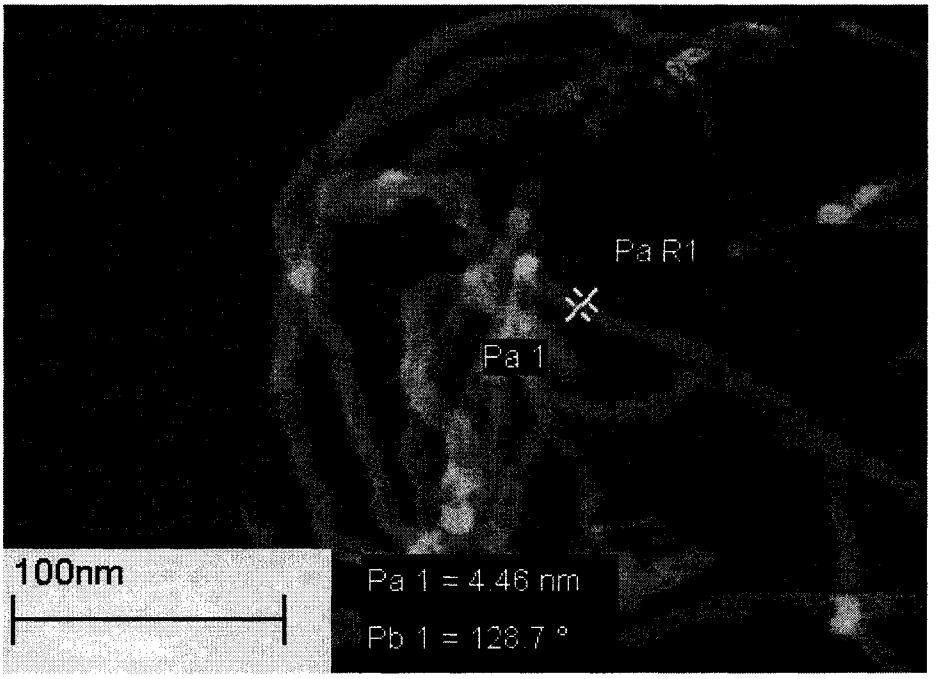

(b)

Figure 3-7 SEM Images of nanotubes (a) low resolution (scale 200 nm), and (b) high resolution (scale 100 nm)

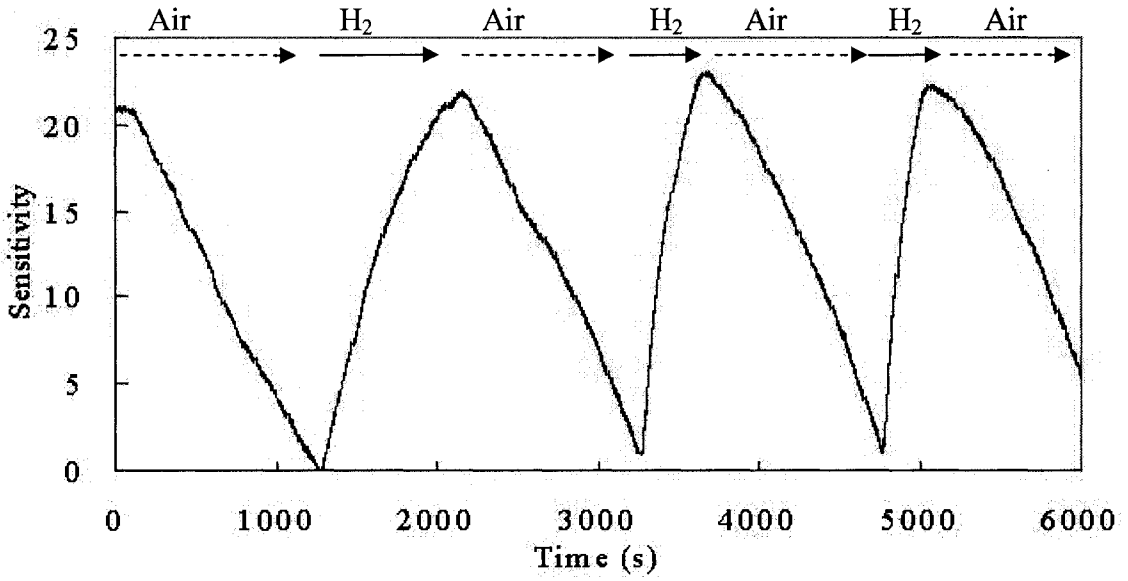

(a)

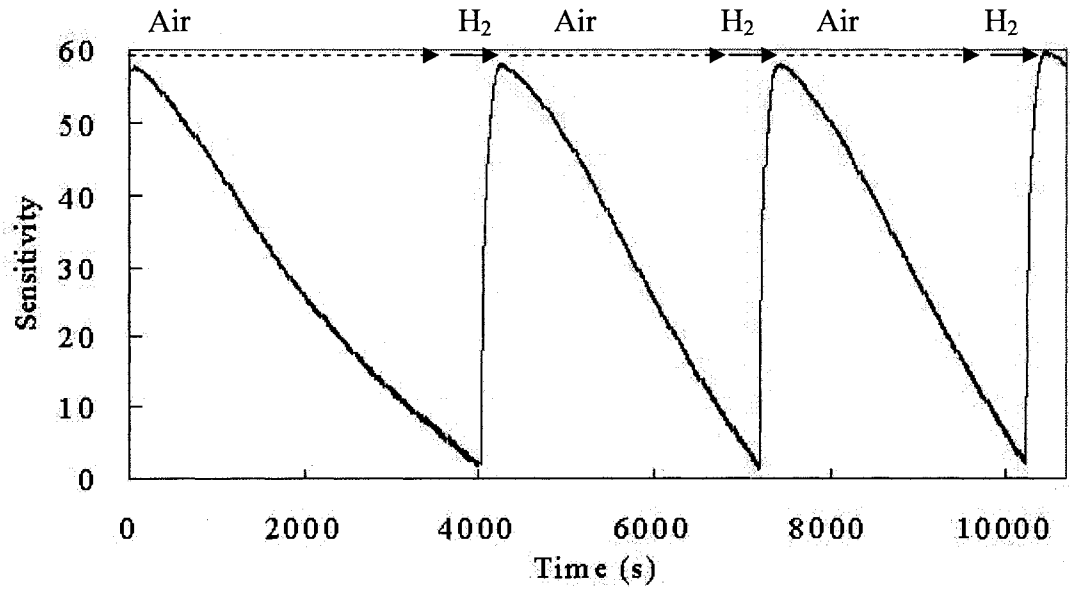

(b)

Figure 3-8 Sensitivity characteristics of MWCNTs based gas sensor for 20% H_2 (5% H_2 in Ar) in air at (a) 150 °C and (b) 300 °C

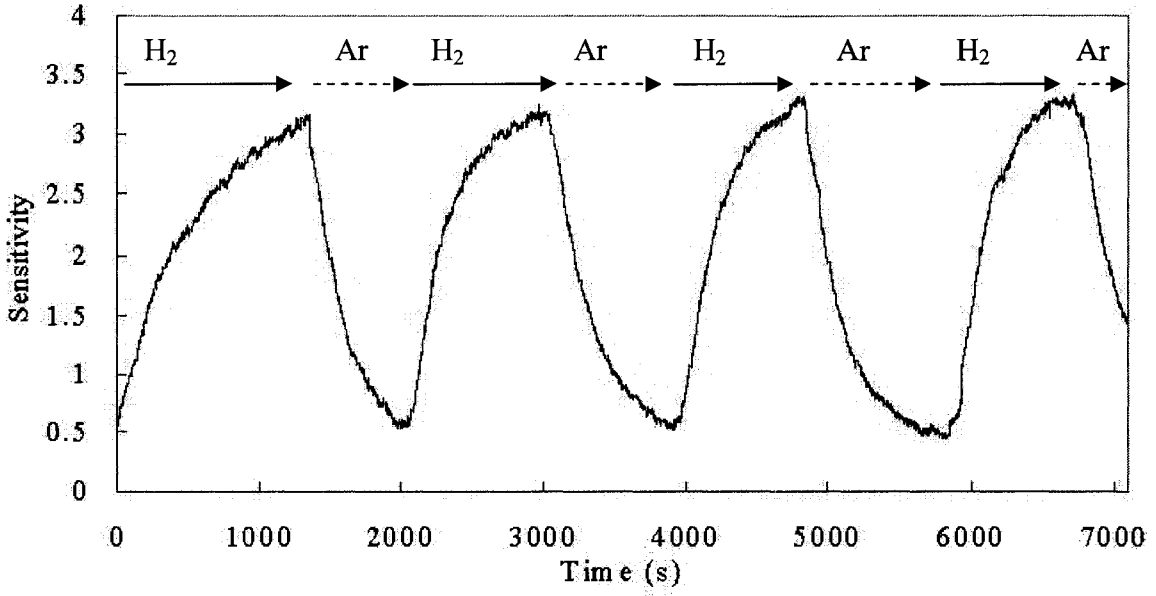

Figure 3-9 Sensitivity of MWCNTs based gas sensor for 5% H_2 in Ar at 80°C

One interesting property to note is that the resistance (conductivity) increases (decreases) with O_2 adsorption [67]. It was also reported that the resistance increased with NO_2 adsorption [128]. Since the O_2 molecule is electrophilic, charges are expected to transfer from CNTs to the physisorbed O_2. The conductivity drop upon gas adsorption can therefore only be explained when the CNTs is n-type. This is in contrast to the belief that the carrier of individual CNTs is p-type [129-131]. This phenomenon can be explained as follows. The CNTs placed between the two electrodes are composed of metallic and semiconducting CNTs, which are entangled and cross linked. We can therefore expect an equivalent parallel circuit as shown in Figure 3-10. The current was governed mostly by the metallic tubes, since the resistance of the semiconducting tubes is presumably large. The adsorption of O_2 on the metallic tubes reduces the number of electrons available and, as a consequence, the resistivity of the nanotubes increases. Since an individual nanotube shows p-type characteristics [12, 132], a critical concentration of the CNTs, where the semiconducting CNTs dominate the

current of the sensor, should exist for the conversion between n-type and p-type.

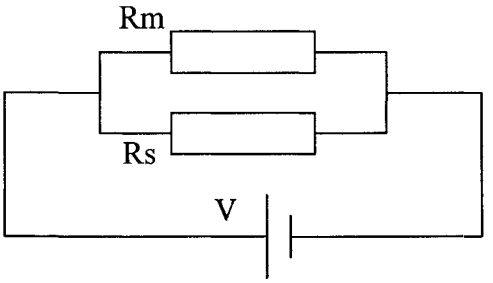

Figure 3-10 Equivalent parallel circuit of gas sensor

3.6 Conclusions

The CNTs were sysnthesized on the catalyst coated on Si/SiO_2 substrates as the core part of the gas detector. Gold was coated on two ends of CNTs film as electrodes. After being assembled, the gas detector was installed in the testing setup. The resistance of CNT-based gas detector was measured by a multimeter and recorded by a Labview computer program when gas (such as H_2) was passed and stopped. It was found that the sensitivity of this CNT-based gas detector was higher at 300 °C than 150 °C.

Chapter Four

4 Application of Carbon Nanotubes in Pressure Sensors

The fabrication and testing of the CNT-based pressure sensor are discussed in this chapter. The principle of the CNT-based pressure sensor is described with illustrations and formulas. The fabrication processes, including making membranes, preparing catalyst patterns, synthesizing CNTs, coating electrodes, and assembling pressure sensors, are described step by step. The testing setup is illustrated. The test results of pressure are discussed in two conditions.

4.1 Introduction

One of the widely used mechanical sensors is the pressure sensor. Currently the piezoelectric sensors were widely used for many applications. The CNTs can also be used to make pressure sensor. The CNT-based pressure sensors provide an alternative. The measurement range of the CNT-based pressure sensor should be very large because the strength of CNTs was high enough to bear huge strain when elongated and bent. A new pressure sensor made of CNTs was developed as shown in Figure 4-1. The CNTs were

synthesized on the membrane, and the CNTs were deformed when the membrane was bent because of the applied pressure.

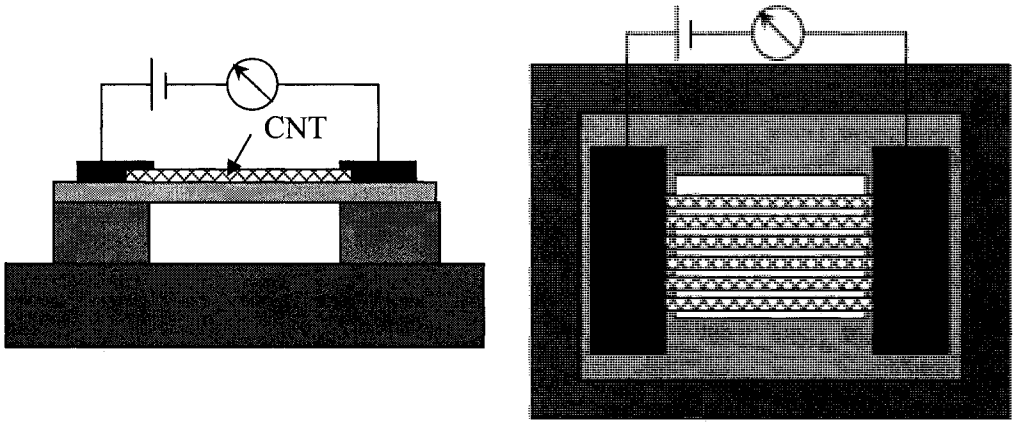

Figure 4-1 Pressure sensor made of CNTs: (a) cross section, (b) top view

4.2 Principle of CNT-based Pressure Sensors

The CNTs are conductive and the resistance of CNTs changes when the CNTs film is deformed by force. The CNTs were grown on membrane of substrates and metal electrodes were coated on the ends of CNTs film to connect the CNTs and the resistance measuring circuit. When pressure was applied on the sensors, the membrane was bent, and the CNTs film was also deformed. The resistance was changed because the connections between CNTs were increased or decreased when the CNTs moved under force. Then the pressure can be achieved by comparing the resistance change of CNTs.

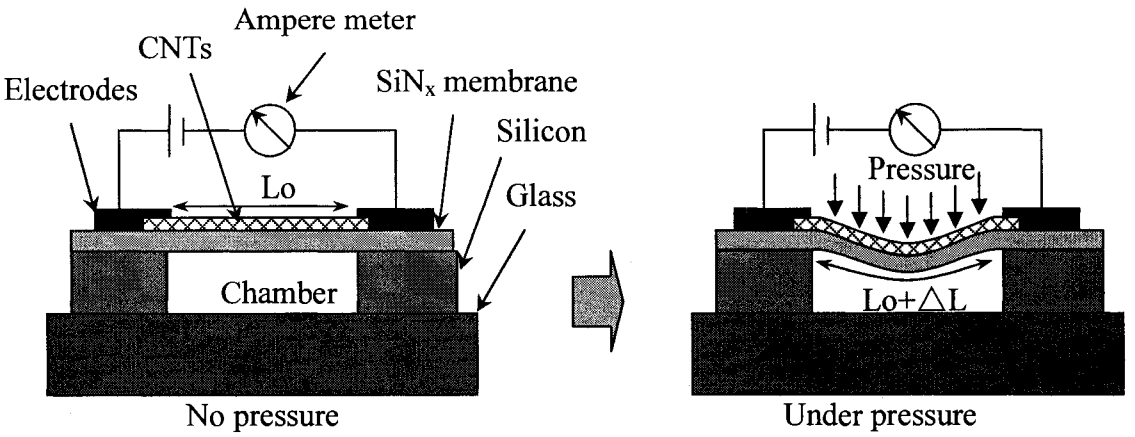

Figure 4-3 Pressure sensors without pressure and under pressure

4.3 Fabrication of CNT-based Pressure Sensors

The CNTs were synthesized on the SiN_x membrane layer on silicon substrates, and the silicon substrates were assembled with glass substrates to make a closed chamber. Gold was coated on the CNTs as electrodes to connect the circuit. The whole fabrication processes was shown in Figure 4-4.

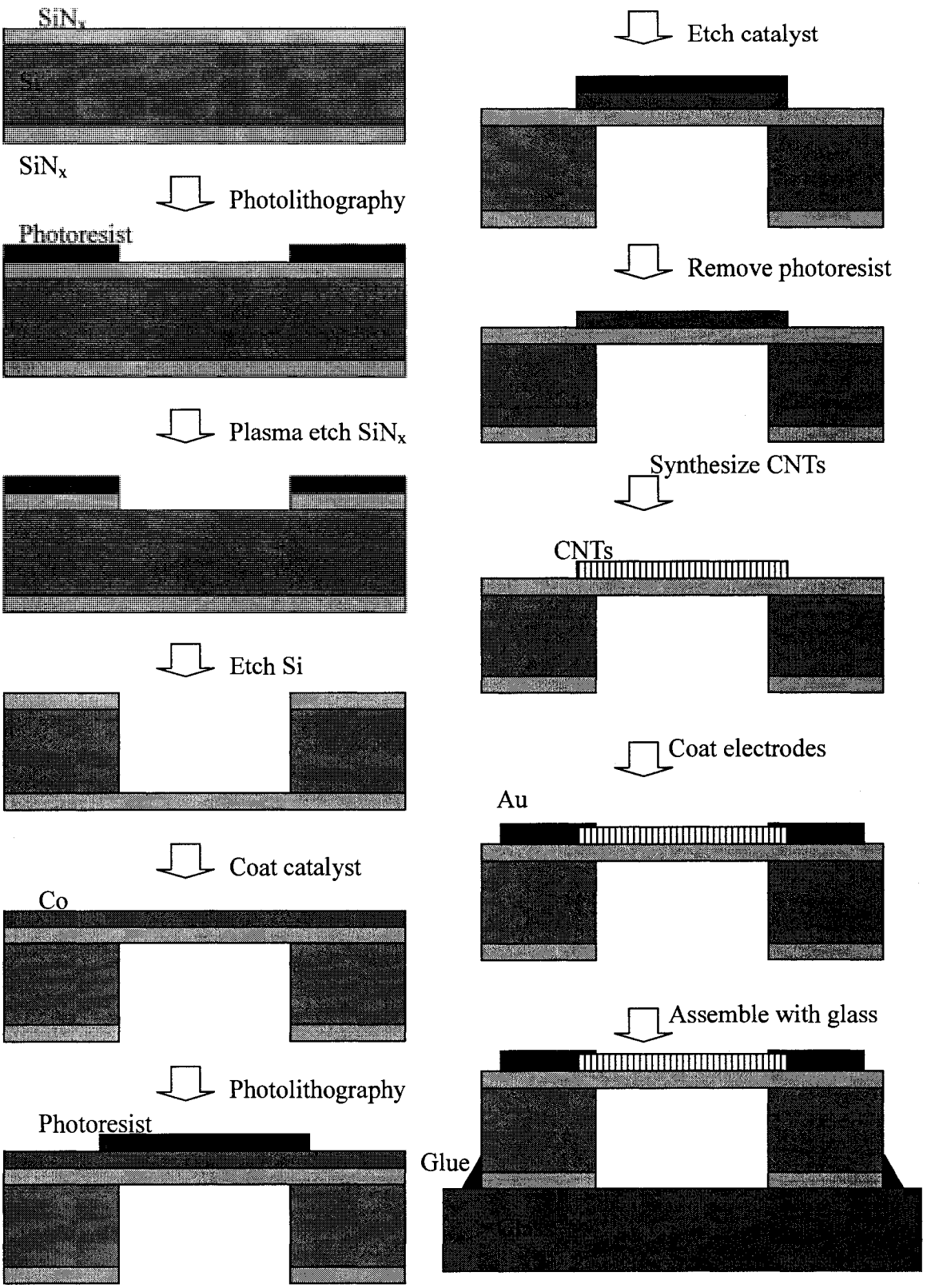

Figure 4-4 Processes of CNT-based pressure sensors

4.3.1 Fabrication of Silicon Nitride Membrane

The silicon wafers with SiN_x layers on both sides were selected as substrates. The thickness of the SiN_x layer is ~ 100 nm. The silicon layer at the middle is ~ 500 microns in thickness. The SiN_x at one side and silicon at the middle layer were etched to make a chamber at the center of substrates, and the other side SiNx was left to serve as membrane.

Firstly, the photoresist was coated on the Si/SiN_x substrates to make a pattern of a square hole. If this coating was to be done by photolithography, the Si/ SiN_x wafer cannot be put on spin coater directly. Otherwise the SiNx thin layer on the substrates will be broken by the absorbing of the air vacuum that cannot be seen by the eyes. There are two ways to avoid this: use the area out of the area absorbed by spin coater to make patterns; use tape to adhere substrates and do not touch the center area to be made into patterns. After the substrates were fixed on the spin coater, photoresist was coated on the substrates. The substrates were put in the oven to be soft baked for 20 min. Then the substrates were taken out and covered by a mask, and exposed under UV light for about 20 s, and put in the oven for 5 min. Next, the substrates were developed in developer solution for about 30 - 40 s, and rinsed with distilled water. After the substrates were dried, the other sides of substrates were totally coated with photoresist by hand to prevent etching. At last the substrates were kept in oven and were hard backed at 100 ^{o}C for 20 min.

This process can also be done by hand because low precision is accepted for this pattern and manual process can be easier and faster. Manually, the photoresist was applied on the substrates by soft material such as paper, and the center of substrates was left without coating. The other sides of substrates were also totally coated with photoresist. Then the substrates were hard baked at 100 ^{o}C for 20 min.

After being coated with photoresist and hard baked, the Si/SiN_x substrates were kept in the OXFORD Plasmalab 800 Plus CV020 Plasma Etching machine to etch the SiN_x layer on one side. The parameters for each step are shown in table 4-1, and there are three steps for plasma etching as shown in table 4-2. The etching was controlled by the automatic process program. After running the program, the nitrogen (N_2), oxygen (O_2) and fluorocarbon (CF_4) gases were mixed and passed in the chamber, high voltage and magnetic field were applied, and the temperature was adjusted to the set point, then the etching began after plasma was generated. The etching was kept for 8 -10 min, and the SiNx layer was totally etched and a little of the silicon was also etched. Then only N_2 was passed in to clean the chamber for 5 min, and then step 20 was run to reset status for finishing.

Table 4-1 Parameters Setting for Process steps of Plasma Etching

Step No.	12	13	20
Gas 1 (N_2) (%)	5	20	0
Gas 2 (O_2) (%)	2	0	0
Gas 3 (CF_4) (%)	10	0	0
LF Power (Watts)	100	0	0
HF Power (Watts)	0	0	0
Pressure (Torr)	0.4	0.4	0
Table Temperature (^oC)	20	20	-101

Table 4-2 Recipe of Plasma Etching

Step No.	Time (min)
12	8
13	5
20	5

After plasma etching, the photoresist on both sides of Si/SiN_x substrates was removed with acetone. The silicon at the middle of the substrates was etched by potassium hydroxide (KOH) solution or mixture of fluoric acid (HF) and nitric acid (HNO_3). 1 g of KOH was dissolved into 2 ml distilled water to make the KOH solution. The etching speed was about 1 μm/min at 80 °C. The HF and HNO_3 were mixed by a ration of 1:49 to make the solution, and the etching speed was about 0.25 μm/min. Usually, KOH solution was selected to etch the silicon. The baker containing KOH solution and Si/SiN_x substrates was heated on hot plate at 80 °C. The silicon layer was then etched totally after about 8 hrs, and the SiN_x layer was left at one side of the substrates. The SiN_x membrane was almost transparent. The substrates with SiN_x membranes were rinsed with distilled water and dried carefully. Part of the membrane on the silicon substrate was shown in Figure 4-5

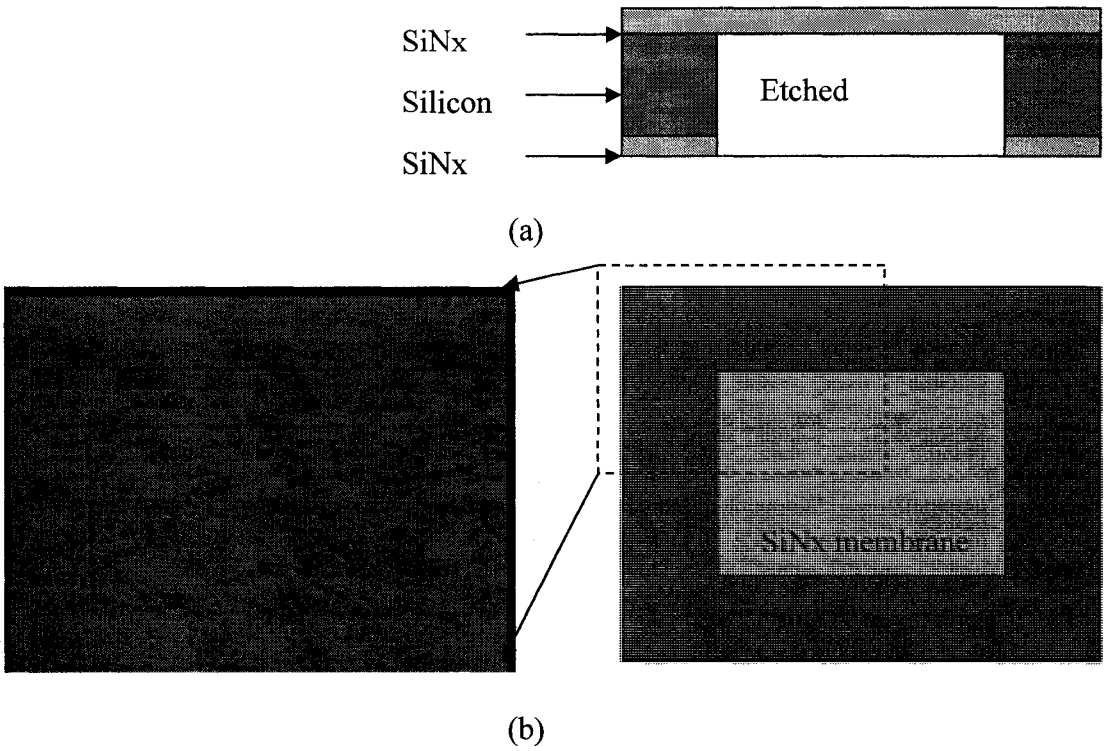

Figure 4-5 Membrane on silicon substrate (right bottom area): (a) cross section, (b) top view

4.2.2 Preparation of Catalyst Pattern on Silicon Nitride Membrane

In order to control the shape of CNTs on the SiN_x membrane, catalyst was etched to make special pattern on the substrates. The PVD was used to coat catalyst thin film on substrates, photolithography was used to make mask pattern of photoresist on the catalyst, and wet etching was used to etch the catalyst to make the pattern.

The Co used as catalyst was coated on the SiN_x membrane side of silicon wafer substrates by PVD. By controlling the thickness of Co coated on substrates, the density of CNTs can be changed, and the conductibility of CNT-based pressure sensors is variable.

Usually, a Co wire of 10 - 20 mm in length and 0.25 mm in diameter was used to be coated on silicon, the distance between catalyst/filament and substrates was 15 - 20 cm, and the thickness of catalyst was controlled at range of 5 - 50nm for pressure sensors.

Photolithography was done in the clean room to make mask of photoresist for etching the catalyst. As same as making SiN_x membrane, tape was used for the silicon substrates to adhere with SiN_x membrane on the spin coater. At first, MICROPOSIT S1813 positive photoresist was coated on the silicon substrates by spin coater. The rotate speed of spin coater was 4000 rpm, and the thickness of photoresist was about 100 μm. The silicon substrates coated with photoresist were soft baked at 80 °C for 20 min in the oven. After that, the silicon substrates were taken out from oven and put on the exposure plate, and the mask with the selected pattern was placed on the silicon substrates. The silicon substrates with photoresist were exposed for 20 s under UV light. The silicon substrates were put in the oven and baked at 80 °C for 5 min. Then the silicon substrates with photoresist were dipped into MICROPOSIT MF–319 developer solution to be developed for about 30 - 40 s. After the unexposed photoresist was removed, the silicon substrates were rinsed in distilled water to remove the developer and clean the silicon surfaces. Then the silicon substrates were put on the spin coater to throw off the water and putted in the oven to be hard baked at 100 °C for 20 min.

Cerium (IV) ammonium sulfate $[(NH)_4Ce(SO_4)_4 \cdot 2H_2O]$ solution was used to wet etch the Co catalyst. Usually, 5 - 20 mg cerium (IV) ammonium sulfate was dissolved into 5 - 20 ml distilled water to make the etching solution. The silicon substrates with photoresist pattern and Co were dipped into the cerium (IV) ammonium sulfate solution for 10 - 60 s. After the Co uncovered by photoresist was etched totally, the silicon substrates were rinsed with

distilled water. Then the photoresist was removed with acetone. At last, the silicon substrates with catalyst patterns were rinsed by distilled water and dried. The substrates were ready for growing CNTs as shown in Figure 4-6.

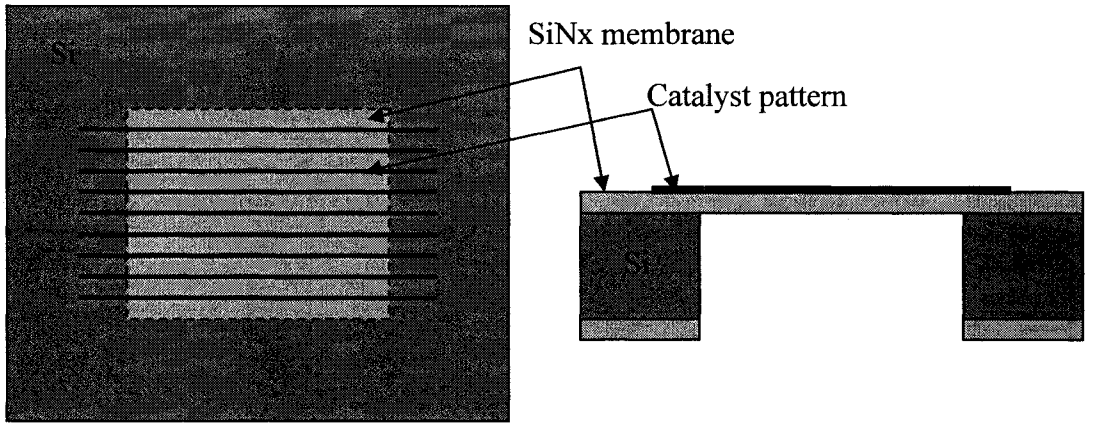

Figure 4-6 Coating catalyst pattern on SiN_x membrane

4.3.3 Synthesis of Carbon Nanotubes on Silicon Nitride Membrane

After the catalyst patterns were made on the SiN_x membrane on silicon substrates, they were put into the CVD system to synthesize CNTs. The silicon substrates were put on the quartz base frame, and the quartz base frame was placed at the center (zone 2) or the end (zone 3) of quartz tube of CVD system. A tungsten wire (15 - 20 cm length, 0.5 mm diameter) was formed into coil to be used as filament to decompose the methane. The filament was attached at the end of two copper electrodes that were fixed on the aluminum cap at the end of quartz tube. The copper electrodes go through the holes on the aluminum cap and were connected to power regulator, which can adjust the AC voltage applied on electrodes from 0 V to 110 V. The electrodes were insulated from the cap by ceramic, and the holes were sealed

well. Then the bolts of cap were tightened to seal the end of quartz tube.

The hydrogen and methane gases were opened for a moment to clean pipes first. The hydrogen flow rate was kept at 50 sccm for 1 – 1.5 hrs to exhaust the air in the CVD quartz tube. The CVD furnace was turned on to heat the quartz tube. The temperature was raised to 400 °C and kept for 1 hr to pre-heat the substrates and transfer the metal oxide into metal in hydrogen environment. Then it was ready to grow CNTs: temperature of CVD furnace was raised to 600 °C, hydrogen flow rate was kept at 50 sccm, methane was open and kept at flow rate 10 sccm, and 10V~15V voltage was applied on the filament to heat it to 1500 °C to 2000 °C. The color of filament was from dark red to orange, until almost white. Those conditions were kept for one to 2 hrs to grow CNTs. After that, voltage on filament was turned off, CVD furnace was turned off, methane was closed, and hydrogen was kept passing until the CVD furnace was cooled down to lower than 100 °C.

After the CVD furnace was cool to room temperature, the silicon substrates with CNTs can be took out from the quartz tube for next process.

4.3.4 Assembling of CNT-based Pressure Sensors

Gold was coated on the CNTs synthesized on the substrates to make a circuit for connection. Firstly, an aluminum film was cut to cover the center part of CNTs pattern on the silicon substrates, and small areas at the two end of CNTs pattern were not covered. The samples were kept in PVD chamber to coat gold at the two ends of CNTs patterns. A gold wire (10 - 15 mm in length, 0.5 mm in diameter) was used for coating. After PVD coating, the aluminum film was removed. Gold was coated on the CNTs and silicon substrates at two ends of the samples. Two wires are connected to the gold coated on the silicon substrates to

connect the CNTs to multi-meter for measuring resistance.

The silicon substrates with SiN_x membrane were adhered on glass substrates by glue to make a small closed chamber between them. The CNTs on the SiN_x membrane face outside. The pressure sensors were ready for testing after the glue was dried. The finished pressure sensor is shown in Figure 4-7.

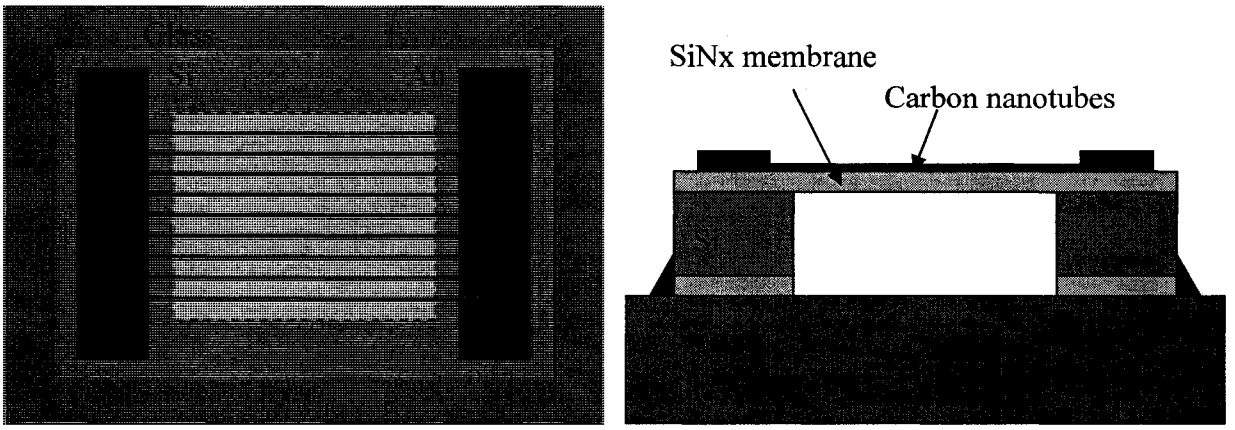

(a)

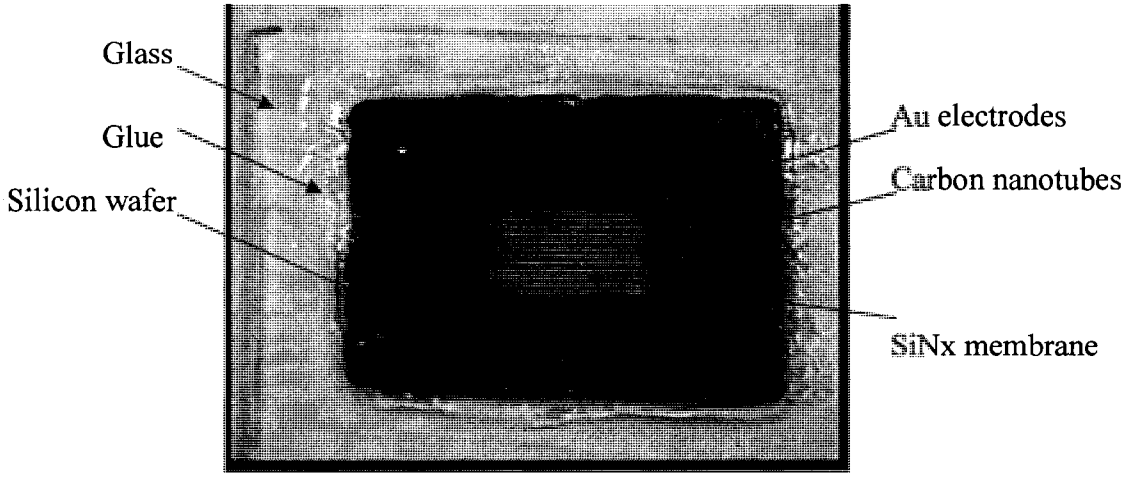

(b)

Figure 4-7 Finished pressure sensor: (a) Schematic of assembled pressure sensor (b) picture of whole pressure sensor

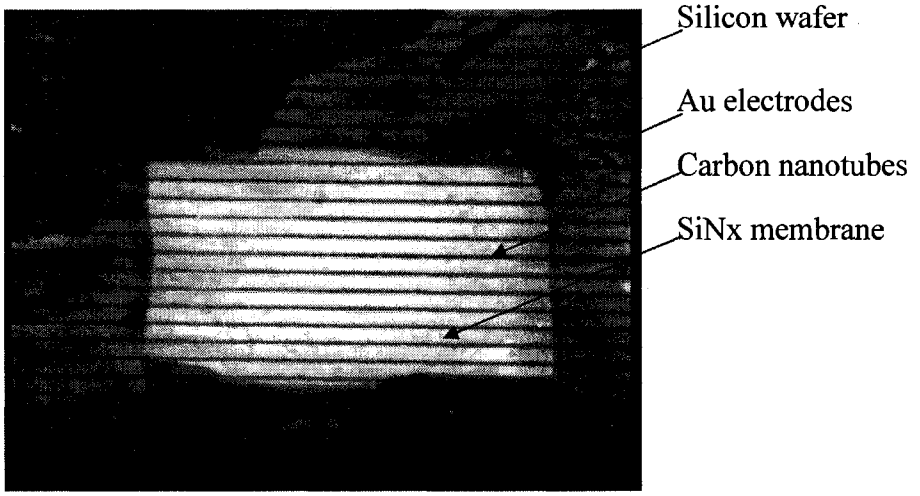

(c)

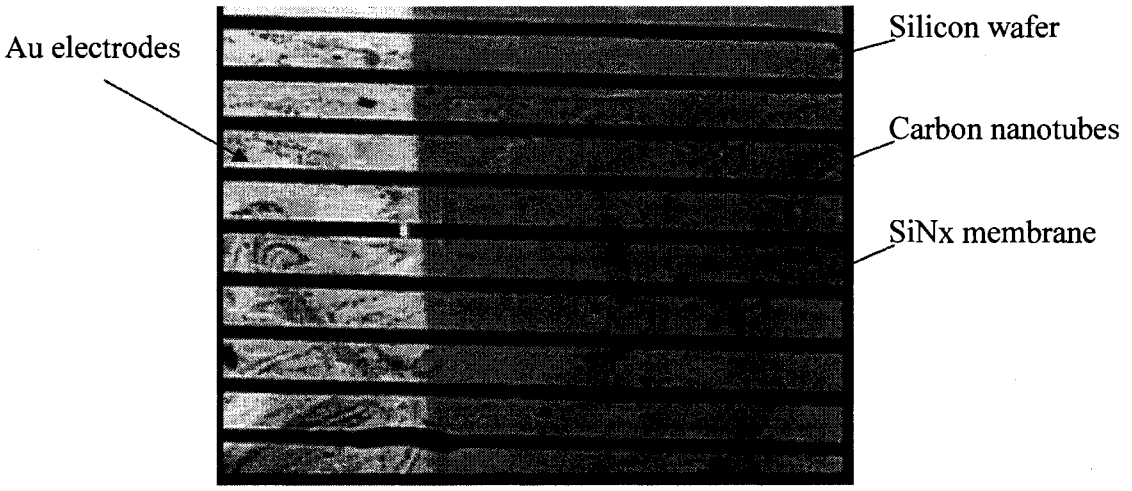

(d)

Figure 4-7 continued: (c) CNTs grown on membrane (central rectangle area) (d) Au electrodes (left area) coated on CNTs

4.4 Testing of CNT-based Pressure Sensors

The CNT-based pressure sensors were installed in the testing setup to test the properties under pressures. The resistance of CNTs was measured by multimeter and recorded by

Labview program when pressure was applied and released.

4.4.1 Testing Setup

The testing setup for CNT-based pressure sensor is shown in Figure 4-8. A small base was made to fix and connect the pressure sensors. Two copper electrodes touched the pressure sensors on the gold electrodes spot and were tighten to push the pressure sensors to fix it on the base. The whole small base was put into a strong container with two metal gas pipes through the cap. The two copper electrodes on the small base were connected to two gas pipes separately, and two gas pipes were connected to multimeter by copper wire. The cap of the bottle was closed and sealed well. One gas pipe was connected to compressed air inlet to apply gas pressure on the sensors. The other gas pipe was connected to a pressure gauge to read the pressure inside the bottle and on the sensors. The multimeter was connected to the pressure sensors to measure the resistance of CNTs and the computer to record the resistance.

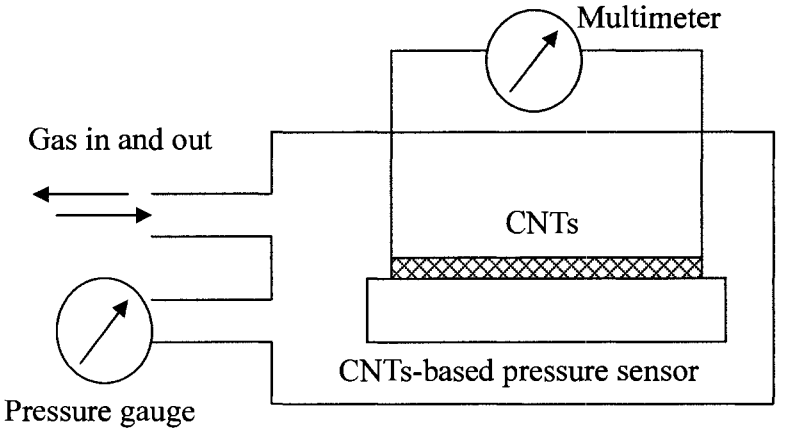

Figure 4-8 Testing setup of CNT-based pressure sensor

4.4.2 Testing Processes

After the container with pressure sensors was connected well to air inlet and pressure gauge, the system was ready for testing. The multimeter was turned on to record the resistance of the pressure sensors. After resistance reading was stable, the air inlet was opened to increase the pressure on the pressure sensors according to the air coming in the container, and the pressure gauge reading was changed too. When the air inlet was closed, the pressure gauge reading should be stable. After the air was out slowly, the pressure gauge reading decreased gradually. The time of opening and closing air, pressure gauge reading, and sensors resistance were recorded at the same time when actions were taken.

4.5 Results and Discussions

After several pressure sensors were tested, there were two different results: resistance of pressure sensors increase when pressure increase as shown in Figure 4-9 (a), and the resistance decrease when pressure increase as shown in Figure 4-9 (b). The difference should be caused by the density and physiognomy of CNTs grown on the pressure sensors.

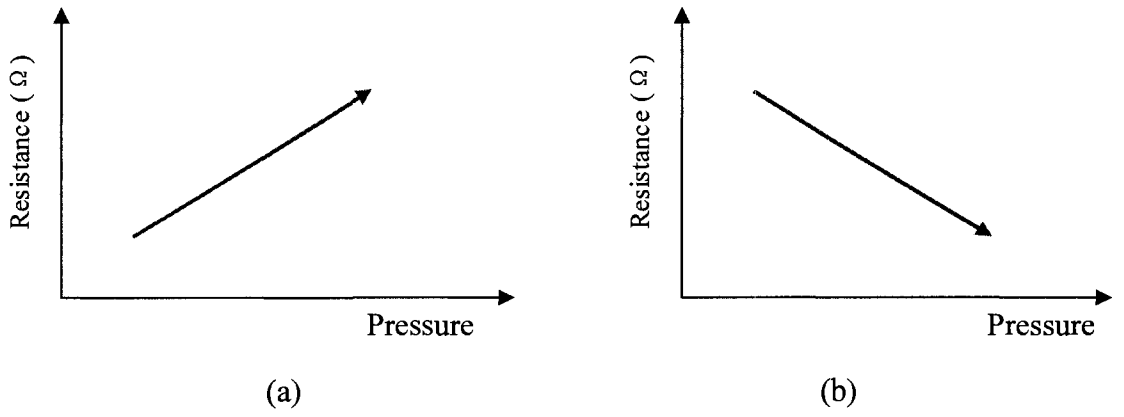

(a) (b)

Figure 4-9 Effects of pressure on resistance change: (a) Resistance increase when pressure increase, (b) Resistance decrease when pressure increase

The transformation of CNTs can be considered from both macro scale of CNTs film and micro scale of single CNT. For macro scale, when the CNTs film was pulled by forces, the length was elongated, and thickness was decreased. When the CNTs film was compressed, the length was decreased, and the thickness was increased. For micro scale, when the CNTs were pulled, each CNT was elongated, and became straight from curve, and some CNTs moved oppositely on the direction of out force. This can be considered as the length of CNTs film was increased at macro scale. The distance between CNTs on the direction perpendicular to out force was decreased. This can be considered as thickness decreased at macro scale. When the CNTs were compressed, each CNT was released from elongation, and some CNTs moved toward each other and became closer. If the movement was stopped by other CNTs on the force direction, the CNTs were bent and some moved on the perpendicular direction of out force, so the CNTs thickness increased.

4.5.1 Resistance Increases when Pressure Increases

If the density of CNTs on the pressure sensors was very low, and the CNTs lied on the surface and cross-linked to each other, the CNTs should move oppositely and the CNTs film was elongated as the SiN_x membrane was bent when pressure increased as shown in Figure 4-10. Some CNTs were not connected to each other anymore because of the elongation. So the resistance R of pressure sensors increased.

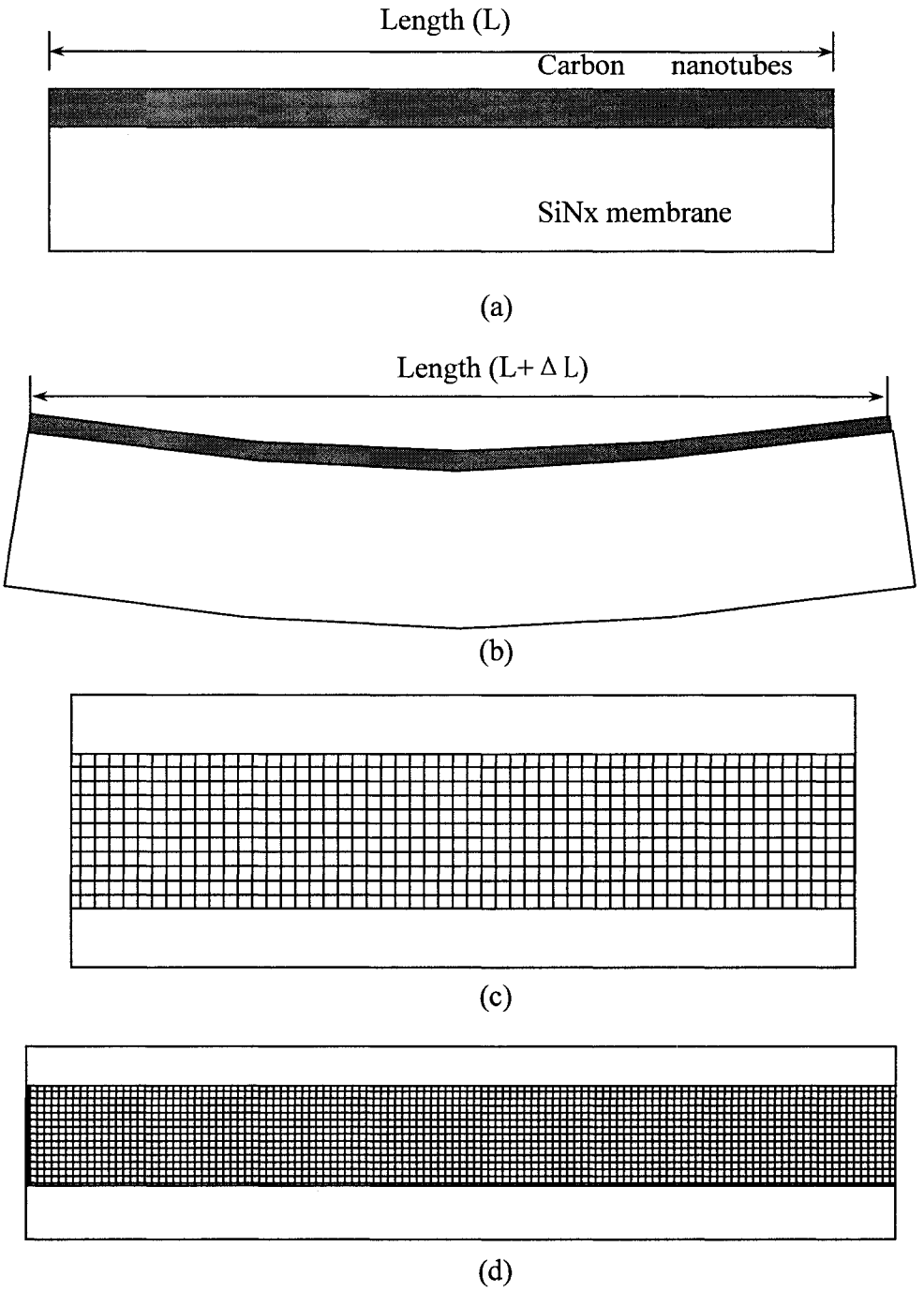

Figure 4-10 Thin film of CNTs was elongated when membrane was bent: (a) cross section without pressure, (b) cross section of elongation when bent under pressure, (c) top view without pressure, (d) top view of elongation under pressure

As shown in Figure 4-11, the resistance of a pressure sensor increased when pressure increased. The resistance was almost stable after the experiment had been started for 900 s, then the pressure was increased to 5 psi, the resistance also increased quickly. And then the resistance was kept at almost the same level when the pressure was kept unchanged. After 900 s, the pressure inside was released, and the resistance pulled back to the original level. After another 200 s, those processes were repeated again, and the resistance increased and pulled back when pressure was increased and released.

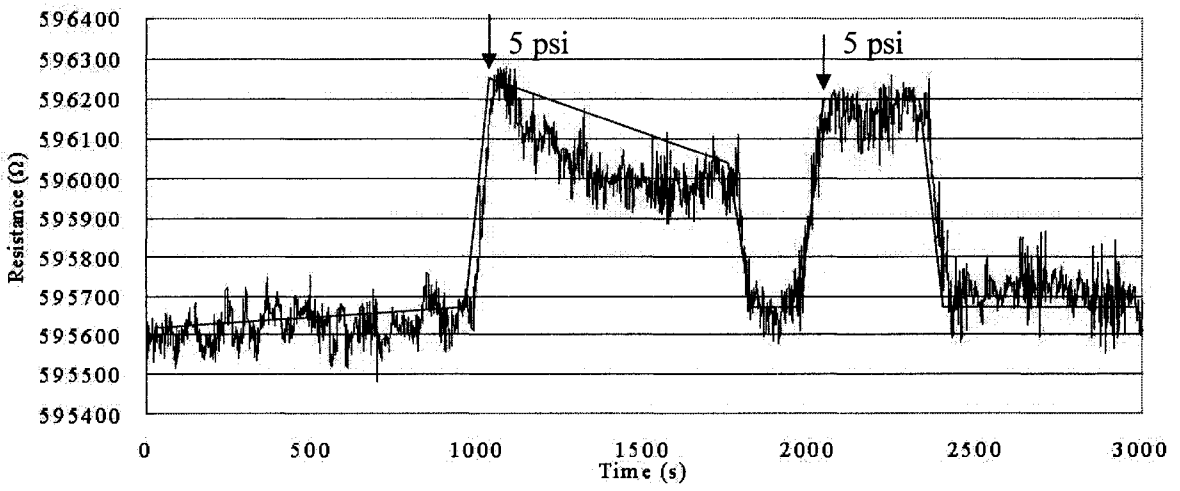

Figure 4-11 Resistance increase at low CNTs density

4.5.2 Resistance Decreases when Pressure Increases

If the density of carbon nanotbues on the pressure sensors was very high, and the CNTs film was thick and CNTs grew upward perpendicular to the substrate, then the film could be considered as multi-layer. The top part of CNTs film was compressed and the CNTs became

closer as the SiN_x membrane was bent when pressure increased as shown in Figure 4-12. More CNTs connected to each other, this could increase the conductance. So the resistance R decreased when pressure increased.

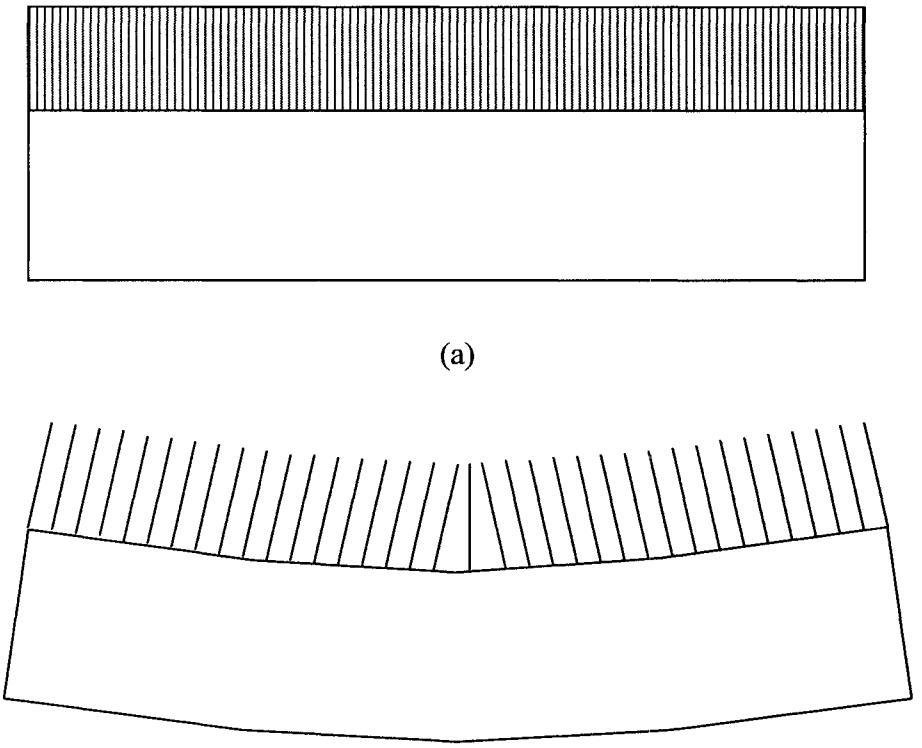

(a)

(b)

Figure 4-12 Thick film of CNTs was compressed when membrane was bent: (a) cross section of CNTs without pressure, (b) cross section of individual CNTs becoming closer when bent under pressure

As shown in Figure 4-13, the resistance of a pressure sensor decreased gradually when pressure increased step by step. The gas was opened to enter the container after the experiment had been started for about 250 s, the pressure increased to 4 psi, and the resistance decreased about 1500 Ω. The pressure was kept at the same level for about 150 s,

and the resistance kept almost the same level. Then the pressure was increased to 6 psi, the resistance was increased again for about 1000 Ω. The pressure was kept for about 100 seconds, then pressure was increased to 8 psi, and the resistance decreased for about 700 Ω.

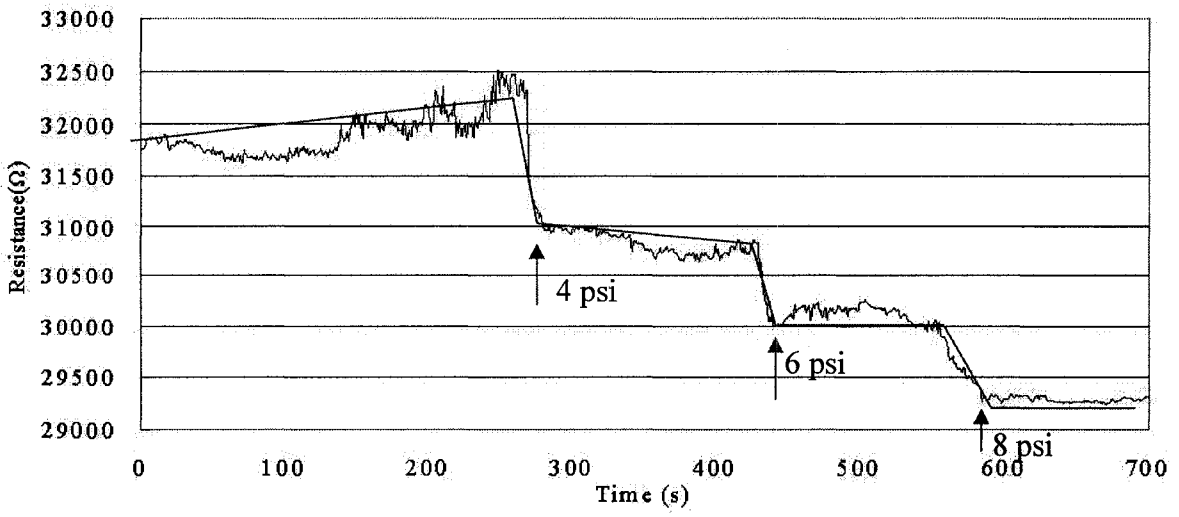

Figure 4-13 Resistance increase at high CNTs density

4.5.3 Full Testing of One Pressure Sensor

The Figure 4-14 shows the resistance of one pressure sensor that was tested continuously by applying and releasing different pressure. Those processes include applying and keeping constant pressure (200 - 700 s), repeating applying certain pressure and releasing pressure (1100 - 1700 s), applying increased pressure at each time (1700 - 2400 s), and increasing and decreasing pressure continuously (2800 - 3200 s).

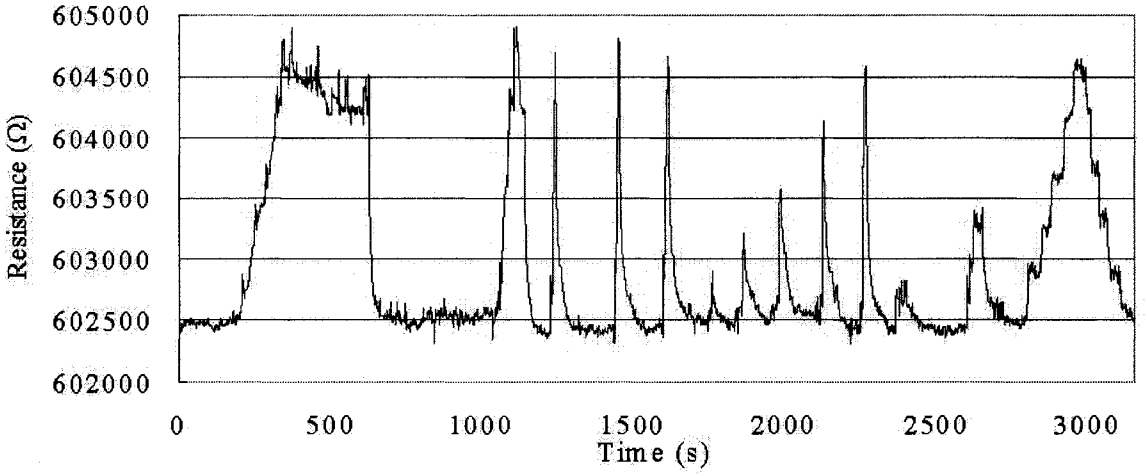

Figure 4-14 All the test data of one pressure sensor

When repeated applying the same pressure at each time, the gas was opened and came in the container containing pressure sensor until the pressure reached 12 psi, then the gas was let out and the pressure was released. The process was repeated for 4 times, and each time the resistance reached almost the same peak and pulled back to the same level as shown in Figure 4-15. This means the pressure sensor is sensitive, constantly repeatable and reusable.

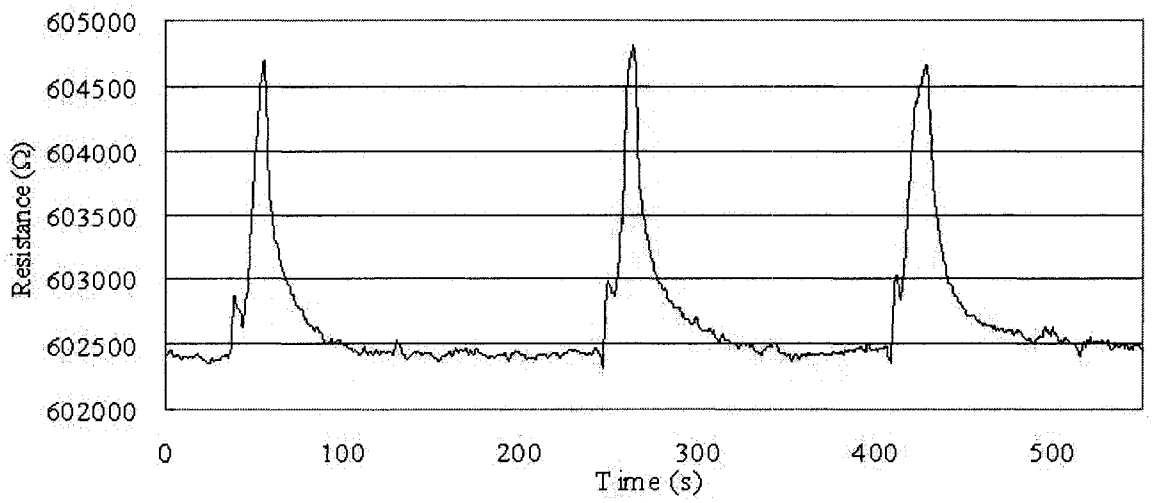

Figure 4-15 Repeatability of sensor under the same pressure

When the pressure was increased time by time, different pressure was applied on the pressure sensor, and then released each time. The pressure increased from 4 to 6, 8, 10, and 12 psi. The resistance increased to higher and higher peaks according to the pressure increasing, and then pulled back after pressure was released as shown in Figure 4-16.

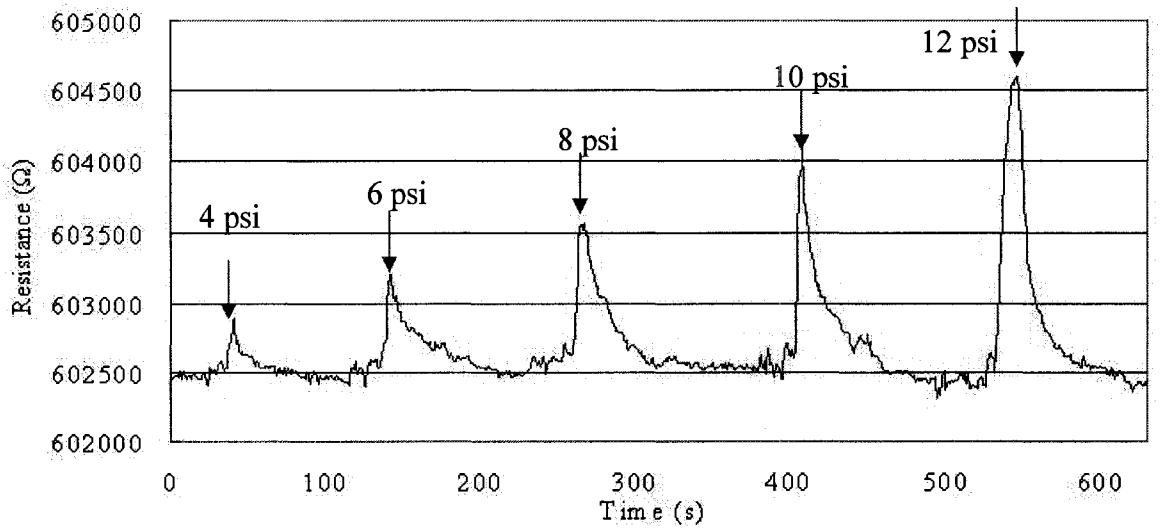

Figure 4-16 Change of sensor signal with increase of pressure

When the pressure was increased continuously, the pressure was increased from 4 to 6, 8, 10, and 12 psi without release, then pressure was decreased step by step from 12 to 10, 8, 6, and 4 psi. The resistance increased and decreased gradually when the pressure was increased and decreased as shown in Figure 4-17.

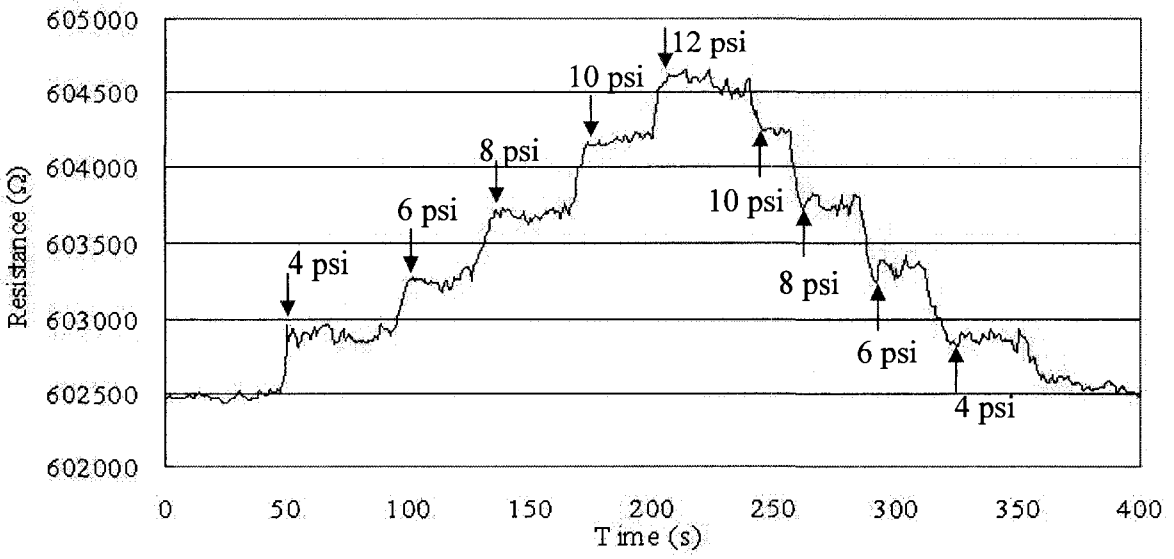

Figure 4-17 Increasing and decrease pressure gradually

The relation between the pressure and resistance of this CNT-based pressure sensor is shown as Figure 4-18.

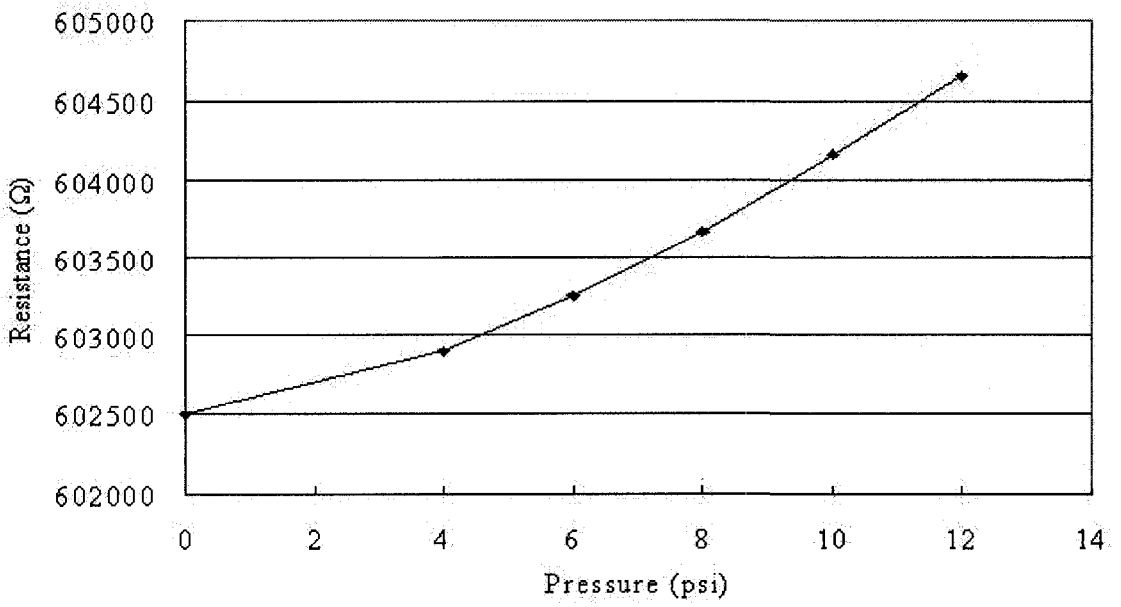

Figure 4-18 Relation of pressure and resistance of CNT-based pressure sensor

This full test of the pressure sensor showed that the sensor was sensitive, scaleable, repeatable and reusable to measure pressure for range of 4 to 12 psi. As the SiN_x membrane was fragile, the pressure sensor can not measure pressure higher than 30 psi currently.

4.6 Conclusions of CNT-based Pressure Sensors

The CNTs were grown on the SiN_x membranes made from silicon wafers with SiN_x layers on both sides, which were assembled with glass substrates to form closed chambers. The membrane was bent when pressure was applied, and the CNTs film was deformed at the same time. According to the different thickness and configuration of CNTs film, there were two responses of the deformation: the resistance increased when the CNTs film was thin, the resistance decreased when the CNTs film was thick. The full testing of one thin film CNT-based pressure sensor showed that the sensor was sensitive, scaleable, and repeatable. The range of the pressure sensor measurement was 0~30 psi currently.

Chapter Five

5 Application of Carbon Nanotubes in Field Emission Display (FED)

The fabrication and testing of CNTs array used as tips for field emission display are discussed in this chapter. The field emission properties of CNTs were discussed with the testing results.

5.1 Introduction

Among possible application of CNTs, electron field emission display (FED) has been widely investigated. Sharp and small tips were used in field emission display to send out electrons. Smaller tip is better for emission, and higher density of tips makes higher resolution. Low emission threshold voltages, high emission current densities, purity, chemical stability and nanostructure of emitters are the advantages of CNTs over other proposed emitters materials. The CNT based prototype FEDs have been demonstrated with low emission threshold (1 - 5 V/μm) and long operation time (> 5000 hrs).

Most of the methods synthesizing CNTs required substrate temperature higher than 700 ^{o}C and vacuum levels better than 50 Torr. Because of high substrate temperature and vacuum

requirements, fabrication of large-area FED using direct coating was difficult. Specially, large-area display devices need low cost substrates like nonalkaline glass which can operate relatively at temperature lower than 600 °C. Due to technical limitation, the CNTs were blended with polymer matrix to print the display matrix on a substrate. It has been demonstrated that the performance of displays have been reached to the requirement in household devices. However, if a methodology is available to coat CNTs without vacuum requirements and substrate temperature below 600 °C, large-area low cost substrates can be used for mass production of FEDs at low cost.

As the CNTs could be grown at low temperature 450 °C using the hot filament CVD system, the CNTs could be grown on nonalkaline glass and silicon substrates which can resist 550 °C. This part of research is to apply the CNTs in FED devices. Therefore, electron field emission properties of CNTs produced by the present method were also investigated.

The field emission display made of CNTs was illustrated in Figure 5-1.

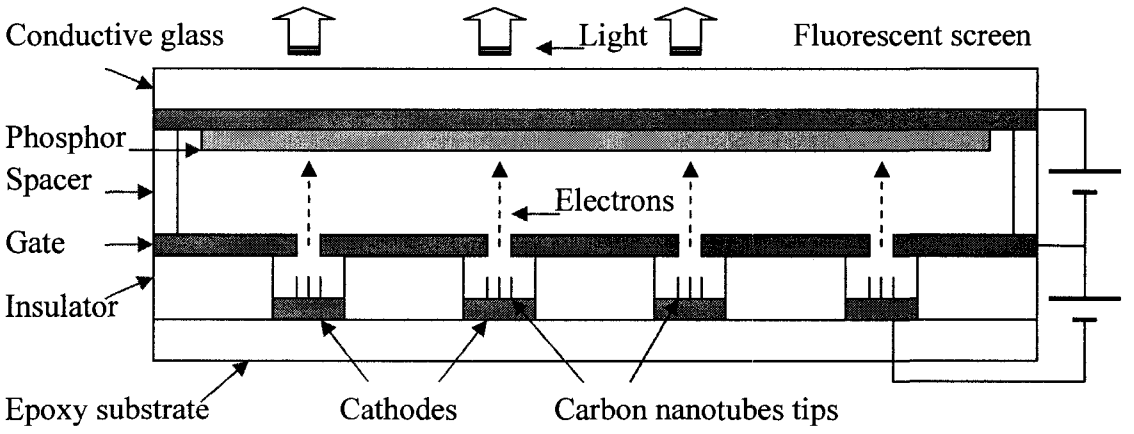

Figure 5-1 Schematic diagram of Field Emission Display made of CNTs

5.2 Fabrication of CNT-based Field Emission Display

Cathodes electrodes and catalyst were coated on glass substrates, and then CNTs were grown on cathode plate by hot filament CVD system. The cathode plate was assembled with ITO glass to make the field emission display unit. The FED was tested by measuring the current passing through the CNTs. The whole process was shown in Figure 5-2.

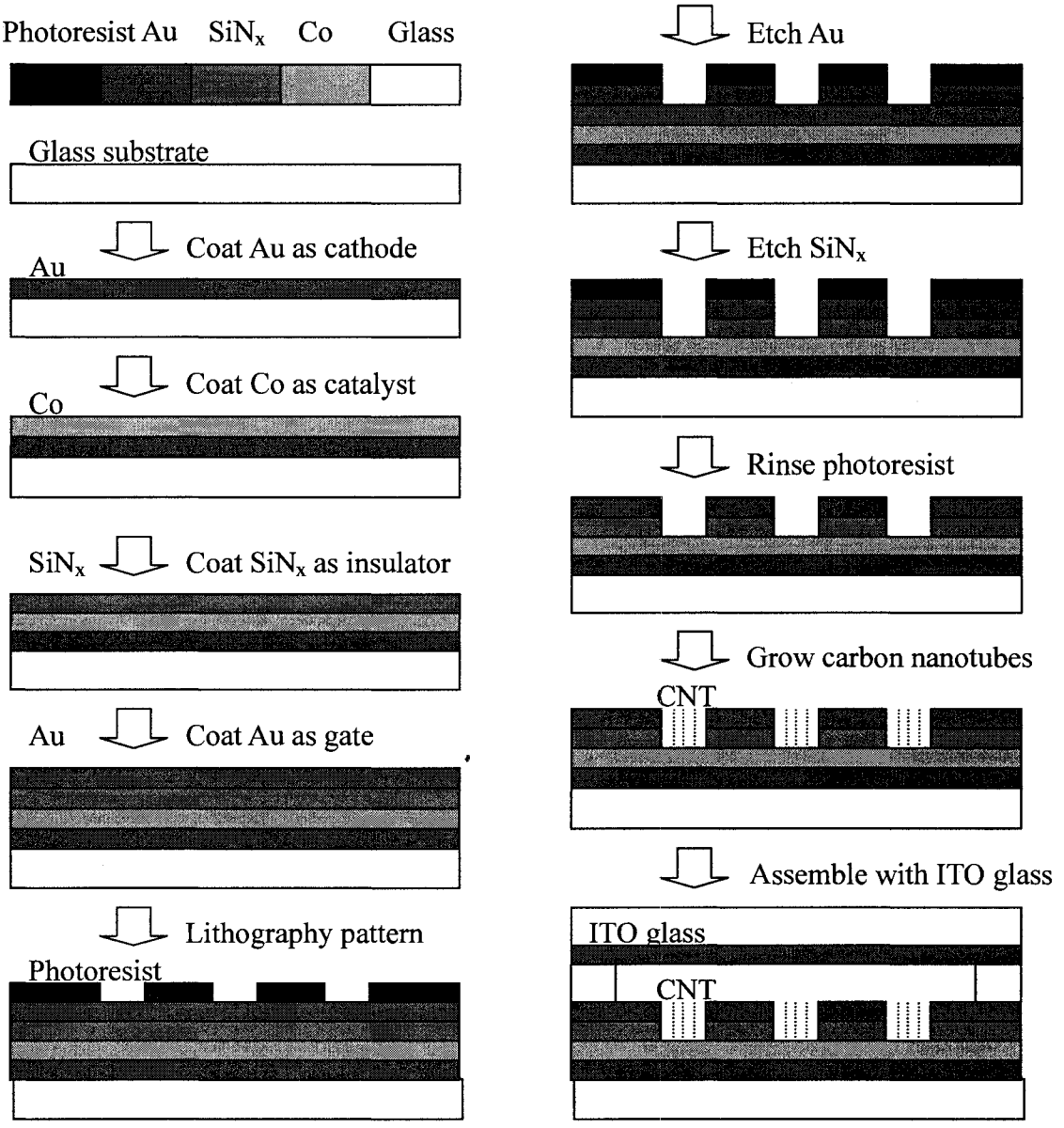

Figure 5-2 Fabrication processes of CNT-based Field Emission Display

5.2.1 Preparation of Substrates

The glass was used as substrate for cathode plate. Gold was coated on the glass first by PVD to be used as cathode electrodes. The Co was coated on the gold for 5 - 10nm in thickness by PVD to be used as catalyst for CNTs synthesis. Then SiN_x was coated on the Co film by PVD to be used as insulator. The pattern array of small holes with 20 μm in diameter was made by photolithography on the substrates. The photoresist was used as mask for etching. The substrates were etched by plasma etching to make holes on SiN_x film. After the photoresist was removed, the substrate was done as shown in Figure 5-3.

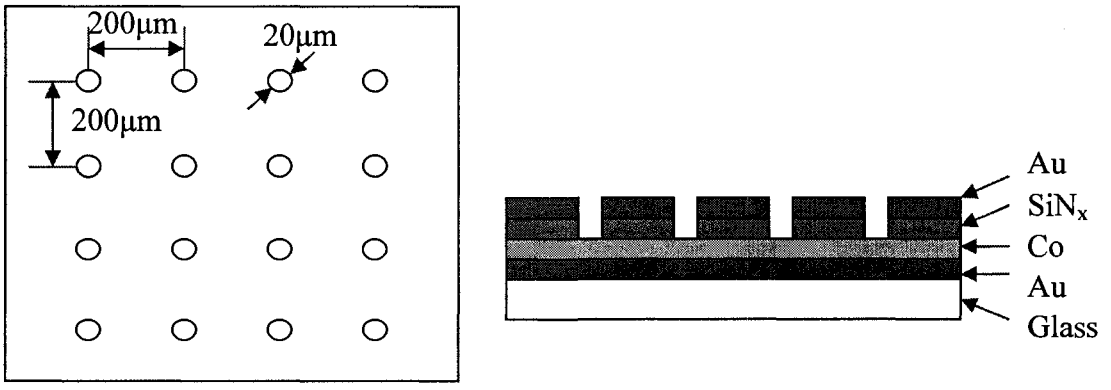

Figure 5-3 Substrates with holes array for CNTs growth

5.2.2 Synthesis of Carbon Nanotubes

The glass substrate coated with Au electrodes, Co catalyst, and SiN_x insulator, was placed in the hot filament CVD system to synthesize CNTs. The CVD furnace was heated to

500 °C lower than the glass melting point. 10 sccm CH_4 and 50 sccm H_2 were passed in to grow CNTs for 1 hr. Cluster of CNTs were grown from the cobalt in the holes of SiN_x film as shown in Figure 5-4.

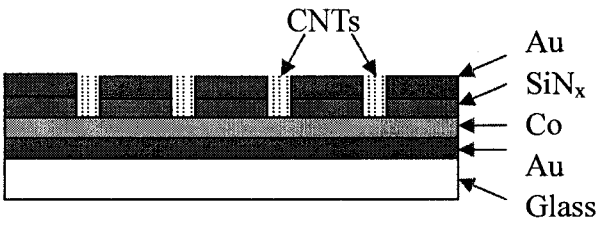

Figure 5-4 CNTs synthesized with Co in the holes of SiN_x film

5.2.3 Assembling of CNT-based Field Emission Display

The cathode plate grown with CNTs was assembled with conductive glass (ITO glass) to make field emission display as shown in Figure 5-5. The ITO glass was separated from the cathode plate by insulating glass of thickness 2 - 4 mm. The ITO glass and cathode plate were fixed together by clamps and sealed by glue.

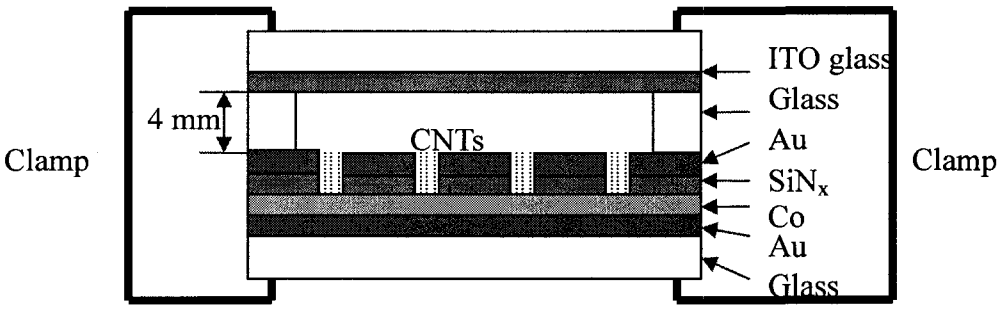

Figure 5-5 Assembled CNT-based FED

5.3 Testing of CNT-based Field Emission Display

Voltage was applied on cathode plate and ITO glass, and the current was recorded as

shown in Figure 5-6. The voltage varied from 5 V to 50 V according to the CNTs and the distance between cathode plate and ITO glass.

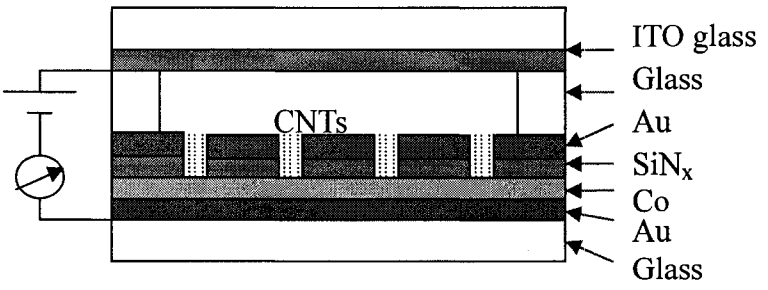

Figure 5-6 Test setup of CNT-based FED

5.4 Characterization

Characterization of the CNTs was carried out using Raman spectrum (532 nm), SEM and TEM. The CNTs array is shown in Figure 5-7. The size of the CNTs dot used as emitter tips is 20 μm. The distance between CNTs dot is 200 μm. Field emission testing was carried out in a vacuum chamber ($<10^{-7}$ Torr). The samples were connected to an insulated micrometer so that distance between electrodes could be determined.

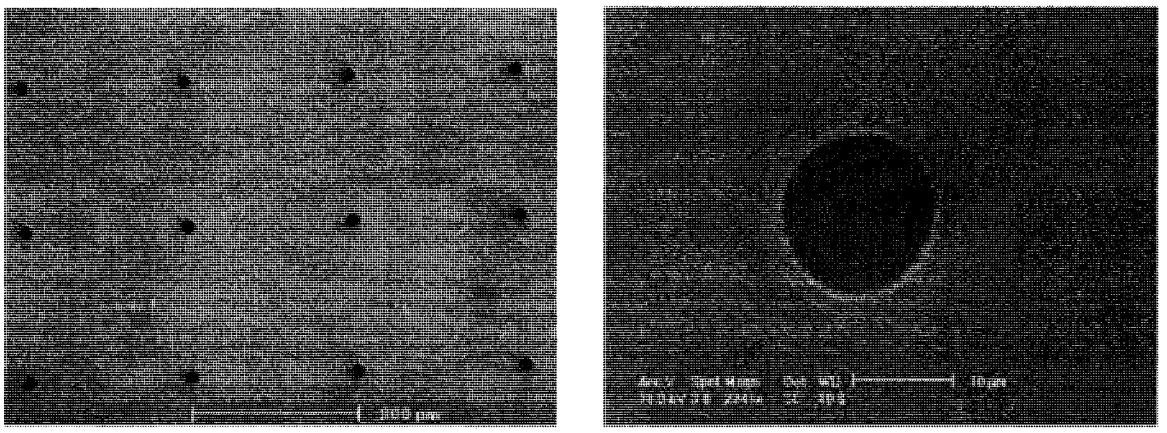

(a) (b)

Figure 5-7 SEM images of CNTs array for FED: (a) pattern array, (b) one pattern

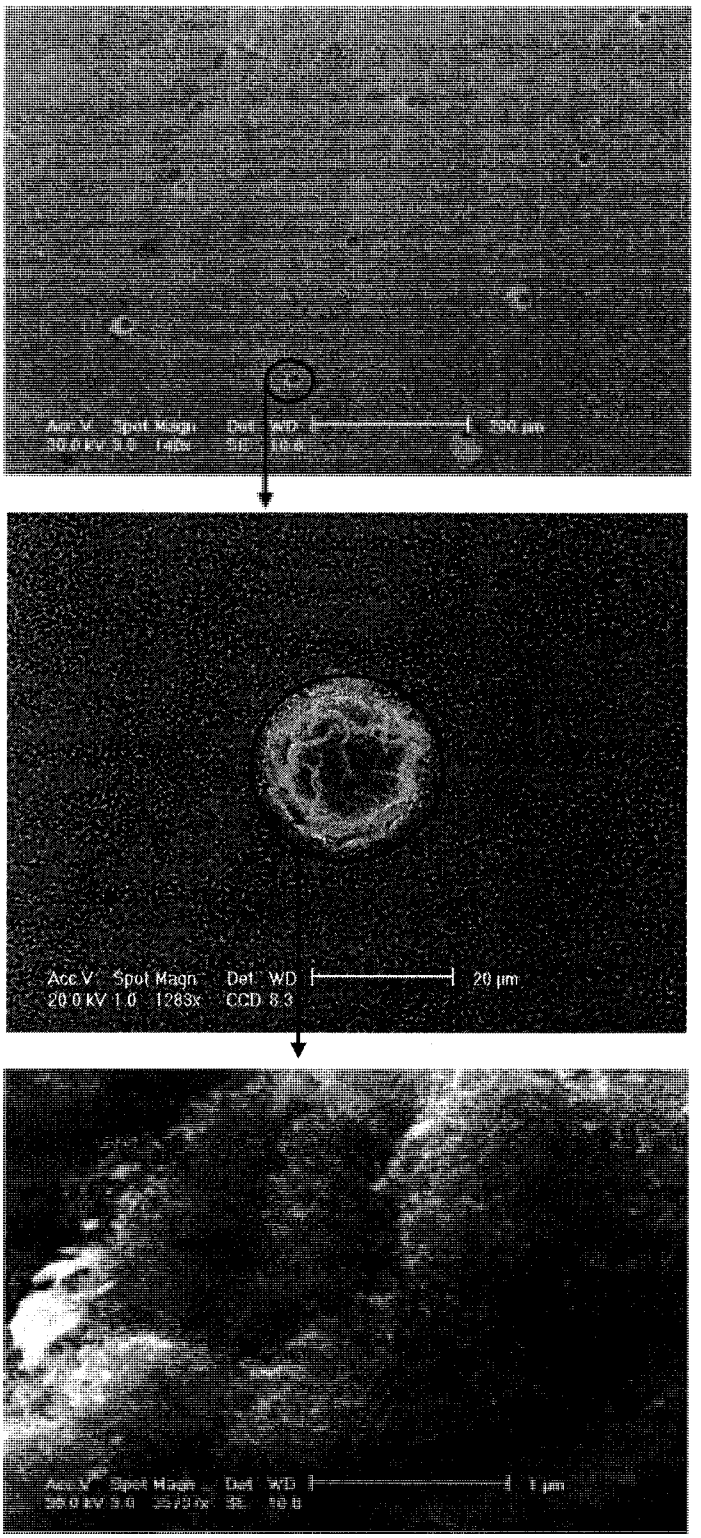

(c)

(d)

(e)

Figure 5-7 continued: (c) large view of emitter array, (d) single emitter, (e) CNTs in the emitter

5.5 Results and Discussions

Figure 5-8 shows the SEM images of CNTs grown on the cathode plate. It can be seen that the CNTs film are thick when they are large as shown in Figure 5-8 (a). When nanotubes are smaller than a certain size, they are thin and grew across the surface as shown in Fig 5-8 (b). The smallest CNTs were about 4 - 5 nm in diameter. The size of nanotubes depends on the size of catalyst particles.

Figure 5-9 shows the Raman spectrum recorded for CNT with diameter of 20 nm and 5 nm samples. They have D-band and G-band corresponding to disordered and primary Raman modes of graphite. When the nanotube size was reduced the intensity in D-band was reduced and G-band was increased.

Figure 5-10 shows the electron field emission characteristics of CNT samples with diameter of 20 nm and 5 nm. The sample with 5 nm CNTs has high emission current levels at a given voltage compared with the sample of 20 nm diameter CNTs. The difference between the threshold voltages of field emission was only 5 V. For voltage of 50 volts, the emission current of 5 nm sample and 20 nm samples were 4 μA and 0.6 μA, respectively. Figure 5-10 (b) shows the Fowler-Nordheim (FN) plots of emission data. The FN equation for electron tunneling from a metal surface is given by

$$I = \alpha(154\beta^2V^2/d^2\,\phi)\exp(-6830d\,\phi^{3/2}/\beta V) \qquad (5\text{-}1)$$

where, α is the area of emission sites, β is the field enhancement factor and ϕ is the

work function of the emission surface. Here d represents the electrode gap in μm which was 80±0.5 μm in the present case. If the emission current follows a tunneling phenomena, the plot of $\ln(I/V^2)$ versus 1/V have to follow a straight line. In this case, the data agree with F-N relation. The β factor of nanotube emitters can be estimated using the gradient of the F-N plots. By assuming that these nanotubes have a work function of graphite (4.9 eV), the estimated value of β is 16723 and 26654 for 20 nm and 5 nm samples, respectively. This fact clearly indicates that the field enhancement factor determines the emission current levels of CNTs.

The electron field emission properties of low temperature grown CNTs indicated that they have low emission threshold voltages and high current levels. These characteristics are very close to the properties reported by CNTs synthesized at high temperature and vacuum conditions in microwave plasma CVD, laser ablation and PECVD. Furthermore, these properties are much improved than emitters made using CNT/polymer composites. Also these CNTs have enhanced emission characteristics than bare metal tips and silicon nanostructures.

In the FED viewpoints, low temperature growth below 500 °C will allow fabrication of emission displays using low cost substrates. Furthermore, proposed FED consists of multilayer device structures such as metal interconnects, gate oxides and gate electrode materials. High temperature processing of these device structures is extremely vulnerable. Another important factor is that synthesis of CNTs in vacuum conditions will hinder scalability and reduction of cost. These factors clearly suggest that the low temperature growth of CNTs in atmospheric CVD conditions provide feasibility to use CNTs in FEDs. The distance and size of CNTs dot array could be made smaller if needed to improve the

resolution of display.

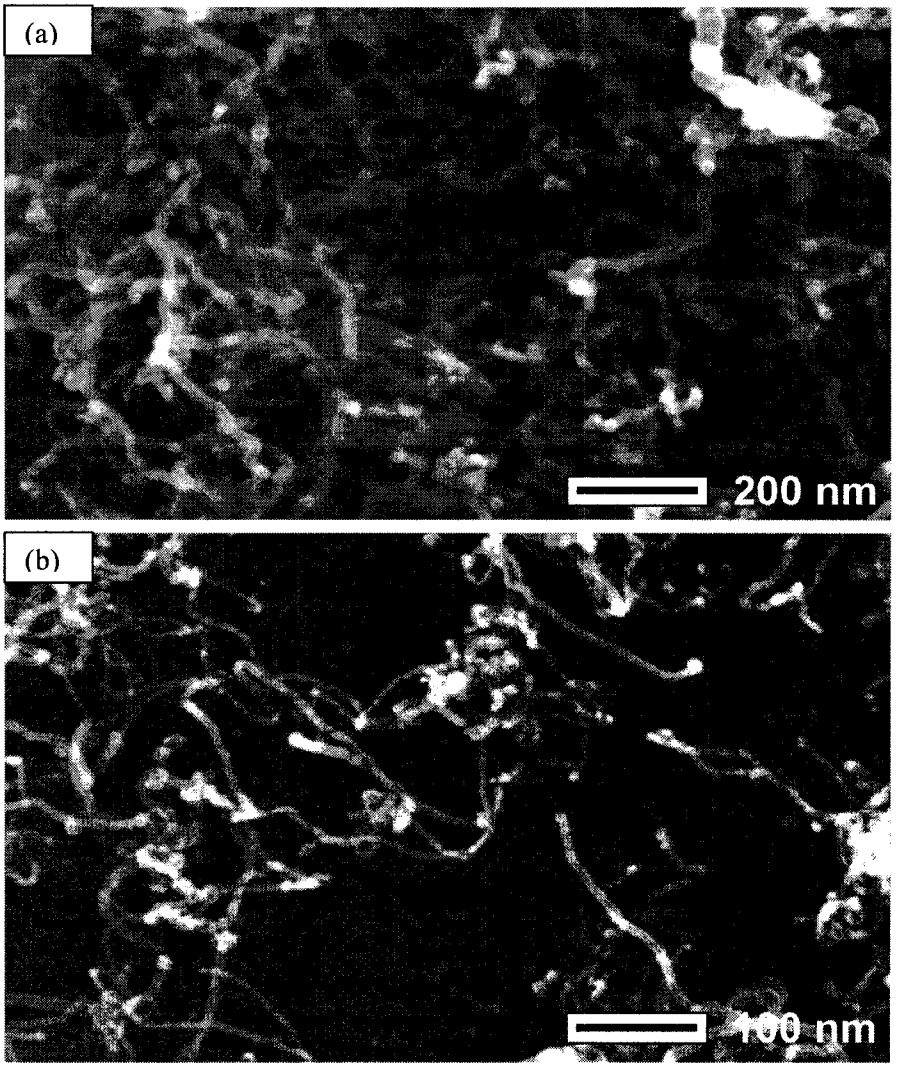

Figure 5-8 SEM images of CNTs synthesized at 500 °C: (a) large diameter, 20 nm and (b) small diameter, 5 nm

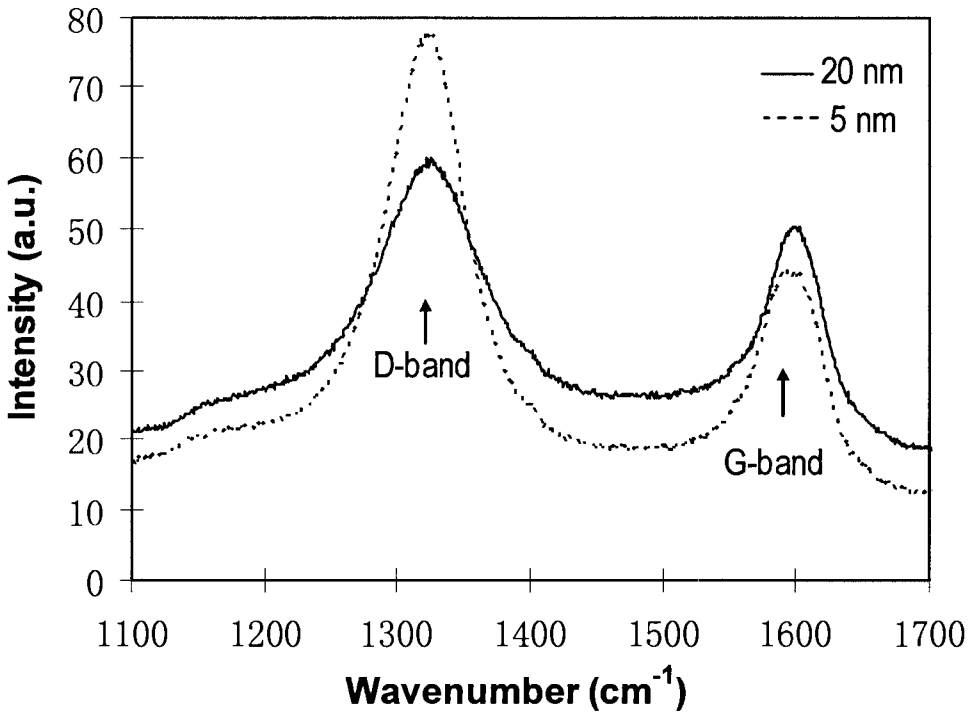

Figure 5-9 Raman spectrum of CNTs with different diameter: large diameter, 20 nm, and small diameter, 5 nm

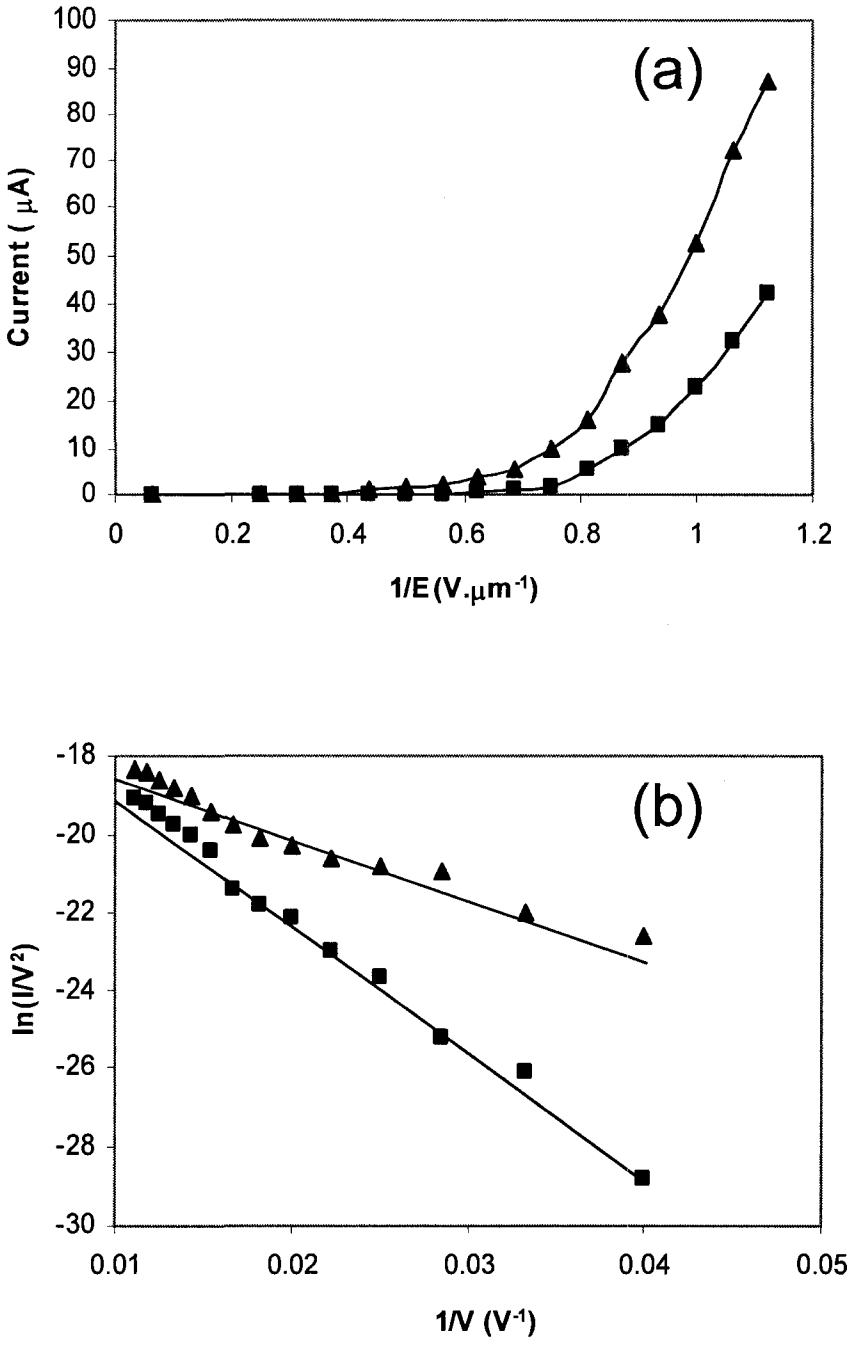

Figure 5-10 Electron field emission characteristics of CNTs grown by hot filament assisted atmospheric CVD: (a) I-E curves of two different diameter CNTs and (b) plot of I-E data with F-N coordinates (▲ for 5 nm nanotubes and ♦ for 20 nm nanotubes)

5.6 Conclusions of CNT-based Field Emission Display

In conclusion, the growth of CNTs was demonstrated in low temperature region (~500 ^{o}C). This low temperature process allows the growth of CNTs directly on large-area device-substrates such as non-alkaline-glass for FEDs. The size of CNTs can be controlled by varying the catalyst particle size. The field emission characteristics indicated that the CNTs have low emission threshold voltage and high emission current levels. In this method, the CNTs can be grown with 1-5% CH_4 in Ar at atmospheric pressure. All these processing conditions are very advantageous regarding FED applications which required large-area growth capability, batch processing and low cost substrates.

Chapter Six

6 Conclusions and Recommendations for Future Research

The conclusions obtained for the research of synthesis and applications of CNTs are included in this chapter. An overview of each main topics and main findings are described. Also, recommendations for future research are listed.

6.1 Conclusions of Current Research

Since the discovery of CNTs, many methods have been discovered to synthesize CNTs, such as arch discharge, laser ablation, CVD, PECVD, and LPCVD. However those methods require high temperature, high gas flow rate, extra energy, and vacuum conditions. All those limitation lead them to complex equipments, high cost in growing CNTs, and some cannot control the position of CNTs. So in this research, a hot filament CVD system was developed to meet the demand. By this hot filament CVD system, the CNTs can be grown at low temperature, low gas flow rate, atmospheric pressure, and on more substrates. The CNTs were applied in fabricating CNT-based gas detector, pressure sensor, and FEDs through techniques such as nanotechnology and NEMS.

The hot filament CVD system was made of quartz tube, furnace with three heating coils, hot filament, and power supply. A tungsten wire was shaped into coil to be used as filament in the CVD system. The carbon source, CH_4, was decomposed into carbon radical species under 2000 °C of the filament applied with 15v or higher voltage. The CNTs were grown on the catalyst coated on substrates when carbon radical species were carried to the reaction zone by Ar (or 5% H_2 in Ar). After growth, the CNTs were characterized by SEM, TEM, RAMAN and XRD. The results were analyzed and discussed to find the optimized conditions to grow CNTs better at low cost. Those conditions included filament, temperature, catalyst, substrate, gas flow rate and so on. It was found that, this hot filament CVD system can grow CNTs at low temperature 450 °C and low gases flow rate 5 sccm, with varies of catalyst such as Co, Ni, Fe, Au and so on, on silicon or glass substrates, under atmospheric pressure.

The CNTs were applied to fabricate gas detectors since the big surface area, which enable CNTs to absorb gases molecular easily. The catalysts were coated on the silicon substrates and made into zigzag pattern to increase the contact surface with gases. The CNTs were grown on the catalyst by the hot filament CVD system. Gold was coated on both ends of the CNTs film as electrodes. The assembled gas detector was put into the chamber of test setup. The electronic multimeter was connected to the gas detector through the electrodes to measure the resistance of CNTs. The multimeter was connected to a computer, and the Labview program running on the computer recorded the readout of multimeter. It was found that the resistance was reduced when H_2 gas was introduced into the chamber, and the sensitivity for H_2 was higher at 300 °C than 150 °C

The CNTs were also applied to fabricate pressure sensor since the resistance was

changed when CNTs were deformed. Silicon wafer with SiN_x layers on both sides were used as substrate. The SiN_x on one side was etched to be used as mask for etching silicon at the middle. After the silicon at the middle was totally etched, and the SiN_x layer on the other side was left, the SiN_x membrane was achieved. The catalyst was coated and made into pattern on the SiN_x membrane, and then the CNTs were grown on the catalyst. Gold was coated on both ends of CNTs pattern as electrodes. The silicon wafer with SiN_x membrane and CNTs was sealed with glass to form a closed chamber between the SiN_x membrane and glass. The pressure sensor was put in a closed container of testing setup, and connected to multimeter to measure the resistance of CNTs. By passing gas in the testing container, the pressure was increased. The pressure was decreased when gas was let out. It was found that, when the CNTs film was thin, the resistance increased when pressure was increased, and resistance decreased when pressure was decreased. When the CNTs film was thick, the resistance decreased when pressure was increased, and resistance increased when pressure was decreased.

The CNTs were applied to make emitter micro tips array for FEDs. Low temperature growth enabled the CNTs to be grown on glass substrates for FEDs. The Au, Co, SiN_x, Au were coated on glass turn by turn to serve as cathode electrode, catalyst, insulator, and extracting gate accordingly. By photolithography, small holes array pattern was made on the substrate. The top gold layer was etched by wet etching, and SiN_x layer was etched by plasma etching, then Co catalyst layer was exposed in the holes. The CNTs were grown on the Co in hot filament CVD system. The cathode plate grown with CNTs array was assembled with ITO glass to fabricate FED unit, and the FED unit was tested by applying voltage on cathode plate and ITO glass, and measuring the current passing through the CNTs.

Many other applications of CNTs were also studied, such as CNTs array for emission filed display, CNTs connecting at step edge and gap, and CNT-based optic sensor. The CNTs were small enough to act as the tiny tips to send out electrons in emission. It was found that the resistance of CNTs was decreased when exposed to light.

In summary, all the objectives of this research have been achieved:

1) The CNTs was synthesized by a hot filament assisted CVD system at temperature as low as 450 ^{o}C, low gas flow rate of 5 sccm CH_4, with varies of catalysts, Co, Ni, Fe and Au, on silicon and glass substrates, at atmospheric pressure conditions;
2) The CNT-based gas detectors were developed. The test of sensitivity was mainly done with H_2;
3) The CNT-based pressure sensors were developed to measure gas pressure;
4) The CNTs array was synthesized for FEDs as emitter tips.

All those results including the characterization of CNTs and applications of the CNTs proved that the hot filament CVD system has advantages to synthesize CNTs compared with other methods and the CNTs have the similar properties to perform as core parts of some applications compared with CNTs synthesized by other methods.

6.2 Recommendations for Future Research

There are still some spaces to improve the hot filament CVD system even it is better than the other methods to grow CNTs. There are some drawbacks for the applications of CNTs in gas detector, pressure sensor, and FEDs. More research should be done for more applications of CNTs.

6.2.1 Synthesis of Carbon Nanotubes

Present research shows the feasibility of hot filament CVD as a competitive technology to synthesize CNTs. More research efforts are required to develop the synthesis of CNTs using this hot filament CVD system at lower temperature and gas flow rate. The temperature monitoring and controlling of the CVD furnace can be operated by computer to adjust temperature as required for CNTs synthesis.

The hot filament CVD system can be redesigned and improved to grow CNTs better using less resource. The size of quartz tube could be reduced to use less gas, which could also reduce the experiment time. Bigger filament, such as grating shape covering the whole cross section of quartz tube, could be used to enhance the efficiency of gas decomposing. The temperature for preheating substrates could be decreased, and more kinds of substrates could be used. More catalyst should be used and compared to find the better and cheaper materials. The growth conditions should be optimized to grow longer and smaller CNTs.

The controlling of CNTs growth can be studied to grow CNTs as required. CNTs can be synthesized on nano-device structures by appropriate design.

6.2.2 Applications of Carbon Nanotubes

Those applications of CNTs still have some drawbacks because of the design or fabrication. Those CNT-based sensors need more research to improve the sensitivity and stability. The fabrication of CNT-based sensors should be adjusted and improved to make smaller devices. The properties of those CNT-based sensors should be tested, and the relations between the detected objects and sensors signals should be built by analyzing the results. There are numerous applications of CNTs to be developed.

(1) Gas detectors

More kinds of catalyst patterns should be used to grow CNTs for gas detectors. The testing conditions should be improved to get stable signals. More gases should be tested and the relations between gases and detectors resistance and sensitivity should be investigated to recognized gases. The gases detectors should be improved to response to lower concentration of gases.

(2) Pressure sensors

As the SiN_x was fragile, the SiN_x membrane was not strong, so the pressure sensor can measure pressure only less than 30 psi. More kinds of materials should be considered to make the membrane. The membrane with high strength could measure high pressure. The fabrication of pressure sensors should be studied to decrease the difficulty of produce: decrease the processes steps and increase the success ratio. The relations between CNTs film thickness and resistance change could be studied to fabricate the proper sensors as needed.

(3) Field emission display

Smaller distance between micro tips of FED could improve the resolution, so the pattern of smaller size of holes and less distance between holes could be used to grow CNTs array for emitter tips. Lower temperature growth should be investigated to grow CNTs on more substrates such as epoxy and glass.

References

[1] Wojciechowski, S., (2000), "New Trends in the Development of Mechanical Engineering Materials", Journal of Materials Processing Technology, 106, pp. 230-235

[2] Ashby, M.F., (1992), "Materials Selection in Mechanical Design", Pergamon Press, Oxford, DC

[3] Hondros, E.D., (1993), "Interfacial Engineering-A Perspective", Mater. Sci. Eng., A166, pp. 1–10

[4] Paradis, M., Goswami, T., (2007), "Carbon Nanotubes – Production and Industrial Applications", Materials and Design, 28, pp. 1477-1489

[5] Biro, L.P., Horvath, Z.E., Szlamas, L., Kertesz, K., Weber, F., Juhasz, G., et al., (2003), "Continuous carbon nanotube production in underwater AC electric arc", Chemical Physics Letters, 372, pp. 399–402

[6] Iijima, S., (1991), "Helical Microtubules of Graphitic Carbon", Nature, 354, pp. 56-58

[7] Kang, I., Schulz, M.J., Kim, J.H., Shanov,V., Shi,D., (2006), "A Carbon Nanotube Strain Sensor for Structural Health Monitoring", Smart Materials and Structure, 15, pp. 737-748

[8] Peng, S., Cho K., (2000), "Chemical Control of Nanotube Electronics", Nanotechnology, 11, pp. 57-60

[9] Burstein, E., (2003), "A major milestone in nanoscale material science: the 2002

Benjamin Franklin Medal in Physics presented to Sumio Iijima", Journal of the Franklin Institute, 340(3–4), pp. 221–42

[10] Judy, J.W., (2001), "Microelectromechanical systems (MEMS): fabrication, design and applications, Smart Materials and Structures", 10, pp. 1115-1134

[11] Kong,J., Franklin, N.R., Zhou, C.,Chapline, M.G., Peng,S., Cho,K., Dai, H., (2000), "Nanotube Molecular Wires as Chemical Sensors", Science, 287, pp. 622-625

[12] Tans, S. J., Verschueren, A. R. M., Dekker, C., (1998), "Room-temperature transistor based on a single carbon nanotube", Nature, 393, pp. 49 - 52

[13] Planeix, J.M., Coustel, N., Coq, B., Brotons, V., Kumbhar, P.S., Dutartre, R., et al., (1994), "Application of cCarbon nanotubes as supports in heterogeneous catalysis", American Chemical Society, 116, pp. 7935-7936.

[14] Saito, S., (1997), "Carbon Nanotubes for Next-Generation Electronics Devices", Science, 278, pp. 77-78

[15] Kim, P., Lieber C.M., (1999), "Nanotube Nanotweezers", Science, 286, pp. 2148-2150

[16] Che, G., Fisher, E.R., Martin, C.R., (1998), "Carbon Nanotubule Membranes for Electrochemical Energy Storage and Production," Nature, 393, pp. 346-349.

[17] Collins, P.G., Zettl, A., Bando, H., Thess, A., Smally, R.E., (1997), "Nanotube Nanodevice", Science, 278, pp. 100-102

[18] Che, G., Lakshmi, B.B., Fisher, E.R., Martin, C.R., (1998), "Carbon nanotubule membranes for electrochemical energy storage and production", Nature, 393, pp. 346-349.

[19] Journet, C., Maser, W.K., Bernier, P., Loiseau, A., Lamy, de la M., Chapelle, S., et al., (1997), "Large-scale production of single-walled carbon nanotubes by the electric-arc

technique", Nature, 388, pp. 756-758

[20] Thostenson, E.T., Ren, Z.F., Chou, Z.W., (2001), "Advances in the science and technology of carbon nanotubes and their composites: a review", Composites Science and Technology, 61, pp. 1899-1912

[21] Iijima, S., Ichihashi, T., (1993), "Single shell carbon nanotubes of one diameter", Nature, 363, pp. 603-605

[22] Alford, J.M., Mason, G.R., Feikema, D.A., (2001), "Formation of carbon nanotubes in a microgravity environment", Sixth international microgravity combustion workshop, NASA Glenn Research Center, Cleveland, OH, CP-2001-210826, p. 293–6, May 22–24.

[23] He, M.S., Zhou, S., Zhang, J., Liu, Z.F., Robinson, C., (2005), "CVD Growth of N-Doped Carbon Nanotubes on Silicon Substrates and Its Mechanism", Journal of Physics and Chemistry B, 109, pp. 9275-9279

[24] Shyu, Y.M., Hong, F.C.N., (2001), "Low-temperature growth and field emission of aligned carbon nanotubes by chemical vapor deposition", Materials Chemistry and Physics, 72, pp. 223-227

[25] http://en.wikipedia.org/wiki/Nanotechnology

[26] Oosterbroek, R.E., Lammerink, T.S.J., Berenschot, J.W., Krijnen, G.J.M., Elewenspoek, M.C., (1999), "A micromachined pressure/flow-sensor", Sensors and Actuators, 77, pp. 167-177

[27] http://en.wikipedia.org/wiki/Carbon_nanotube

[28] Collins, P.G., Avouris, P., (2000), "Nanotubes for electronics", Scientific American, 283(6), pp. 62–69.

[29] Du, C.S., Pan, N., (2005), "CVD growth of carbon nanotubes directly on nickel substrate", Materials Letters, 59, pp. 1678-1682

[30] Lee, K.H., Cho, J.M., Sigmund, W., (2003), "Control of growth orientation for carbon nanotubes", Applied physics letters, Volume 82, Number 3, pp. 448-450

[31] Frogley, M.D., Ravich, D., Wagner, H.D., (2003), "Mechanical properties of carbon nanoparticle-reinforced elastomers", Composites Science and Technology, 63, pp. 1647-1654

[32] Nuriel, S., Liu, L., Barber, A.H., Wagner, H.D., (2005), "Direct measurement of multiwall nanotube surface tension", Chemical Physics Letters, 404 (4-6), pp. 263-266

[33] Bellucci, S., (2005), "Carbon nanotubes: physics and applications", Physica Status Solidi, (c) 2(1), pp. 34-47

[34] Chae, H.G., Kumar, S., (2006), "Rigid Rod Polymeric Fibers", Journal of Applied Polymer Science, 100, pp. 791-802

[35] Demczyk, B.G., Wang, Y.M., Cumings, J., Hetman, M., Han, W., Zettl, A., Ritchie, R.O., (2002), "Direct mechanical measurement of the tensile strength and elastic modulus of multiwalled carbon nanotubes", Materials Science and Engineering, A 334, pp. 173-178

[36] Meo, M., Rossi, M., (2006), "Prediction of Young's modulus of single wall carbon nanotubes by molecular-mechanics based finite element modelling", Composites Science and Technology, 66, pp. 1597-1605

[37] Sinnott, S.B., Andrews, R., (2001), "Carbon Nanotubes: Synthesis, Properties, and Applications", Critical Reviews in Solid State and Material Sciences, 26(3), pp. 145-249

[38] Juang, Z.Y., Chien, I.P., Lai, J.F., Lai, T.S., Tsai, C.H., (2004), "The effects of ammonia on the growth of large-scale patterned aligned carbon nanotubes using thermal chemical vapor deposition method", Diamond and Related Materials, 13, pp. 1203–1209

[39] Taschner, Ch., Pacal, F., Leonhardt, A., Spatenka, P., Bartsch, K., Graff, A., Kaltofen, R., (2003), "Synthesis of aligned carbon nanotubes by DC plasma-enhanced hot filament CVD", Surface and Coatings Technology, 174 –175, pp. 81–87

[40] Saito, Y., Nishikubo, K., Kawabata, K., Matsumoto, T., (1996), "Carbon nanocapsules and single-layered nanotubes produced with platinum-group metals (Ru, Rh, Pd, Os, Ir, Pt) by arc discharge", Journal of Applied Physics, 80(5), pp. 3062–3067

[41] Journet, C., Bernier, P., (1998), "Production of carbon nanotubes", Applied Physics A: Materials Science & Processing, 67, pp. 1–9

[42] Yasuda, A., Kawase, N., Mizutani, W., (2002), "Carbon-Nanotube formation mechanism based on iin situ TEM observation", Journal of Physics and Chemistry B, 106, pp. 13294-13298

[43] Sharma, R., (2004), "Understanding the carbon nanotube growth mechanism by In-Situ microscopy", Microscopy Microanalyst, 10 (supply 2), pp. 368-369

[44] Louchev, O.A., Sato, Y., Kanda, H., (2002), "Growth mechanism of carbon nanotube forests by chemical vapor deposition", Applied Physics Letters, 80, pp. 2752-2754

[45] Endo, M., Kroto, H.W., (1992), "Formation of carbon nanofibers", Journal of Physics and Chemistry, 96, pp. 6941-6944

[46] Saito, Y., Okuda, M., Tomita, M., Hayashi, T., (1995), "Extrusion of single-wall carbon nanotubes via formation of small particles condensed near an arc evaporation source",

Chemical Physics Letters, 236, pp. 419-426

[47] Hirmke, J., Hempel, F., Stancu, G.D., Ropcke, J., Rosiwal, S.M., Singer, R.F., (2006), "Gas-phase characterization in diamond hot-filament CVD by infrared tunable diode laser absorption spectroscopy", Vacuum, 80, pp. 967-976

[48] Joe, R., Badgwell, T.A., Hauge, R.H., (1998), "Atomic carbon insertion as a low-substrate-temperature growth mechanism in diamond CVD", Diamond and Related Materials, 7, pp. 1364-1374

[49] Brukh, R., Mitra, S., (2006), "Mechanism of carbon nanotube growth by CVD", Chemical Physics Letters, 424, pp. 126-132

[50] Yudasaka, M., Yamada, R., Sensui, N., Wilkins, T., Ichihashi, T., Iijima, S., (1999), "Mechanism of the effect of NiCo, Ni and Co catalysts on the yield of single-wall carbon nanotubes formed by pulsed Nd:YAG laser ablation", Journal of Physics and Chemistry B, 103, pp. 6224-6229

[51] Qin, L.C., Iijima, S., (1997), "Fibrilliform growth of carbon nanotubes", Materials Letter, 30, pp. 311-314

[52] Fujita, Y., Bandow, S., Iijima, S., (2005), "Formation of small-diameter carbon nanotubes from PTCDA arranged inside the single-wall carbon nanotubes", Chemical Physics Letters, 413, pp. 410-414

[53] Kokai, F., Takahashi, K., Yudasaka, M., Iijima, S., (1999), "Growth dynamics of carbon-metal particles and nanotubes synthesized by CO2 laser vaporization", Applied Physics A - Materials Science and Processing, 69

[54] Nasibulin, A.G., Pikhitsa, P.V., Queipo, P., Choi, M., Kauppinen, E.I., (2006), "Investigations of mechanism of carbon nanotube growth", Physica Status Solidi (b),

243 No.13, pp. 3095-3100

[55] Vodenitcharova,T., Zhang, L.C., (2004), "Mechanism of bending with kinking of a single-walled carbon nanotube", Physical Review B, 69, pp. 115410-115412

[56] Han, S.S., Lee, K.S., Lee, H.M., (2004), "Nucleation mechanism of carbon nanotube", Chemical Physics Letters, 383, pp. 321-325

[57] Kasuya, D., Yudasaka, M., Takahashi, K., Kokai, F., Iijima, S., (2002), "Selective production of single-wall carbon nanohorn aggregates and their formation mechanism", Journal of Physics and Chemistry B, 106, pp. 4947-4951

[58] Bonard, J.M., Croci, M., Conus, F., Stockli, T., Chatelain, A., (2002), "Watching carbon nanotubes grow, Applied Physics Letters", Vol.81, No.15, pp. 2836-2838

[59] Porter, D.A., Easterling, K.E., (1992), "Phase Transformation in Metal and Alloys", Stanleey Thornes Ltd, United Kingdom

[60] Tang, Z.K. et al., (2001), "Superconductivity in 4 Angstrom Single-Walled Carbon Nanotubes", Science, 292, pp. 2462-2465

[61] Tennent, H.G., (1987), US Patent 4,663,230 (5 May 1987).

[62] Baugham, R., Zakhidov, A., Heer, W., (2002), "Carbon nanotubes – the route toward applications", Science, 297, pp. 787–792

[63] Wang, W.K., Cao, L.M., (2001), "Transformation of carbon nanotubes to diamond at high pressure and high temperature", Russian Physics Journal, 44(2), pp. 178–182

[64] Ajayan, P., Zhou, O., (2001), "Applications of carbon nanotubes, carbon nanotubes", University of North Carolina, pp. 391–425

[65] Takao, Y., Miyazaki, K., Shimizu, Y., Egashira, M., (1994), "High Ammonia Sensitive Semiconductor Gas Sensors with Double-Layer Structure and Interface Electrodes",

Journal of the Electrochemical Society, 141, pp. 1028-1034

[66] Cheah, K., Forsyth, M., Truong, V. T., (1998), "Ordering and stability in conducting polypyrrole", Synthetic Metals, 94, pp. 215-219

[67] An, K. H., Jeong, S. Y., Hwang, H. R., Lee, Y. H., (2004), "Enhanced sensitivity of a gas sensor incorporating single-walled carbon nanotube-polypyrrole nanocomposites", Advanced Materials, 16, pp. 1005-1009

[68] Chopra, S., McGuire, K., Gothard, N., Rao, A. M., (2003), "Selective gas detection using a carbon nanotube sensor", Applied physics letters, Volume 83, Number 11, pp. 2280-2282

[69] Suehiro, J., Zhou, G. B., Imakiire, H., Ding, W. D., Hara,M., (2005), "Controlled fabrication of carbon nanotubes NO2 gas sensor using dielectrophoretic impedance measurement", Sensors and Actuators B, 108, pp. 398–403

[70] Park, D., Kim, Y. H., Lee, J. K., (2003), "Synthesis of carbon nanotubes on metallic substrates by a sequential combination of PECVD and thermal CVD", Carbon, 41, pp. 1025–1029

[71] http://en.wikipedia.org/wiki/Piezoelectric_sensor

[72] Ayerdi, I., Castano, E., Garcia-Alonso, A., Gracia, J., (1997), "High-temperature ceramic pressure sensor", Sensors and Actuators, A 60, pp. 72-75

[73] Stankevic, V., Simkevicius, C., (1996), "Semiconductor pressure-pulse sensor", Sensors and Actuators, A 51, pp. 159-163

[74] Lim, H.C., Schulkin, B., Pulinkal, M.J., Liu, S., Petrova, R., Thomas, G., Wagner, S., Sidhu, K., Federici, J.F., (2005), "Flexible membrane pressure sensor", Sensors and Actuators A, 119, pp. 332–335

[75] LI, C. Y., CHOU, T. W., (2006), "Atomistic Modeling of Carbon Nanotube-based Mechanical Sensors", JOURNAL OF INTELLIGENT MATERIAL SYSTEMS AND STRUCTURES, 17, pp. 247-254

[76] Ilic, B., Czaplewski, D., Craighead, H.G., Neuzil, P., Campagnolo, C., Batt, C., (2000), "Mechanical Resonant Immunospecific Biological Detector", Applied physics letters, 77(3), pp. 450–452.

[77] Li, C. Y., Chou, T. W., (2003), "Single-walled Carbon Nanotubes as Ultrahigh Frequency Nanomechanical Resonators", Physical Review B, 68(7), pp. 073405-073407

[78] Li, C. Y., Chou, T. W., (2004), "Vibrational Behaviors of Multiwalled Carbon Nanotube-based Nanomechancial Resonators", Applied physics letters, 84(1), pp. 121–123

[79] Huang, X. M. H., Zorman, C. A., Mehregany, M., Roukes, M. L., (2003), "Nanodevice Motion at Microwave Frequencies", Nature, 421(6922), pp. 496

[80] Froes, F.H., (1994), "Advanced Metals for Aerospace and Automotive Use", Material Science and Engineering, A 184, pp. 119

[81] Dohn, S., Kjelstrup-Hansen, J., Madsen, D.N., Molhave, K., Boggild, P., (2005), "Multi-walled carbon nanotubes integrated in microcantilevers for application of tensile strain", Ultramicroscopy, 105, pp. 209–214

[82] Dharap, P., Li, Z. L., Nagarajaiah, S., Barrera, E. V., (2004), "Nanotube Film Based on Single-wall Carbon Nanotubes for Strain Sensing", Nanotechnology, 15(3), pp. 379–382.

[83] Kang, I., Schulz, M. J., Kim, J. H., Shanov, V., Shi, D. L., (2006), "A carbon nanotube

strain sensor for structural health monitoring", Smart Material Structure, 15, pp. 737–748

[84] http://en.wikipedia.org/wiki/Field_emission_display

[85] Jonge, N.D., Bonard, J.M., (2004), "Carbon nanotube electron sources and applications", Philosophical Transactions of the Royal Society of London, A 362, pp. 2239-2266

[86] Deng, S.Z., Wu, Z.S., Xu, N.S., Chen, J., (2001), "Characterization of a high voltage flat panel display unit using nanotube-based emitters", Ultramicroscopy, 89, pp. 105-109

[87] Lee, N. S., Chung, D. S., Han, I. T., (2001), "Application of carbon nanotubes to field emission displays", Diamond and Related Materials, 10, pp. 265-270

[88] Wei, L., Zhang, X.B., Zhu, Z.Y., (2007), "Application of ZnO nanopins as field emitters in a field-emission-display device", Journal of Vacuum Science and Technology, B 25(2), pp. 608-610

[89] Chen, J., Xu, N.S., Deng, S.Z., She, J.C., Chen, J., (2003), "Effects of the interface and surface nanostructures on field emission of amorphous diamond film", Journal of Vacuum Science and Technology, B 21(1), pp. 581-586

[90] Givargizov, E. I., Zhirnov, V. V., Chubun, N. N., Stepanova, A. N., (1997), "Fabrication of field emission display prototype based on Si field emission arrays with diamond coating", Journal of Vacuum Science and Technology, B 15(2), pp. 450-453

[91] Lee, J.D., Oh, C.W., Park, J.W., Park, B.G., (2003), "Metal-oxide-semiconductor field effect transistor-controlled field emission display, Journal of Vacuum Science and Technology, B 21(1), pp. 519-522

[92] Taniyasu, Y., Kasu, M., Makimoto, T., (2004), "Field emission properties of heavily Si-doped AlN in triode-type display structure", Applied Physics Letters, Vol.84, No.12, pp. 2115-2117

[93] Nakayama, Y., Akita, S., (2001), "Field-emission device with carbon nanotubes for a flat panel display", Synthetic Metals, 117, pp. 207-210

[94] Chen, J., Dai, Y.Y., Luo, J., Li, Z. L., Deng, S. Z., She, J. C., Xu, N. S., (2007), "Field emission display device structure based on double-gate driving principle for achieving high brightness using a variety of field emission nanoemitters", Applied Physics Letters, 90, pp. 253105-253107

[95] Nagao, M., Yasumuro, C., (2007), "Field emitter array with a memory function for ultrahigh luminance field emission display", Journal of Vacuum Science and Technology, B 25(2), pp. 464-468

[96] Wang, L.L., Sun, Z., Chen, T., Que, W.X., (2006), "Growth temperature effect on field emission properties of printable carbon nanotubes cathode", Solid-State Electronics, 50, pp. 800-804

[97] Shiroishi, T., Hosono, A., Sono, A., Nishimura, K., Suzuki, Y., Nakata, S., Okuda, S., (2006), "Improvement of emission characteristics uniformity of carbon nanotubs field emission display by surface treatment", Journal of Vacuum Science and Technology, B 24(2), pp. 979-982

[98] Liu, D.P., Benstetter, G., Frammelsberger, W., (2006), "Nano-scale electron field emission from the bare, hydrogenated, and graphitelike-layer-covered tetrahedral amorphous carbon films", Journal of Applied Physics, 99, pp. 044303

[99] Wei, L., Zhang, X. B., Yang, G. D., Xie, M. Y., (2006), "Study of the triode structure in

a field emission display element", Journal of Vacuum Science and Technology, B 24(2), pp. 962-966

[100] Zeng, F. G., Zhu, C. C., Liu, W. H., Liu, X. H., (2006), "The fabrication and operation of fully printed carbon nanotube field emission displays", Microelectronics Journal, 37, pp. 495-499

[101] Choi, W.B., Jin, Y.W., Kim, H.Y., Lee, S. J., Yun, M.J., Kang, J.H., Choi, Y.S., Park, N.S., Lee, N.S., Kim, J.M., (2001), "Electrophoresis deposition of carbon nanotubes for triode-type field emission display", Applied Physics Letters, 78(11), pp. 1547-1549

[102] Siegel, R.W., Hu, E., Roco, M.C., (1998), "R&D Status and Trends in Nanoparticles, Nanostructured, Materials, and Nanodevices in the United States", World Technology Evaluation Center (WTEC) Workshop Report (May 8-9, 1997), NSF

[103] http://grin.hq.nasa.gov/ABSTRACTS/GPN-2000-001535.html

[104] Harper, T., (2003), "What is Nanotechnology?", Nanotechnology, Volume 14, issue 1

[105] http://en.wikipedia.org/wiki/List_of_nanotechnology_applications

[106] Bustillo, J., Howe, R. T., Muller, R. S., (1998), "Surface micromachining for microelectro-mechanical systems Proc", IEEE, 86, pp. 1552–1574

[107] Klaassen, E. H., Petersen, K., Noworolski, J. M., Logan, J., Maluf, N. I., Brown, J., Storment, C., McCulley, W., Kovacs, G. T. A., (1995), "Silicon fusion bonding and deep reactive ion etching; a new technology for microstructures Proc.", Int. Solid-State Sensors and Actuators Conf., Transducers '97 (Stockholm), pp. 556–559

[108] Zee, F., Judy, J. W., (1999), "MEMS chemical gas sensor using a polymer-based array Proc.", Int. Solid-State Sensors and Actuators Conf., Transducers '99 (Sendai), pp. 1169–1172

[109] iMEMS: www.analog.com/iMEMS/

[110] Mizuno, K., Hata, K., Saito, T., Ohshima, S., Yumura, M., Iijima, S., (2005), "Selective Matching of Catalyst Element and Carbon Source in Single-Walled Carbon Nanotube Synthesis on Silicon Substrates", Journal of Physics and Chemistry B, 109, pp 2632-2637

[111] Lee, W.Y., Liao, T.X., Juang, Z.Y., Tsai, C.H., (2004), "Patterned aligned growth of carbon nanotubes on porous structure templates using chemical vapor deposition methods", Diamond and Related Materials, 13, pp. 1232–1236

[112] Zhang, Z.J., Dewan, C., Kothari, S., Mitra, S., Teeters, D., (2005), "Carbon nanotube synthesis, characteristics, and microbattery applications", Materials Science and Enginering B, 116, pp 363-368

[113] Dresselhaus, M.S., Dresselhaus, G., Jorio, A., Souza Filho, A.G., Saito, R., (2002), "Raman spectroscopy on isolated single wall carbon nanotubes", Carbon, 40, pp. 2043-2061

[114] Xu, G., Feng, Z.C., Popovic, Z., Lin, J.Y., Vittal, J.J., (2001), "Nanotube Structure Revealed by High-Resolution X-ray Diffraction", Advanced Materials, 13, No.4, pp. 264-267

[115] Yusa, H., Watanuki, T., (2005), "X-ray diffraction of multiwalled carbon nanotube under high pressure: Structural durability on static compression", Carbon, 43, pp. 519-523

[116] Li, Z.Q., Lu, C.J., Xia, Z.P., Zhou, Y., Luo, Z., (2007), "X-ray diffraction patterns of graphite and turbostratic carbon", Carbon, 45, pp. 1686-1695

[117] Suehiroa, J., Sano, N., Zhou, G.B., Imakiire, H., Imasaka, K., Hara, M., (2006),

"Application of dielectrophoresis to fabrication of carbon nanohorn gas sensor", Journal of Electrostatics, 64, pp. 408–415

[118] Sayago, I., Terrado, E., Lafuente, E., Horrillo, M.C., Maser, W.K., Benito, A.M., Navarro, R., Urriolabeitia, E.P., Martinez, M.T., Gutierrez, J., (2005), "Hydrogen sensors based on carbon nanotubes thin films", Synthetic Metals, 148, pp. 15-19

[119] Sayago, I., Terrado, E., Aleixandre, M., Horrillo, M.C., Fernandez, M.J., Lozano, J., Lafuente, E., Maser, W.K., Benito, A.M., Martinez, M.T., Gutierrez, J., Munoz, E., (2007),"Novel selective sensors based on carbon nanotubes for hydrogen detection", Sensors and Actuators B, 122, pp. 75-80

[120] Ding, D.Y., Chen, Z., Rajaputra, S., Singh, V., "Hydrogen sensors based on aligned carbon nanotubes in an anodic aluminum oxide template with palladium as a top eletrode", Sensors and Actuators B, 124, pp. 12-17

[121] Niu, Li., Luo, Y.L., Li, Z.Q., (2007), "A highly selective chemical gas sensor based on functionalization of multi-walled carbon nanotubes with poly (ethylene glycol)", Sensors and Actuators B, 126, pp. 361-367

[122] Varghese, O.K., Kichambre, P.D., Gong, D., Ong, K.G., Dickey, E.C., Grimes, C.A., (2001), "Gas sensing characteristics of multi-wall carbon nanotubes", Sensors and Actuators B, 81, pp. 32-41

[123] Liu, Y.L., Yang, H.F., Yang, Y., Liu, Z.M., Shen, G.L., Yu, R.Q., (2006), "Gas sensing properties of tin dioxide coated onto multi-walled carbon nanotubes", Thin Solid Films, 497, pp. 355-360

[124] Ueda, T., Norimatsu, H., Bhuiyan, M.M.H., Ikegami, T., Ebihara, K., (2006), "Properties of CNTs gas sensors prepared using PLD/CVD method", Material Research

Society Symposium Proceedings, Vol. 900E, 0900-o09-08

[125] Han, P.G., Wong, H., Poon, M.C., (2001), "Sensitivity and stability of porous polycrystalline silicon gas sensor", Colloids and Surfaces A, 179, pp. 171-175

[126] Sakai, G., Matsunaga, N., Shimanoe, K., Yamazoe, N., (2001), "Theory of gas-diffusion controlled sensitivity for thin film semiconductor gas sensor", Sensors and Actuators B, 80, 125-131

[127] Cantalini, C., Valentini, L., Armentano, I., Lozzi, L., Kenny, J.M., Santucci, S., (2003), "Sensitivity to NO_2 and cross-sensitivity analysis to NH_3, ethanol and humidity of carbon nanotubes thin film prepared by PECVD", Sensors and Actuators B, 95, 195-202

[128] Chang, H. J., Lee, J. D., Lee, S. M., Lee, Y. H., (2001), "Adsorption of NH3 and NO2 molecules on carbon nanotubes", Applied Physics Letters, 79, pp. 3863-3865

[129] Collins, P. G., Bradley, K., Ishigami, M., Zettl, A., (2000), "Extreme Oxygen Sensitivity of Electronic Properties of Carbon Nanotubes", Science, 287, pp. 1801-1804

[130] Zhou, C., Kong, J., Dai, H., (2000), "Electrical measurements of individual semiconducting single-walled carbon nanotubes of various diameters", Applied Physics Letters, 76, pp. 1597-1599

[131] Martel, R., Derycke, V., Lavoie, C., Appenzeller, J., Chan, K. K., Tersoff, J., Avouris, P., (2001), "Ambipolar Electrical Transport in Semiconducting Single-Wall Carbon Nanotubes", Physical Review Letters, 87(25), pp. 256805-256807

[132] Zhou, C., Kong, J., Yenilmez, E., Dai, H., (2000), "Modulated Chemical Doping of Individual Carbon Nanotubes", Science, 290, pp. 1552